U.S. DEPARTMENT OF ENERGY

PNNL-19245

Prepared for the U.S. Department of Energy
under Contract DE-AC05-76RL01830

The Role of Cohesive Particle Interactions on Solids Uniformity and Mobilization During Jet Mixing: Testing Recommendations

PA Gauglitz
BE Wells
JA Bamberger
JA Fort
J Chun
JJ Jenks

April 2010

Pacific Northwest
NATIONAL LABORATORY

Proudly Operated by Battelle *Since 1965*

DISCLAIMER

PACIFIC NORTHWEST NATIONAL LABORATORY
operated by
BATTELLE
for the
UNITED STATES DEPARTMENT OF ENERGY
under Contract DE-AC05-76RL01830

Printed in the United States of America

Available to DOE and DOE contractors from the
Office of Scientific and Technical Information,
P.O. Box 62, Oak Ridge, TN 37831-0062;
ph: (865) 576-8401
fax: (865) 576-5728
email: reports@adonis.osti.gov

Available to the public from the National Technical Information Service,
U.S. Department of Commerce, 5285 Port Royal Rd., Springfield, VA 22161
ph: (800) 553-6847
fax: (703) 605-6900
email: orders@ntis.fedworld.gov
online ordering: http://www.ntis.gov/ordering.htm

This document was printed on recycled paper.
(9/2003)

PNNL-19245

The Role of Cohesive Particle Interactions on Solids Uniformity and Mobilization During Jet Mixing: Testing Recommendations

PA Gauglitz
BE Wells
JA Bamberger
JA Fort
J Chun
J Jenks

April 2010

Prepared for
the U.S. Department of Energy
under Contract DE-AC05-76RL01830

Pacific Northwest National Laboratory
Richland, Washington 99352

Executive Summary

Radioactive waste that is currently stored in large underground tanks at the Hanford Site will be staged in selected double-shell tanks (DSTs) and then transferred to the Waste Treatment and Immobilization Plant (WTP). Before being transferred, the waste will be mixed, sampled, and characterized to determine if the waste composition meets the waste feed specifications. Washington River Protection Solutions (WRPS) is conducting a Tank Mixing and Sampling Demonstration Program to determine the mixing effectiveness of the current baseline mixing system that uses two jet mixer pumps to mobilize and mix waste in DSTs and to determine the adequacy of the planned sampling method. The overall purpose of the demonstration program is to mitigate the technical risk associated with the mixing and sampling systems meeting the feed certification requirements for transferring waste to the WTP.

A critical aspect of meeting the feed certification requirements is ensuring that the collected samples will adequately represent the contents of the tank and that all batches of transferred waste are sufficiently uniform so that they all are equivalent to the characterized samples. However, the tank waste contains slurries of solid particles that settle and may become progressively more concentrated towards the bottom of the tank. Obtaining a perfectly uniform distribution of waste in the DSTs with a mixing system may not be possible. To determine how close this ideal can be approached, the expected performance of the DST mixing and sampling systems must be quantified. There have been a number of laboratory studies and full-scale tank farm studies that evaluated mixing behavior; these studies are discussed later in this report. However, these studies do not provide adequate quantitative information to evaluate the performance of the planned sampling and the batch uniformity. Accordingly, WRPS' demonstration program is focusing specifically on quantifying the uniformity of samples and batch transferred material to reduce the technical risk associated with these systems.

The first phase of the demonstration program is to conduct scaled tests that appropriately match full-scale behavior and to evaluate sampling methodologies and the uniformity of batch transfers. The initial scaled testing will use non-cohesive particles where the particles do not have cohesive interactions that would cause the particles to stick together. The purpose of this report is to analyze existing data and evaluate whether scaled mixing tests with cohesive simulants are needed to meet the overall objectives of the small-scale mixing demonstration program. This evaluation will focus on estimating the role of cohesive particle interactions on various physical phenomena that occur in parts of the mixing process. A specific focus of the evaluation will be on the uniformity of suspended solids in the mixed region.

The evaluation shows that cohesive particle interaction will have multiple effects through a number of different mechanisms. Some of the effects improve solids uniformity while others will likely degrade uniformity. An overall assessment was made that estimated the combined behavior. A very striking and consistent observation from all the tank farm and scaled test data is that during jet mixing operations, the waste particles segregate into an upper mixed region of an essentially constant concentration that is independent of elevation and a region at the bottom of the tank that contains a higher concentration of particles.

Tank farm and scaled-test data suggest that a substantial fraction of the waste solids is not lifted above the bottom region of the tank but remains towards the bottom as a stratified layer. The evaluation suggests that the solids concentration in this layer is sufficiently high that the slurry will be non-Newtonian with a small but still significant yield stress. The non-Newtonian behavior and yield stress are

thought to be caused primarily by cohesive particle interactions. Studies have shown that even a small yield stress reduces the jet momentum in the fluid at a distance from the jet and thus reduces the ability of the jet to mobilize solids. It is expected that any significant shear thinning behavior in a non-Newtonian fluid will have the same effect as a fluid having a yield stress, which is a specific type of shear thinning fluid. Accordingly, in the expected stratified condition of a jet-mixed tank, cohesive particle interactions will reduce the ability of the jet to lift particles into the upper region of the tank. The conclusion of this overall assessment is that stratification will likely occur, and cohesive particle interactions will reduce the fraction of particles lifted into the upper region of the tank. The cohesive particle interactions do not, on their own, cause the stratified layer and reduced particle lifting to occur, but the cohesive interactions if present will accentuate this behavior although the magnitude of the impact is difficult to estimate. Hence, the conclusion is that testing with only non-cohesive particles will create technical uncertainty in meeting the objectives of the Tank Mixing and Sampling Demonstration Program.

The evaluation also shows that for the particles that are lifted into the upper region of the tank, the total particle concentration and the relative amounts of different size particles are extremely uniform. However, in comparison to the overall concentration in the tank and the initial relative amounts of particles of different size, the material in the upper region is clearly different.

Finally, this study conducted an extensive review of the literature on the uniformity of suspended solids in jet mixed tanks. There are no existing studies or data that specifically quantify the role of cohesive interactions on uniformity. The absence of definitive data further suggests that at least some testing with cohesive particles as part of the Tank Mixing and Sampling Demonstration Program will be needed to determine the impact of the cohesive particle interactions.

Based on the evaluation presented in this report and the absence of definitive studies, the recommendation is to conduct scoping tests to determine the magnitude of the impact caused by cohesive particle interactions on mixing. If the impact is determined to be significant, the recommendation is to conduct quantitative mixing tests at multiple scales with cohesive particles to augment the initial testing with non-cohesive particles. If initial testing can demonstrate that the impact of cohesive interactions is small over the range of important test conditions, then extensive scaled testing should not be necessary.

Acronyms and Abbreviations

ADMP	advanced design mixer pump
CFD	computational fluid dynamics
DOE	U.S. Department of Energy
DST	double-shell tank
ECR	effective cleaning radius
ESP	Environmental Simulation Program
ft	feet
HLW	high-level waste
hp	horsepower
ICD-19	Interface Control Document for Waste Feed
in.	inch(es)
K	$C_1 \exp\{-C_2[\tan\theta]^2\}$
MVST	Melton Valley Storage Tanks
OHF	old hydrofracture
ORNL	Oak Ridge National Laboratory
PNNL	Pacific Northwest National Laboratory
PSDD	particle size and density distribution
SRNL	Savannah River National Laboratory
rpm	revolutions per minute
SRS	Savannah River Site
SSP	suspended solids profiler
TSPP	tetra sodium pyrophosphate
UDS	undissolved solids
WRPS	Washington River Protection Solutions
WTP	Hanford Waste Treatment and Immobilization Plant

Symbols

A_v	flow area between vanes
D	diameter of tank
d	average spacing between vanes or gap between vane and pump housing
DC	duty cycle = t_D / t_C
D_0	nozzle diameter
D*	nondimensional critical suspension parameter
Ga	Galileo number
g	gravitational constant
g_c	constant
gpm	gallons per minute
H_C*	nondimensional cloud height
h_B	sediment depth
h_T	liquid surface level
K	$C_1 \exp\{-C_2[\tan\theta]^2\}$
N	number of installed jets or pulse tubes
N_J	number of operating jets/pulse tubes
n_v	number of vanes
Re	jet Reynolds number = U_0D_0/ν
s	density ratio, ratio of particle density to liquid density = ρ_s/ρ_l
t_C	cycle time
t_D	drive time, discharge time, pulse time, time at end of pressurization during pulse discharge
u(z)	maximum time averaged velocity
U_{CS}	critical suspension velocity, all solids suspended at the end of the pulse
U_T	unhindered terminal settling velocity
U_{TH}	hindered terminal settling velocity
U_0	nozzle exit velocity
V	apparent velocity determined by total flow
V_P	volume of pulse (per PJM)
V_{PT}	volume of pulse tube
V_{REF}	reference volume based on the volume of a right circular cylinder of diameter D where height equals diameter, $V_{REF} = (\pi D^3)/4$
V_{tip}	tip velocity
w_M	UDS mass fraction
w_S	UDS sediment mass fraction

X	mass fraction
z	distance

Greek Letters

ρ	density
ρ_B	bulk sediment density
ρ_L	liquid density
ρ_S	UDS density
η	Suspension viscosity in Figure 2.2
η_o	Suspension viscosity in the limit of zero shear rate in Figure 2.2
η_∞	Suspension viscosity in the limit of infinite shear rate in Figure 2.2
ν	kinematic viscosity = μ/ρ_l
μ	viscosity
ϕ_J	jet density = $N_J d^2/D^2$
ϕ_{max}	packing fraction
ϕ_p	pulse volume fraction = $N V_P / V_{REF}$
ϕ_{PT}	ratio of pulse tube to vessel cross-sectional area = $N D_{PT}^2/D^2$
ϕ_S	ratio of volume of solids particulate to reference volume = $V_S/V_{REF} = V_S/(\pi D^3/4)$
θ	jet half angle
τ_0	yield stress

Contents

Figures

Tables

1.0 Introduction

Radioactive waste that is currently stored in large underground tanks at the Hanford Site will be staged in selected double-shell tanks (DSTs) and then transferred to the Waste Treatment and Immobilization Plant (WTP) (Certa and Wells 2009). Before being transferred, the waste will be mixed, sampled, and characterized to determine if the waste composition meets the waste feed specifications (Hall 2008). Washington River Protection Solutions (WRPS) is conducting a Tank Mixing and Sampling Demonstration Program to determine the mixing effectiveness of the current baseline mixing system that uses two jet mixer pumps to mix and mobilize waste in DSTs and to determine the adequacy of the planned sampling method (Townson 2009). The overall purpose of the demonstration program is to mitigate the technical risk associated with the mixing and sampling systems meeting the feed certification requirements for transferring waste to the WTP.

A critical aspect of meeting the feed certification requirements is ensuring that the collected samples will adequately represent the contents of the tank and that all batches of transferred waste are sufficiently uniform so that they all are equivalent to the characterized samples. However, the tank waste contains slurries of solid particles that settle and may become progressively more concentrated towards the bottom of the tank. Obtaining a perfectly uniform distribution of waste in the DSTs with a mixing system is an ideal that can be approached, but is not practically achievable. Accordingly, the expected performance of the planned DST mixing and sampling systems must be quantified. There have been a number of laboratory studies and full-scale tank farm studies that evaluated mixing behavior; these studies are discussed later in this report. However, these studies do not provide adequate quantitative information to evaluate the performance of the planned sampling method and the batch uniformity. Accordingly, WRPS' demonstration program is focusing specifically on quantifying the uniformity of samples and batch transferred material to reduce the technical risk associated with these systems.

The first phase of the demonstration program is to conduct scaled tests that appropriately match full-scale behavior and to evaluate sampling methodologies and the uniformity of batch transfers. Computational models are also being developed to support the program objectives. The initial scaled testing will use non-cohesive particles. A simple definition of cohesiveness is when particles stick together by surface forces (Parker 1984), and non-cohesive particles do not stick together. The distinction between cohesive and non-cohesive materials is commonly used in the discussion of sediments and their behavior (Winterwerp and Van Kesteren 2004; Day 2006), even though it is recognized that it is difficult to give a sound scientific definition of a cohesive sediment (Winterwerp and Van Kesteren 2004). In tank mixing systems, slurries of non-cohesive or cohesive particles may behave differently depending on the particle characteristics and solids concentrations (Gauglitz et al. 2009; Meyer et al. 2009). For sufficiently dilute systems, many slurries will behave as Newtonian fluids and cohesive interactions may be negligible (Gauglitz et al. 2009). As discussed throughout this report, there are numerous studies on mixing of both non-cohesive and cohesive slurries. However, these studies do not specifically show whether the presence or absence of cohesive particle interactions will play a significant role in waste uniformity during mixing. Accordingly, it is not clear if testing is needed with cohesive particles to supplement the initial tests using non-cohesive materials.

The purpose of this report is to analyze existing data and evaluate whether scaled mixing tests with cohesive simulants are needed to meet the overall objectives of the small-scale mixing demonstration program. This evaluation will focus on estimating the role of cohesive particle interactions on the vertical

distribution of suspended solids. The specific objectives are to describe the difference between cohesive and non-cohesive materials during the processes of sediment (settled sludge) mobilization and the vertical distribution of solids and to discuss the role of cohesive particle interactions on scaled tests. The final result of this evaluation will be a recommendation on whether scaled mixing tests with cohesive particles are needed to augment the initial testing with non-cohesive particles.

In the following subsections, the general role of cohesive particle interactions is described and the significant relationship between cohesive forces and non-Newtonian slurry rheology is introduced. In Section 1.2, the general problem of jet mixing in DSTs is divided into a series of regions that each has specific physical behavior that can be described and evaluated. Section 1.3 is a summary of specific previous studies that are pertinent to jet mixing behavior and Section 1.4 summarizes the overall objectives and approach for the tank mixing and sampling demonstration program. Section 2 focuses on an evaluation and examples of how solids concentration and the magnitude of cohesive particle interactions affect slurry rheology. Section 3 provides data and analysis on waste properties for the anticipated waste feed that will be staged for transfer to the WTP. In Section 4, each region that was described in Section 1.2 is evaluated in detail, and the specific studies that highlight the role of cohesive particle interactions are presented. Section 4 also includes brief discussions on previous studies that provide information on the scale-up behavior. Finally, Section 5 provides a discussion of the overall impact of cohesive interactions on the uniformity of solids in the mixed region of the tanks, and Section 6 summarizes the conclusions and recommendations.

1.1 Cohesive Material Behavior

Particles that may stick together due to surface forces are classified as cohesive particles, while particles with negligible surface attractive forces are non-cohesive (Parker 1984). The phenomenon of particles sticking together causes a slurry of cohesive particles to behave differently than a non-cohesive slurry in a number of significant ways. Figure 1.1 depicts the particle behavior with cohesive and non-cohesive materials. For the cohesive particles, when the material is stagnant or being sheared very slowly, the particles stick together. If the connected particles span a sufficient distance, the material is essentially a gel and will possess a yield stress or shear strength or simply behave as a strongly shear thinning fluids (for a discussion of yield stress, shear strength, and shear thinning behavior see Poloski et al. 2007). If the material is sheared, the connections between particles are progressively disrupted as the shearing increases, and the particle networks get broken into progressively smaller aggregates of particles. This is depicted in Figure 1.1 and results in the cohesive slurry being a shear thinning (non-Newtonian) fluid. Figure 1.1 also shows the qualitative behavior of a slurry composed of non-cohesive particles. Here, the particles do not stick together, so the suspension does not form connections between particles and does not behave as a gel. Suspensions of non-cohesive particles may be slightly shear thinning and may be a bit more viscous than the suspending fluid due to the presence of the particles. However, as we will show in Section 2, a slurry of cohesive particles will have a significantly higher viscosity than an equivalent slurry of non-cohesive particles. This difference in fluid behavior, such as the increased viscosity and presence of a yield stress (or shear strength), is one of the main differences between a cohesive and non-cohesive slurry. It is important to note that when sufficiently dilute, a slurry of cohesive particles will be unable to form connections of attached particles that span long distances, and these dilute slurries will behave similar to non-cohesive slurries.

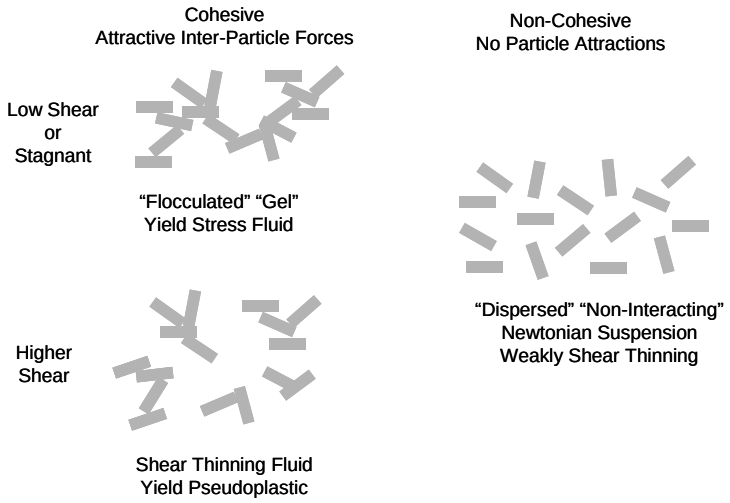

Figure 1.1. Cohesive and Non-Cohesive Material Particle Behavior

Cohesive and non-cohesive slurries will also behave differently in terms of the tendency of the particles to flocculate into aggregates. For cohesive particles, aggregates may form that will settle more quickly than the individual primary particles. The behavior will be important in the mixed region of the tank. As reported in Wells et al. (2007), high-level waste (HLW) includes insoluble solids consisting primarily of oxides and hydroxides of metals used in the fabrication and reprocessing of nuclear fuels. These solid particles range in size and density from small dense primary particles to large, low-density diffuse flocs or soft agglomerates and large, relatively dense, cemented aggregates and stable agglomerates (collectively termed hard agglomerates). Figure 1.2 (from Ilievski and White 1994) depicts these different particles. Individual primary particles can combine to form flocs and partially cemented aggregates. In the absence of surface forces to bind the primary particles together (i.e., non-cohesive particles), large, soft, and hard agglomerates will not be developed. The settling rates of the individual primary particles, soft agglomerates, and hard agglomerates are different, and thus, the cohesive properties of the primary particulate can affect the settling rate of the material.

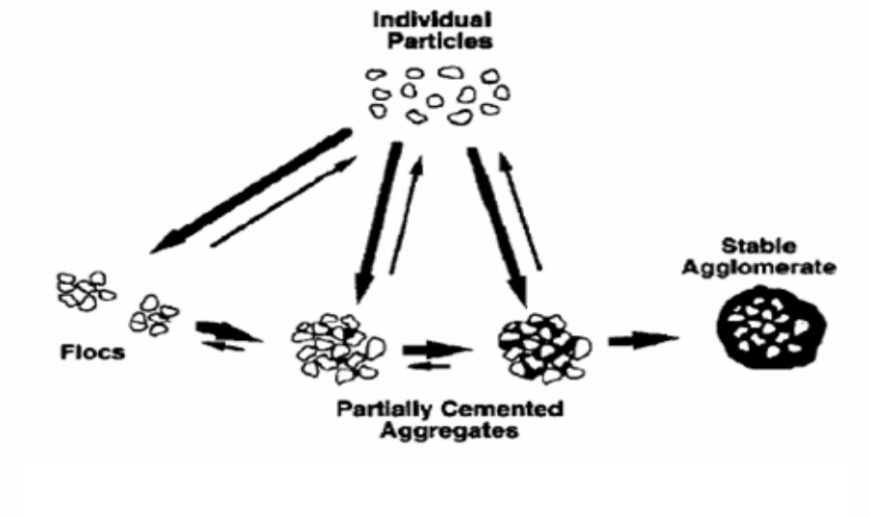

Figure 1.2. Solid Particles and Soft and Hard Agglomerates (from Ilievski and White 1994)

1.2 Regions of Behavior during Jet Mixing and Settling of Cohesive Slurries

In tank mixing systems, slurries with cohesive particles will affect different regions of behavior. Figure 1.3 shows the important regions of jet mobilization and suspension.

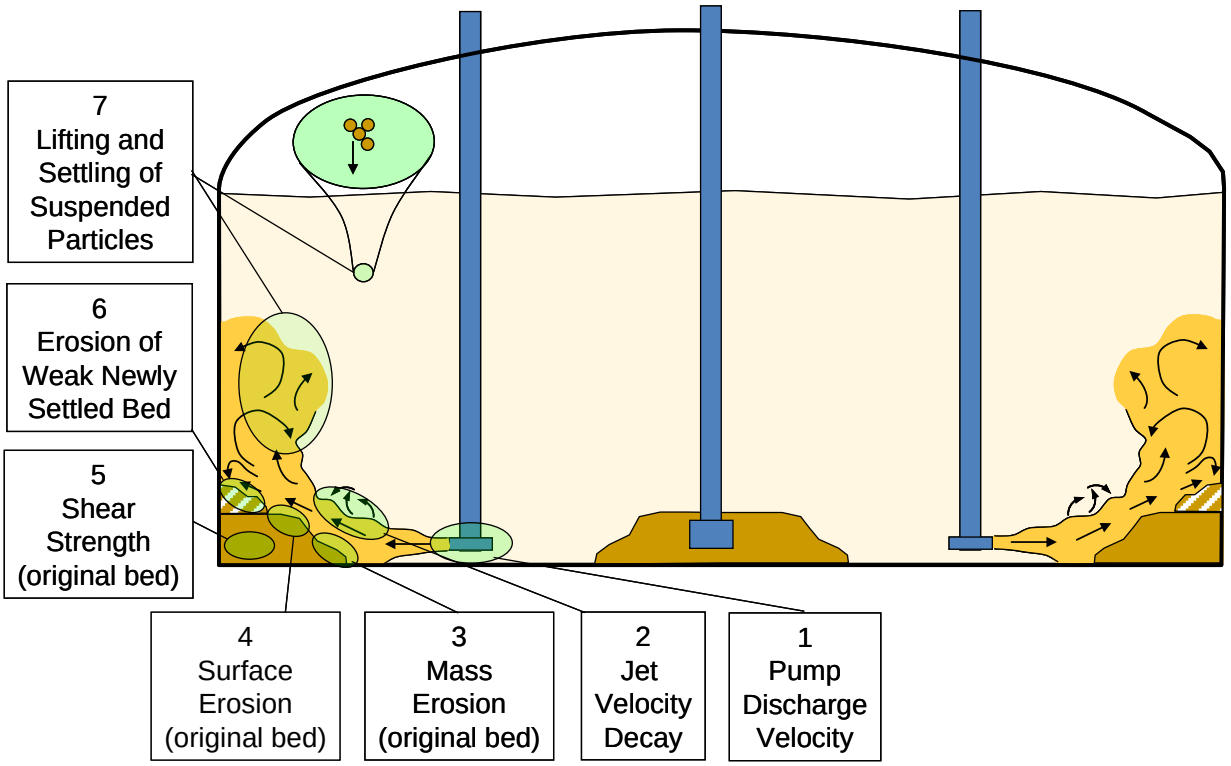

Figure 1.3. Regions of Behavior During Jet Mixing and Settling of Cohesive Slurries

Region 1 – Pump Discharge Velocity. This region is associated with the pump performance. For a specific pump, the performance is typically characterized by the manufacturer using water. How cohesive properties affect pump performance will impact jet mobilization and suspension.

Region 2 – Jet Velocity Decay. This region is associated with the decay in jet velocity downstream of the nozzle and the lateral velocity distribution. The impact of cohesive properties on the jet velocity decay will affect jet mobilization and suspension.

Region 3 – Mass Erosion. This is the region in which the jet removes large portions of the sediment material independent of particle action at the surface of the sediment. The cohesive properties of the sediment impact the extent of mass erosion.

Region 4 – Surface Erosion. This is the region in which the sediment material is eroded by the jet via the removal of individual particles from the sediment surface. The cohesive properties of the sediment impact the extent of surface erosion and the non-Newtonian rheology of the jet, which is influenced by the cohesive properties of the particles, will also affect surface erosion.

Region 5 – Shear Strength. The initial sediment will be eroded by the jet via surface or mass erosion. If the shear strength of the sediment is sufficient, erosion resistance will be increased. The sediment shear strength is a function of the cohesive properties of the material.

Region 6 – Erosion of Weak Newly Settled Bed. This region is associated with the erosion, or resuspension, of recently mobilized material that has settled to form a new sediment. As with Region 5, the cohesive properties of the material will affect the extent of erosion due to the jet.

Region 7 – Lifting and Settling of Suspended Particles. The particle lifting and settling that occur in this region are the critical behaviors affecting the overall uniformity in the mixed region. Whether or not the particles are cohesive can impact the particle lifting and settling in this region.

1.3 Overview of Previous Work Relating to Solids Mixing and Mobilization

This overview summarizes research published by the U.S. Department of Energy (DOE)'s Savannah River National Laboratory (SRNL), Pacific Northwest National Laboratory (PNNL), WTP, tank farm, etc.), industry, and university sources that demonstrate similarities and differences in mixing behavior observed between cohesive and non-cohesive particulates. This overview augments several broadly based and thorough reviews including: 1) the historical perspective regarding jet mixing at Hanford and other DOE sites by Powell et al. (1997), 2) assessments of jet mixing by Fort et al. (2007), 3) retrieval issues identified by Fellinger et al. (2009), and 4) a summary of research and tank farm operations related to mobilization, mixing, and transport across the DOE complex by Dimenna et al. (2008).

1.3.1 Savannah River Studies

Savannah River Site (SRS) activities related to mixing and mobilization including: 1) scaled testing and computational fluid dynamics (CFD) modeling of mobilization and mixing, 2) development of the advanced design mixer pump (ADMP), and 3) evaluation of Flygt mixers for solids suspension are summarized in the following subsections.

1.3.1.1 Mixer Pumps

In the late 1970s, SRNL introduced the precursor to the mixer pump concept currently in use, replacing the use of fresh water added through high-pressure (~3000 psig) nozzles to resuspend the sludge and slurry (Hill 1967). The benefits of the new system were elimination of dilution and a $1/6^{th}$ reduction in required power. The mixer pumps were used for two activities: salt dissolution and sludge mobilization and mixing (Hill and Parsons 1977).

SRS research included scaled tests with clay simulant (Bradley et al. 1977) to develop effective cleaning radius (ECR) relationships (Churnetski 1981, 1982). Horowitz (1980) conducted 1/12-scale tests to demonstrate the ability to remove residual piles of solids discovered under risers in Tank 16. Motuka (1981) conducted 1/12-scale tests to evaluate the effectiveness of mixer pumps to remove thick sludge deposits trapped between cooling coil assemblies. Poirier et al. (2003) conducted ~1/6 scale tests to evaluate resuspension of sludge and monosodium titanite slurries using a four-blade, flat-blade impeller using three scaling approaches: equal power per unit volume, equal tip speed, and equal cavern diameter.

Hamm et al. (1989) developed models for ECR and suspension rate as a function of time. Full-scale sludge suspension experiments conducted with sludge simulants (Hay and Lee 1994) using rotating mixer pumps showed that cleaning radius was determined to be less than expected. Poirier (1995) evaluated slurry pump operation in Tank 48. Poirier and Monson (1998) evaluated gas-liquid mass transfer in agitated tanks containing non-Newtonian fluids.

Full-scale demonstrations and operations included a one-pump test in Tank 16 to demonstrate using low-velocity hydraulic cleaning to slurry and transfer sludge (West 1979), tests with three mixer pumps installed in Tank 16 to determine the minimum number of pumps required to slurry all the sludge in the waste tank (Comley 1979), and removal of over 1-million gallons of radioactive waste salt from Tank 19 through dissolution (Goslen 1984). Tests of a new submersible mixer pump showed that the pump was permitting solids stratification to occur (Hansen and Williams 2005) based on particle size analysis of the kaolin/sand slurries used during the testing.

CFD studies were used to assist in tank farm operations including: code benchmarking (Lee and Dimenna 1995, 2005), recommending pump operating strategies for heel removal (Lee and Dimenna 2002, 2004, 2008; Lee 2003b, 2004), modeling transfer of liquid salt solution (Tamburello et al. 2008a, 2009), and evaluating mixing and sedimentation characteristics using transfer and recirculation pumps (Tamburello et al. 2008b). Savannah River Technology Center also used CFD to model conventional bladed mixer performance (Lee 2002).

Transport studies included evaluating the flow characteristics of simulated slurries (Carstens 1982), and pipeline plugging tests (Fazio and Ebra 1987; Motyka 1981a, b, 1983).

1.3.1.2 Advanced Design Mixer Pump Tests

SRS installed an ADMP in the center riser of Tank 18F. Enderlin et al. (2003) tested a geometrically scaled (1/4.53 of full scale) mockup of the ADMP and found that for fast settling (>1 cm/s) zeolite simulant, solids stratification occurred: the solids concentration passing through the ADMP was on the order of two to four times of that passing through the transfer pump. CFD was used to model the ADMP and modified ADMP performance (Lee and Dimenna 2001a, b).

Lee (2003a), Leishear et al. (2004), and Lee et al. (2007) used the FLUENT™ CFD code to simulate Tank 18 operations with and without a cohesive sludge mound. Sensitivity results show that higher tank level and lower elevation of pump nozzle would result in better performance in suspending and removing the sludge.

1.3.1.3 Flygt Mixers

SRS teamed with PNNL, Oak Ridge National Laboratory (ORNL), and ITT Flygt Corporation to evaluate shrouded axial propeller mixers (Flygt mixers) for heel removal (Poirier et al. 1998a, b, c, 1999) in SRS Tank 19 (Powell et al. 1999a, b, c; Poirier and Rodwell 1999) in scaled and full-scale tests. Key conclusions and recommendations (Powell et al. 1999c): scale-up of the Flygt mixers for the mixing of rapidly settling particles apparently follows a constant-power-per-unit-volume relationship over the range of tank sizes and simulant compositions tested, and sludge mobilization tests imply a correlation exists between sludge shear strength and required mixer thrust.

Lee and Dimenna (2000) developed CFD models of the FLYGT mixer using FLUENT™: a sensitivity analysis showed that pump speed, not non-uniform inlet velocity or surface roughness of the shroud inner wall, was the most sensitive parameter in terms of flow performance and pump loading.

Pacquet and Leshikar (2000) evaluated using Flygt mixer propellers for DST HLW auxiliary solids mobilization.

1.3.2 PNNL Mixer Pump Studies

Staff at PNNL conducted experimental studies to understand jet mobilization, mixing, and slurry transport, which are described in the sections below.

1.3.2.1 Sludge Mobilization Studies

At PNNL, Powell et al. (1995a, b) and Powell (1996) conducted scaled research to investigate jet mobilization. Powell et al. (1997) reviewed a wide range of ECR data and correlations from a number of studies that used cohesive sediments and concluded that the ECR scales with U_0D_0 and also depends on the shear strength of the sediment being mobilized for some but not all materials. Shekarriz et al. (1997) examined fundamental mechanisms expected during mobilization of the waste within the DSTs at Hanford to develop scaling relationships based on experiments conducted at $1/50^{th}$, $1/25^{th}$ and $1/12^{th}$ scale. They concluded that the use of the current empirical correlations for ECR should be done cautiously taking into account the appropriate properties of the material for yielding. Mahoney and Trent (1995) developed correlation models for waste tank sludge and slurries. Others also studied bank erosion (Thorne 1981) and erosion by jets (Rajaratnam 1980, 1981, 1982; Rajaratnam and Berry 1977; Rajaratnam and Beltaos 1977). In addition to mobilization, jet forces on in-tank components were studied (Allemann 1989; Bamberger 1992; Bamberger et al. 1990a, 1992, 1999c; Waters and Heimbigner 1992).

For solidified wastes, a scarifier was developed and tested (Bamberger and Steele 1993; Bamberger et al. 1993a, 1994; Hatchell et al. 1995).

1.3.2.2 Mixing and Uniformity Studies

SY-101 Studies

Fort et al. (1993) conducted 1/12-scale experiments to support hydrogen mitigation in tank SY-101. The tests included ultrasonic characterization and grab samples to quantify slurry uniformity during mixing as a function of time. Eschbach and Enderlin (1993) conducted 1/12-scale experiments to visualize the mixing interface and evaluate buoyant particle release to support hydrogen mitigation. Chang and Beaver (1993) conducted scaled mixing tests in a wedge shaped test tank. Antoniak (1993) analyzed historical trends of waste level and temperature.

In tank SY-101, *in situ* rheology and void fraction were measured by Shepard et al. (1994 a, b, 1995) and Stewart et al. (1995, 1998) to assess hydrogen generation. Full-scale tests were conducted to evaluate using pump mixing to release hydrogen (Stewart 1994; Stewart et al. 1994) and Trent and Michener (1993) used CFD to model jet mixing concepts for the tank.

1/12-Scale Uniformity Studies

A significant start toward the direct goal of predicting mixture uniformity in the DST mixer pump system began in 1990. A strategy was developed for a combined experimental and computational program (Bamberger et al. 1990a; Liljegren and Bamberger 1992) that recommended scaled testing to be conducted in 1/12- and 1/4-scale models of a 1-million-gallon DST. The 1/12-scale test plan and test results were recently published (Bamberger et al. 2007; Bamberger and Liljegren 1994; Bamberger and Meyer 2007). The 1/12-scale tests were conducted over a range of mixer pump operating conditions including 25, 50, 75, and 100% of U_0D_0 (the scaled parameter to model pump operation), thereby providing the ability to address curvature in the correlation. During these initial tests, nozzle diameter was not varied, and the test was conducted at a single, relatively small scale. In spite of these limitations, this testing was a very good start toward obtaining the information that is needed. To provide continuous monitoring of the solids concentration during these tests, ultrasonic sensors were developed (Bamberger and Greenwood 2004a, b). This instrumentation was used to provide real-time measurements of the concentration profiles obtained during the 1/12-scale tests (Bamberger and Meyer 2001). The correlation presented in the experimental results report gives the solids concentration achievable with a single mixer pump as a function of jet velocity, particle size, and liquid viscosity.

1/4-Scale Evaluation of Russian Retrieval Equipment

Enderlin et al. (1997) conducted an experimental study to evaluate the performance of a 1/4-scale model of a pump system to be used to retrieve hazardous waste.

CFD Studies

In the early 1990s, PNNL staff began developing models of mixer pump performance at Hanford (Allemann et al. 1992; Bamberger et al. 1993b). These studies included some general investigations on the difference between Newtonian and non-Newtonian fluids in mixing problems (Recknagle and Shekarriz 1998). The majority of the studies eventually focused on turbulent jet mixing in Hanford waste tanks, and a summary of the studies that are relevant to current mixing and mobilization problem are discussed below. Eyler and Michener (1992) modeled mixer pump operations for two cases: low jet velocity and high settling velocity, which produces a non-uniform distribution, and high jet velocity and low settling velocity, which produces a uniform distribution. Trent and Michener (1993) used the TEMPEST code to investigate mobilization of the SY-101 sediment using a jet mixer. TEMPEST is a time-varying three-dimensional CFD code (Onishi and Trent 1999).

TEMPEST has been validated for gas release plume studies (Meyer and Fort 1993; Eyler et al. 1983). The validation testing has included the modeling of hydrogen transport in reactor containment structures under a variety of conditions, resulting in good agreement of model results with the experimental data (Trent and Eyler 1991). Antoniak and Recknagle (1997) used TEMPEST to investigate waste tank headspace flammability following a plume-type gas release from the waste and reported reasonably good agreement with the experimental and analytical study of buoyant jets.

The TEMPEST code has been shown to reproduce literature results of jet behavior in homogeneous fluids for the jet centerline velocity for a three dimensional jet (Trent and Michener 1993). A comparison of TEMPEST predictions of jet behavior in AZ-102 with the same ideal literature results for a homogeneous jet, showed basic similarity in jet behavior, with the differences attributed to jet rotation,

differences in the jet density and rheology relative to the surrounding sediment and supernatant (all of which may very temporally and spatially), the jet penetration being impacted by the non-erodible portion of the sediment, interaction between the jet and the tank bottom and walls, and interaction of the jet with tank internals such as ALCs and heating coils (Onishi et al. 2000).

TEMPEST has been used to investigate numerous aspects of Hanford waste retrieval including:

- mobilization and mixing of sediment in SY-102 (Onishi et al. 1996)
- concentration of plutonium in the pump housings in AZ-101 during sediment mobilization and mixing (Onishi and Recknagle 1997b)
- adequacy of a single mixer pump to fully mix wastes in AP-102 and AP-104 (Onishi and Recknagle 1998)
- ability of a densitometer in AY-102 to represent the mass of solids transferred during retrieval of C-106 (Onishi and Recknagle 1999)
- mobilization and mixing of sediment in AZ-102 (Onishi et al. 2000)
- mobilization and mixing of sediment in AN-105 after transfer and dilution (Onishi et al. 2003a)
- feasibility of a single mixer pump to adequately mobilize and mix AN-101 (Onishi et al. 2003b)
- liquid waste mixing of S-112 and SY-101 (Onishi et al. 2003c)
- feasibility of a single mixer pump to adequately mobilize and mix AY-102 (Onishi and Wells 2004).

These TEMPEST simulations include undissolved solids (UDS) concentration and strain rate-driven rheological models for the waste, and usually used a narrow distribution of particle size at a single bulk UDS density. The predictions typically showed that the suspended UDS was uniformly distributed. When size and density distributed UDS were considered, stratification was observed. An undocumented scoping comparison of TEMPEST ECR results for AZ-101 to the full-scale AZ-101 results (Carlson et al. 2001) showed that TEMPEST produced a reasonable range of ECR results.

TEMPEST has also been used for thermal modeling of Hanford tanks AW-101 and AN-104 (Antoniak and Recknagle 1995). Additionally, TEMPEST has been combined with a thermodynamic chemical code to provide chemically reacting, time-varying, three-dimensional CFD predictions for non-Newtonian slurries and sediment with a shear strength (Onishi et al. 2001a, b; Onishi and Wells 2001).

Slurry Characterization

PNNL staff and collaborators developed and deployed ultrasonic methods to provide *in situ*, real-time measurement of slurry properties (Atkinson and Kytomaa 1991, 1992; Bamberger et al. 1998b, c, 1999b; Bamberger and Greenwood 2002, 2003, 2004a, b, c; Greenwood et al. 1993; Greenwood and Bamberger 2002; Kytomaa 1993; Kytomaa and Corrington 1994; Shekarriz et al. 1998; Shekarriz and Sheen 1998). In addition, a pipeline probe was developed and demonstrated in SY-101 transfer piping to measure density of slurries during retrieval (Bamberger and Greenwood 2000, 2001; Witwer et al. 2001).

1.3.2.3 Pipeline Transport

In pipeline transport, particles can settle and form layers depending on the particles and velocity. This phenomenon has similarity to the focus of this report, which is mobilizing and suspending particles in DSTs with turbulent jets, so some pertinent literature is discussed. Shekarriz et al. (1997b) summarized results of a technical panel review of the methodology for accepting waste for transport through the Hanford Replacement Cross-Site Transfer System, which was constructed to replace the existing pipelines that hydraulically connect the 200 West and 200 East Areas. Poloski et al. (2009a, b) conducted transport studies to determine deposition velocities for non-Newtonian and Newtonian slurries in pipelines to support Waste Treatment Plant operations. Earlier investigations related to Hanford were conducted by Bamberger and Liljegren (1993), Estey (1998), Eyler and Lombardo (1980), Eyler et al. (1982), and McKay et al. (1994). Of the large literature on pipeline transport, the studies by Hanks (1987) and Doron and Barnea (1993, 1995, 1996) where they developed transport models and flow maps are particularly useful.

1.3.3 PNNL Pulse Jet Mixer Studies

Pulse jet mixers (PJMs) are being used in the WTP vessels to maintain slurries in suspension. PJMs are non-steady jet mixing devices that use compressed air as the motive force. PJMs, installed inside the vessel, differ from mixers that sustain a steady jet to provide mixing. Downward-facing jets are formed by alternating pressure and suction on fluid in vertically oriented pulse tubes coupled with jet nozzles, creating a pulsating flow. The nozzle end of the tube is immersed in the tank with the nozzle facing the vessel floor. Periodic pressure, vacuum, and venting are supplied to the opposite end to initiate pulsed jets. In the right conditions, multiple pulse tubes, operating either in parallel or in sequence, can be used to effectively provide mixing in liquid/solid systems. The pulse tubes are oriented in rings one or two radii from the tank center. The PJMs are distributed uniformly around the vessel circumference (Meyer et al. 2009).

Mixing requirements for the WTP are described in Olsen (2008a, b). Meyer et al. (2009) conducted pulse jet mixing tests at three vessel scales (small – 15-in.-diameter, mid – 34-in.-diameter, and large – 70-in.-diameter) with noncohesive solids to develop correlations to predict two measures of mixing performance in full-scale vessels: cloud height, H_C, (the height to which solids will be lifted by the PJM action) and critical suspension velocity, U_{CS}, (the minimum velocity needed to ensure that all solids are suspended off the floor, though not fully mixed). Prior to the scaled tests described in Meyer et al. (2009), PNNL conducted tests to demonstrate the ability to mix in a small-scale PJM test facility (Johnson et al. 2003), and scaling relationships were proposed by Bamberger and Meyer (2007).

Additionally, PNNL staff have conducted significant experimental and analytical studies investigating PJM performance for mixing non-Newtonian slurries (Bamberger et al. 2005; Johnson et al. 2005; Meyer et al. 2005, 2006; Kurath et al. 2007; Meyer and Etchells 2007; Bamberger et al. 2008) and conducted tests with neutralized current acid waste simulant (Bontha et al. 2000). The work with non-Newtonian slurries was expanded to determine the technical basis for scaling air sparging systems for mixing non-Newtonian slurries (Poloski et al. 2005; Guerrero and Restivo 2004). Experiments have been conducted to evaluate the performance of specific vessels, including the ultrafiltration feed process (UFP) and HLW lag storage (LS) vessels (Bates et al. 2003). These studies were expanded to define the technical bases for

predicting mixing and flammable gas behavior in the UFP and LS vessels (Bontha et al. 2005). PJM controller and instrumentation performance were also evaluated (Bontha et al. 2007). CFD studies of PJM operation include Bontha et al. (2003a, b).

1.3.4 Hanford Tank Operations

Centrifugal jet mixer pumps have been used in three Hanford tanks: AZ-101 (baseline configuration mixer pump test, Carlson et al. [2001]), SY-101 (mitigation of sediment gas retention, e.g., Allemann et al. 1994, Stewart et al. 1994), and AP-102 (mixing efficiency, Hunter 1988). An evaluation of the data from these mixer pump operations in terms of sediment mobilization and solids uniformity and the role of cohesive particle interactions is discussed in Section 4. A brief summary of these tests is given below.

The 241-AP-102 in-tank mixer operability test (October 19, 1987–February 12, 1988) verified the functional operation of the in-tank mixer (Hunter 1988). The performance was analyzed based upon suspension of solids and mixing with respect to liquids. The following criteria were used to determine mixing time: tank contents would be mixed when vertical and radial variabilities were not significantly larger than the sampling and analytical variabilities for two consecutive time periods and constituent averages were sufficiently close to theoretical values. Based on these criteria, the contents of 241-AP-102 were mixed with respect to dye tracer within 9 hours. A second liquid component used in a much larger volume than the dye tracer was distributed within 30 minutes. Also, approximately 10% of solids were evenly suspended after 12 hours of mixing.

CFD modeling was used to make recommendations for retrieval of tank 241-SY-102 (Onishi and Hudson 1996; Onishi et al. 1996) and assess the criticality issue in tank 241-AZ-101(Onishi and Recknagle 1997b).

Tests were conducted in tank 241-AZ-101 using two 300-hp mixer pumps to provide baseline mixer pump operational data (Carlson et al. 2000, 2001; Douglas 2000; MacLean 2000; Staehr 1999; Templeton 2000). These tests are described in Section 4.1.2.3.

Most recently, Adamson et al. (2009b) conducted a small-scale demonstration of simulated waste transfers from Tank AY-102.

1.3.5 Oak Ridge Studies

Studies were conducted to support waste mobilization, mixing, and transport at ORNL. Characterization studies were conducted by Giaquinto et al. (1997), Keller et al. (1996, 1997a, b), and Sears et al. (1995). Mobilization focused on the Melton Valley Storage Tanks (MVST) (Hylton et al. 1994, 1995; Shor and Cummins 1991; Ceo et al. 1990), Gunite Tanks (Ehrlich and Weeren 1979; Weeren 1984; Rule et al. 1998) and a design for a waste handling and packaging plant (Shor et al. 1990). Bamberger et al. (1998a, 1999a, b) developed the borehole miner for removal of wastes at the old hydrofracture (OHF) tanks (Francis and Herbes 1997; Keller et al. 1997b). Perona et al. (1994) studied jet mixing in the horizontal storage tanks at ORNL. Kent et al. (1998) demonstrated using PJMs for use in the horizontal storage tanks.

Eyler et al. (1993) and Terrones and Eyler (1993) investigated using submerged liquid jets to mobilize and mix non-Newtonian sludge in horizontal, cylindrical, waste storage tanks (similar to the

ORNL Melton Valley Storage Tanks) using the modified time-dependent, finite-volume TEMPEST computer program. The sludge was covered by a layer of particle-free supernatant. Rheology of the sludge exhibits a power law character; non-linearity was considered because dilution occurred during mixing. Mahoney et al. (1994) and Eyler and Mahoney (1995) modeled mobilization and mixing in the horizontal storage tanks.

Dahl et al. (1999) investigated transfers from the C Tanks. Youngblood et al. (1991) investigated transport of radioactive sludges at ORNL.

1.3.6 West Valley Studies

Schiffhauer et al. (1985) documented waste removal activities at West Valley. Schiffhauer and Inzana (1987) used a 1/16-scale model to develop the design for the West Valley mobilization system. The mobilization system consisted of five mixer pumps installed in strategic locations within the tank. The scale-model system was also used to identify the design basis for the zeolite retrieval equipment, which is part of the Supernatant Treatment System. McMahon (1990) descried the design of the sludge mobilization system. Fow et al. (1989) evaluated the mixing system for the West Valley melter feed hold tank.

1.3.7 Idaho Studies

Bamberger et al. (2001) reviewed retrieval and closure plans at the Idaho National Engineering and Environmental Laboratory INTEC tank farm facility. Meyer (1994) modeled jet mixing for the INEL waste tanks. Stanisch et al. (1991) developed sampling and analysis plans for several site liquid waste tanks.

1.4 Overall Objectives and Approach for the Tank Mixing and Sampling Demonstration Program

The overall objective of the Tank Mixing and Sampling Demonstration Program is to determine the mixing effectiveness of the current baseline mixing system that uses two jet mixer pumps to mix and mobilize waste in DSTs and to determine the adequacy of the planned sampling method (Townson 2009). The approach to meeting this objective is to combine scaled testing with modeling to estimate full-scale behavior, with an initial emphasis on the feed delivery tank AY-102, and then conduct a full-scale test in AY-102. The combination of the results from the scaled testing, modeling, and full-scale test should significantly mitigate the technical risk associated with the mixing and sampling systems meeting the feed certification requirements for transferring waste to the WTP.

The initial phase of the demonstration program is to conduct scaled tests that appropriately match full-scale behavior of waste mixing in AY-102 and to evaluate sampling methodologies and the composition of individual batch transfers. For the actual feed delivery to the WTP, the design basis assumes each staged HLW feed tank is homogenously mixed and feed is delivered in 160,000-gallon batches that have nearly equal chemical composition and UDS content (Townson 2009). The scaled tests will be conducted in two geometrically scaled vessels of different size using test conditions that will allow estimates of full-scale performance to be extrapolated from the small-scale test results. The small-scale test platforms will include 1/21 and 1/7.5 vessels (42.5- and 120-in. vessels in comparison to the 75-ft-

diameter full-scale DST), and all tank internals, pumps and associated systems will be scaled prototypically where possible (Townson 2009). The initial scaled testing will use non-cohesive particles.

As discussed previously in this section, the purpose of this report is to evaluate whether these scaled mixing tests need to include cohesive simulants to meet both the overall objectives of the program and the specific focus of estimating the full-scale behavior of sampling and batch transfers from tank AY-102. Slurries of non-cohesive or cohesive particles may behave differently, although for sufficiently dilute systems, many slurries will behave as Newtonian fluids and cohesive interactions may be negligible (Gauglitz et al. 2009). The Interface Control Document for Waste Feed (ICD-19 2008) gives an upper limit of 200 g/L (~ 16 wt% UDS) for total (unwashed) solids in feed delivery batches, and the average concentration in many feed delivery tanks will be well below this limit (for example, Table 3.6 in this report gives UDS concentrations of 10 wt% for AY-102 and 4 wt% for AZ-101 if these tanks are perfectly homogenized). Actual waste is known to have a wide range of behavior, and the solids loading will also vary depending on the tank and the specific mixing conditions. In the following section, we discuss how slurry rheology changes due to cohesive particle interactions and through changes in the UDS concentration because a change in rheology is the key element of how cohesive interactions affect mixing effectiveness.

2.0 Cohesive Effects on Rheology

The flow behavior of a fluid or slurry is typically described as its rheology. For a general discussion of suspension rheology, see Russel et al. (1989) or Poloski et al. (2007). For the simplest case of a Newtonian fluid, the viscosity is a constant that does not depend on the shear rate or how the shear rate has changed over time (memory effects). The viscosity of a Newtonian fluid or slurry may, however, depend on a number of parameters other than shear rate such as fluid temperature and composition and the concentration of suspended particles. There are a number of different non-Newtonian fluid behaviors, and some general descriptions will be used in this discussion of how cohesive particle interactions affect mixing. One way to compare differences in fluid rheology is to make the comparisons in terms of viscosity. When the viscosity of a fluid decreases with increasing shear rate, the fluid is shear thinning and non-Newtonian. The magnitude of the shear rate dependence can be small (weakly non-Newtonian) or large. One example of a strongly shear-thinning fluid is a fluid that is described by a Bingham model and has a yield stress, which we will refer to here as a non-Newtonian yield-stress fluid. In the mixing and mobilization problem being addressed in this report, the shear rate varies from extremely high in the jet pump and jet as it exits the nozzle to negligibly small in regions away from the influence of the jet and at the walls of the tank. For any strongly shear-thinning fluid, there will be a large variation in fluid viscosity, and hence local mixing behavior as a result of the variation in shear rate.

The rheology and viscosity of a slurry of particles depends on a number of factors, including the magnitude of inter-particle cohesive forces and the particle concentration. The particle shape and size also play significant roles, but for the discussion here we will focus on the magnitude of cohesive forces and concentration. Figure 2.1 depicts the general ranges of behavior for slurries. At lower concentrations and for weaker interparticle forces, the slurry will be Newtonian. If the particles are non-cohesive but at a higher concentration, the slurry will be weakly non-Newtonian with an elevated viscosity. If the particles are cohesive but the suspension is dilute, the slurry will again be weakly non-Newtonian. The most dramatic effect on slurry rheology occurs when the slurry is concentrated and the particles are cohesive. In the remainder of this section, data on slurry rheology are presented that demonstrate this general behavior for simulants and actual waste.

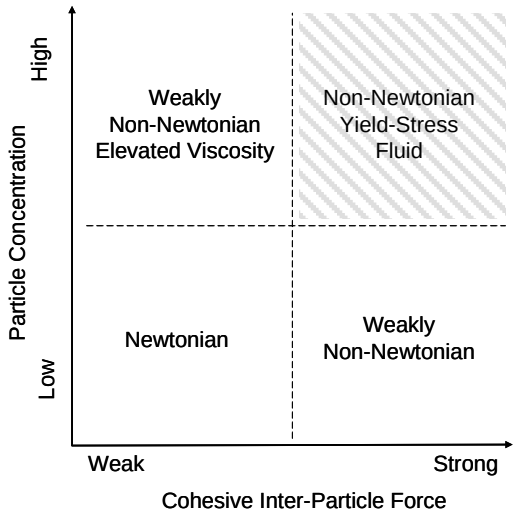

Figure 2.1. Qualitative Role of Particle Concentration and Magnitude of Cohesive Particle Interactions on Slurry Rheology

2.1 Role of Cohesive Particle Interactions on Slurry Rheology

There are extensive studies in the literature on the rheology of non-cohesive slurries (see Russel et al. (1989) or Poloski et al. (2007) for a general discussion). Figure 2.2 shows the effect of particle concentration on the viscosity of suspensions of non-cohesive particles (Russel et al. 1989, see Figure 14.4). The upper curve in Figure 2.2 is the suspension viscosity in the limit of low shear rate, and the lower curve is the viscosity in the limit of high shear rate. The particle concentration is given in terms of the volume fraction of solids. For typical waste slurries, the volume fraction of solids is about half the weight fraction of undissolved solids (UDS) (Gauglitz et al. 2009), so even a very concentrated waste slurry of 40 wt% UDS will only be about 20% solids by volume. The typical range for tank waste slurries, including the example of a very concentrated slurry, is highlighted in the figure. Figure 2.2 shows that at 0.2 (20%) solids volume fraction there is very little difference between the low and high shear rate viscosities, so this slurry is at most very weakly non-Newtonian. The slurry viscosity is elevated in comparison to the liquid suspending particles by about a factor of two. In summary, this result shows that suspensions of non-cohesive particles will typically have an elevated viscosity and be nearly Newtonian.

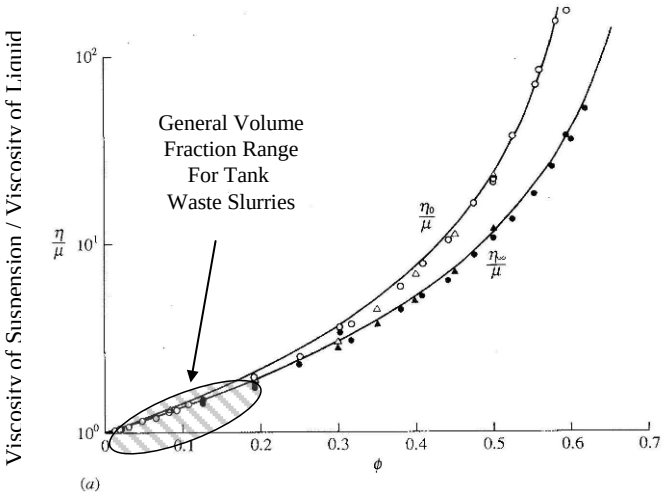

Figure 2.2. Effect of Particle Concentration on Suspension Viscosity and Shear Thinning Behavior for Non-Cohesive Particles

There are very few specific examples in the literature that demonstrate the specific role of cohesive particle interactions on suspension rheology, but the behavior of kaolin clay suspensions provides one example. Litzenberger (2003) has shown that slurries of cohesive kaolin particles can be changed into slurries of non-cohesive particles by the addition of the dispersant tetra sodium pyrophosphate (TSPP). In these slurries, the TSPP adsorbs on the clay particles, making all surfaces strongly negatively charged and the particles all repulsive and non-cohesive. Litzenberger (2003) also showed that the apparent viscosity of kaolin slurries decreases dramatically with the addition of TSPP.

In a recent study, Poloski et al. (2009b) varied the concentration of kaolin clay and TSPP in simulants to adjust the rheology of the slurries. Some preliminary scoping studies were done where TSPP was

added to a kaolin slurry that had a Bingham yield stress of about 45 Pa.[1] Figure 2.3 shows the viscosity of the kaolin clay suspension decreased dramatically with the addition of small amounts of the dispersant TSPP. Without TSPP, the kaolin slurry was strongly shear thinning, or non-Newtonian, and was much more viscous that the water used in the suspension. For the highest concentrations of TSPP, the kaolin slurry had a viscosity of about 4 cP, or 4 times higher than water and the viscosity was essentially independent of the shear rate. With this behavior, this slurry would be described as a Newtonian fluid.

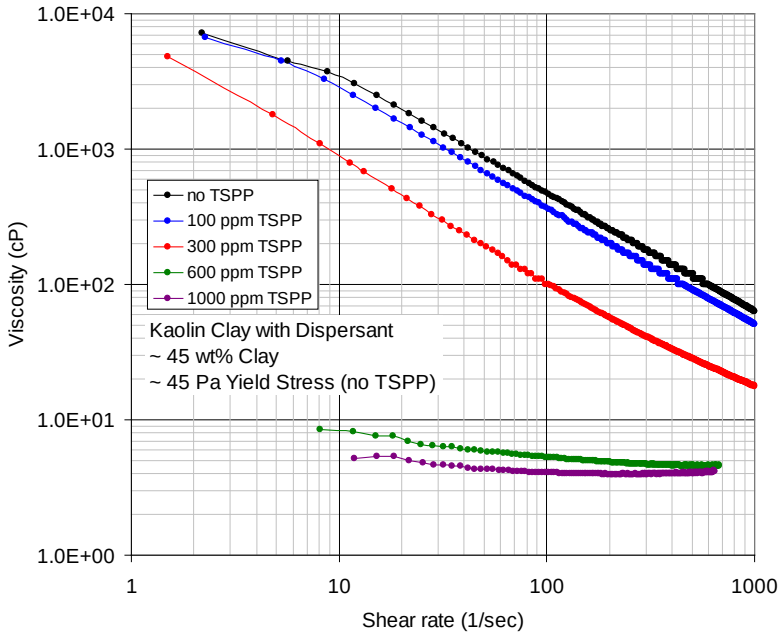

Figure 2.3. Reduction in Suspension Viscosity due to Reducing Particle Cohesive Interactions in Kaolin Slurries by Adding the Dispersant Tetra Sodium Pyrophosphate (TSPP). The Kaolin Slurry had a Bingham Yield Stress of about 45 Pa.

In terms of understanding the role of cohesive particle interaction, these data show that a moderately concentrated suspension of non-cohesive particles again behaves as Newtonian fluids in terms of viscous behavior. When cohesive particle interactions are present, this same slurry can become strongly non-Newtonian (a shear thinning yield stress fluid) with a significant yield stress and a viscosity that is much higher than water unless the shear rate is very high.

Figure 2.4 gives an actual waste example demonstrating the important behavior of a slurry becoming more non-Newtonian as the undissolved solids concentration increases. In Figure 2.4, the data show the apparent viscosity of AZ-102 waste (Warrant 2001) becoming more shear thinning and increasing with increasing UDS concentration.[2] At 32 wt% UDS, the slurry is strongly shear thinning and non-Newtonian over the entire range of shear rates reported, while the 3 wt% slurry has a much smaller change in viscosity between shear rates of 100 to 1000 s^{-1}. In the remainder of this report where we

[1] The results of this specific test were not reported in Poloski et al. (2009), but the test used the materials described in Poloski et al. (2009).

[2] Reported wt% UDS taken from PNNL Letter Report to CH2M HILL: Wells BE. 2004. *Evaluation of Waste Data for Rheological Models Used in Waste Pipeline Transfer Assessment*. TWS05.001, Pacific Northwest National Laboratory, Richland, Washington.

evaluate mixing behavior of slurries, particular emphasis will be place on studies that show the role of a yield stress or viscosity increases because these changes represent the key change due to the presence of cohesive particle interactions.

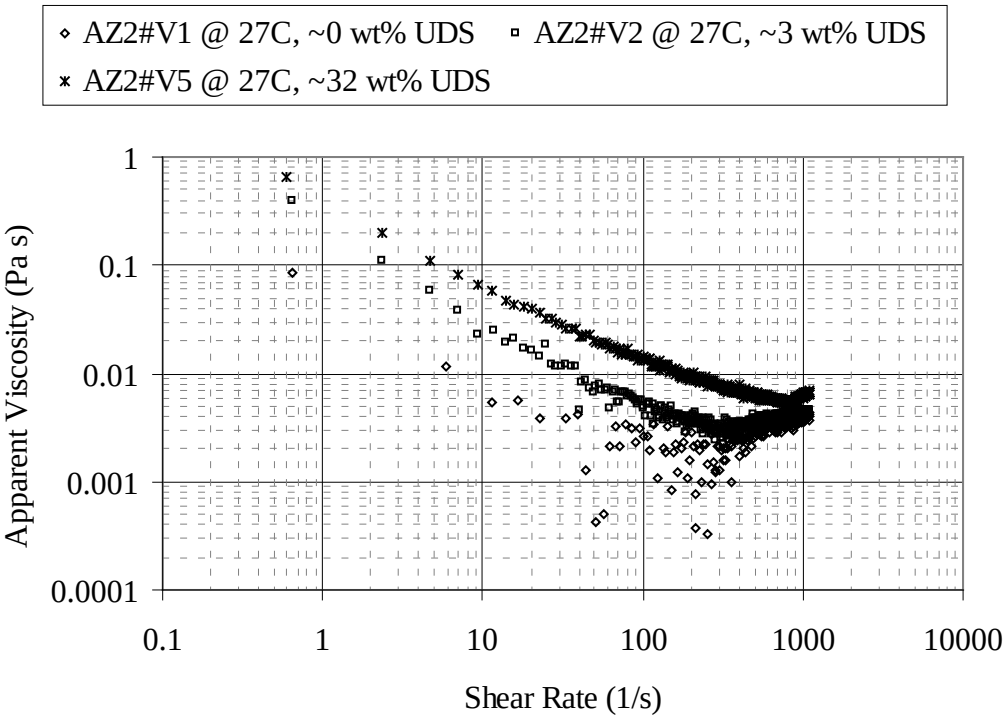

Figure 2.4. AZ-102 Slurry Apparent Viscosity as a Function of UDS Concentration. Data from Warrant (2001).

3.0 WTP High-level Waste Feed Staging Tank Properties

Hanford DSTs will be used as feed staging tanks for the WTP. Although subject to alteration as the Waste Feed Delivery Plan is optimized, 17 DSTs are identified as HLW feed tanks and include AN, AZ, AY, AW, and AP farm tanks (Greenwell 2009). Specific tanks may include AN-101, AN-106, AZ-101, AZ-012, AY-101, AY-102, AW-101 through AW-106, AP-101 through AP-104, and AP-108. The current waste content of the WTP HLW feed tank, AY-102, will be the commissioning feed. Thus, the waste properties pertinent to cohesive behavior for AY-102 are presented. Although not in a feed configuration, waste properties for AZ-101, in which the baseline feed delivery pumps were operated, are also presented. Given the breadth and changing nature of retrieval scenarios, the feed staging tanks as a whole are considered based on the measured properties of the HLW tanks (i.e., those tanks with the UDS that primarily comprise insoluble solids and are commonly referred to as sludge tanks, e.g., Weber 2008).

Waste properties pertinent to cohesive behavior include the particle size and shape and UDS concentration. The particle size and density distribution (PSDD) data are presented in Section 3.1 together with a brief discussion of the particle settling rate data. Particle shapes for the Hanford sludge have not been quantified per se, but particle shape may be observed to be unique and varied with the solid phase compound (e.g., Wells et al. 2007). Thus, shape may be inferred from the chemical solid phase composition, which is reflected in the density of the particulate.

The solid concentration in Hanford settled layers (sediment) is presented in Section 3.2, and the solid concentration for fully or partially mixed conditions in the feed staging tanks is discussed. These solid concentrations may be related to the probability of cohesive behavior of HLW in the feed staging tanks as presented in Section 3.3.

3.1 High-level Waste Undissolved Solids Properties

PSDDs for AY-102, AZ-101 and Hanford sludge are presented in Section 3.1.1. Settling rate data for this particulate is briefly discussed in Section 3.1.2.

3.1.1 Particle Size and Density Distribution

Solid particulate can be characterized by a PSDD. The PSDDs for AY-102 and AZ-101 from Wells and Ressler (2009) developed from the Case 3 approach of Wells et al. (2007) are provided in Table 3.1 and Table 3.2, respectively. The Case 3 PSDD approach is recommended by WTP project memorandum CCN 186332, from AW Etchells, Dupont Technology Consulting, to SA Saunders, Bechtel National, Inc., on January 29, 2007, “Comments on the Input Particle Size Report,” as “...the most accurate and most conservative” approach.

Table 3.1. AY-102 PSDD (Wells and Ressler 2009)

	Solid Phase Compounds and Density (g/mL)										
	Fe_2O_3	$Al(OH)_3$	$Ca_5OH(PO_4)_3$	MnO_2	$Ni(OH)_2$	$Na_2U_2O_7$	$LaPO_4 \cdot 2H_2O$	Bi_2O_3	Ag_2CO_3	ZrO_2	PuO_2
	5.24	2.42	3.14	5.026	4.1	5.617	6.51	8.9	6.077	5.68	11.43
Particle Size (μm)	Solid Volume Fraction										
0.22	3.4E-05	5.3E-05	5.3E-06	5.2E-06	1.2E-06	1.0E-06	4.8E-07	2.4E-08	8.6E-09	6.5E-09	3.9E-09
0.28	4.6E-04	7.1E-04	7.2E-05	7.0E-05	1.6E-05	1.4E-05	6.5E-06	3.3E-07	1.2E-07	8.8E-08	5.3E-08
0.36	6.5E-04	1.0E-03	1.0E-04	1.0E-04	2.2E-05	2.0E-05	9.2E-06	4.7E-07	1.7E-07	1.2E-07	7.5E-08
0.46	6.6E-04	1.0E-03	1.0E-04	1.0E-04	2.3E-05	2.0E-05	9.3E-06	4.7E-07	1.7E-07	1.3E-07	7.6E-08
0.6	9.5E-04	1.5E-03	1.5E-04	1.5E-04	3.3E-05	2.8E-05	1.3E-05	6.8E-07	2.4E-07	1.8E-07	1.1E-07
0.77	5.6E-03	8.7E-03	8.7E-04	8.6E-04	1.9E-04	1.7E-04	7.9E-05	4.0E-06	1.4E-06	1.1E-06	6.5E-07
1	2.3E-02	3.5E-02	3.5E-03	3.4E-03	7.7E-04	6.7E-04	3.2E-04	1.6E-05	5.7E-06	4.3E-06	2.6E-06
1.29	3.7E-02	5.7E-02	5.7E-03	5.6E-03	1.3E-03	1.1E-03	5.2E-04	2.6E-05	9.3E-06	7.0E-06	4.2E-06
1.67	3.4E-02	5.2E-02	5.2E-03	5.1E-03	1.2E-03	1.0E-03	4.7E-04	2.4E-05	8.5E-06	6.4E-06	3.9E-06
2.15	3.0E-02	4.7E-02	4.8E-03	4.6E-03	1.0E-03	9.1E-04	4.3E-04	2.2E-05	7.7E-06	5.8E-06	3.5E-06
2.78	3.1E-02	4.9E-02	4.9E-03	4.8E-03	1.1E-03	9.4E-04	4.4E-04	2.3E-05	7.9E-06	6.0E-06	3.6E-06
3.59	2.8E-02	4.4E-02	4.4E-03	4.3E-03	9.6E-04	8.4E-04	4.0E-04	2.0E-05	7.1E-06	5.4E-06	3.2E-06
4.64	2.7E-02	4.2E-02	4.3E-03	4.2E-03	9.4E-04	8.2E-04	3.8E-04	2.0E-05	6.9E-06	5.2E-06	3.1E-06
5.99	2.5E-02	3.8E-02	3.8E-03	3.8E-03	8.5E-04	7.4E-04	3.5E-04	1.8E-05	6.2E-06	4.7E-06	2.8E-06
7.74	2.0E-02	3.2E-02	3.2E-03	3.1E-03	7.0E-04	6.1E-04	2.9E-04	1.5E-05	5.2E-06	3.9E-06	2.4E-06
10	1.7E-02	2.6E-02	2.6E-03	2.6E-03	5.7E-04	5.0E-04	2.4E-04	1.2E-05	4.2E-06	3.2E-06	1.9E-06
12.92	1.6E-02	2.5E-02	2.5E-03	2.5E-03	5.5E-04	4.8E-04	2.3E-04	1.2E-05	4.1E-06	3.1E-06	1.9E-06
16.68	1.5E-02	2.3E-02	2.3E-03	2.3E-03	5.2E-04	4.5E-04	2.1E-04	1.1E-05	3.8E-06	2.9E-06	1.7E-06
21.54	6.4E-03	1.0E-02	1.0E-03	9.8E-04	2.2E-04	1.9E-04	9.1E-05	4.6E-06	1.6E-06	1.2E-06	7.4E-07
27.83	2.0E-03	3.1E-03	3.1E-04	3.0E-04	6.8E-05	5.9E-05	2.8E-05	1.4E-06	5.0E-07	3.8E-07	2.3E-07
35.94	1.1E-03	1.8E-03	1.8E-04	1.7E-04	3.9E-05	3.4E-05	1.6E-05	8.1E-07	2.9E-07	2.2E-07	1.3E-07
46.42	1.4E-03	2.2E-03	2.3E-04	2.2E-04	5.0E-05	4.3E-05	2.0E-05	1.0E-06	3.6E-07	2.8E-07	1.7E-07
59.95	1.7E-03	2.7E-03	2.7E-04	2.6E-04	5.9E-05	5.2E-05	2.4E-05	1.2E-06	4.4E-07	3.3E-07	2.0E-07
77.43	2.3E-03	3.6E-03	3.6E-04	3.6E-04	8.0E-05	7.0E-05	3.3E-05	1.7E-06	5.9E-07	4.4E-07	2.7E-07
100	3.2E-03	5.0E-03	5.0E-04	4.9E-04	1.1E-04	9.5E-05	4.5E-05	2.3E-06	8.0E-07	6.1E-07	3.7E-07
129.15	4.1E-03	6.4E-03	6.4E-04	6.3E-04	1.4E-04	1.2E-04	5.8E-05	3.0E-06	1.0E-06	7.9E-07	4.8E-07
166.81	3.1E-03	4.8E-03	4.8E-04	4.7E-04	1.1E-04	9.2E-05	4.3E-05	2.2E-06	7.8E-07	5.9E-07	3.5E-07
215.44	2.6E-03	4.1E-03	4.1E-04	4.0E-04	8.9E-05	7.8E-05	3.7E-05	1.9E-06	6.6E-07	5.0E-07	3.0E-07
278.26	2.1E-04	3.3E-04	3.3E-05	3.2E-05	7.3E-06	6.4E-06	3.0E-06	1.5E-07	5.4E-08	4.1E-08	2.4E-08
Total Solid-Phase Volume Fraction	0.34	0.53	0.053	0.052	0.012	0.010	0.005	0.0002	0.00009	0.00006	0.00004

Table 3.2. AZ-101 PSDD (Wells and Ressler 2009)

Particle Size (μm)	Solid Phase Compounds and Density (g/mL)								
	$Al(OH)_3$	Fe_2O_3	ZrO_2	$Ca_5OH(PO_4)_3$	$Ni(OH)_2$	$Na_2U_2O_7$	MnO_2	$LaPO_4•2H_2O$	PuO_2
	2.42	5.24	5.68	3.14	4.1	5.617	5.026	6.51	11.43
	Solid Volume Fraction								
0.22	3.8E-04	7.7E-05	2.4E-05	6.9E-06	6.7E-06	4.9E-06	1.1E-06	3.7E-06	2.5E-08
0.28	9.1E-03	1.9E-03	5.7E-04	1.7E-04	1.6E-04	1.2E-04	2.7E-05	9.0E-05	6.0E-07
0.36	1.0E-02	2.1E-03	6.4E-04	1.9E-04	1.8E-04	1.3E-04	3.1E-05	1.0E-04	6.8E-07
0.46	1.3E-02	2.7E-03	8.4E-04	2.5E-04	2.4E-04	1.7E-04	4.0E-05	1.3E-04	8.8E-07
0.60	1.8E-02	3.6E-03	1.1E-03	3.2E-04	3.1E-04	2.3E-04	5.3E-05	1.7E-04	1.2E-06
0.77	2.2E-02	4.5E-03	1.4E-03	4.0E-04	3.9E-04	2.9E-04	6.5E-05	2.2E-04	1.4E-06
1.00	5.4E-02	1.1E-02	3.4E-03	9.9E-04	9.6E-04	7.0E-04	1.6E-04	5.3E-04	3.6E-06
1.29	5.1E-02	1.0E-02	3.2E-03	9.3E-04	9.0E-04	6.6E-04	1.5E-04	5.0E-04	3.4E-06
1.67	4.6E-02	9.4E-03	2.9E-03	8.5E-04	8.2E-04	6.0E-04	1.4E-04	4.6E-04	3.0E-06
2.15	6.1E-02	1.2E-02	3.8E-03	1.1E-03	1.1E-03	7.9E-04	1.8E-04	6.0E-04	4.0E-06
2.78	5.6E-02	1.1E-02	3.5E-03	1.0E-03	1.0E-03	7.3E-04	1.7E-04	5.6E-04	3.7E-06
3.59	6.0E-02	1.2E-02	3.8E-03	1.1E-03	1.1E-03	7.9E-04	1.8E-04	6.0E-04	4.0E-06
4.64	6.8E-02	1.4E-02	4.3E-03	1.3E-03	1.2E-03	8.9E-04	2.0E-04	6.8E-04	4.5E-06
5.99	6.2E-02	1.3E-02	3.9E-03	1.1E-03	1.1E-03	8.1E-04	1.8E-04	6.1E-04	4.1E-06
7.74	6.3E-02	1.3E-02	4.0E-03	1.2E-03	1.1E-03	8.3E-04	1.9E-04	6.3E-04	4.2E-06
10.00	3.6E-02	7.3E-03	2.2E-03	6.6E-04	6.3E-04	4.7E-04	1.1E-04	3.5E-04	2.4E-06
12.92	3.5E-02	7.2E-03	2.2E-03	6.5E-04	6.2E-04	4.6E-04	1.0E-04	3.5E-04	2.3E-06
16.68	3.2E-02	6.6E-03	2.0E-03	6.0E-04	5.8E-04	4.2E-04	9.7E-05	3.2E-04	2.1E-06
21.54	2.8E-02	5.7E-03	1.8E-03	5.2E-04	5.0E-04	3.7E-04	8.4E-05	2.8E-04	1.8E-06
27.83	2.3E-02	4.7E-03	1.5E-03	4.3E-04	4.1E-04	3.0E-04	6.9E-05	2.3E-04	1.5E-06
35.94	4.7E-03	9.5E-04	2.9E-04	8.6E-05	8.3E-05	6.1E-05	1.4E-05	4.6E-05	3.1E-07
Total Solid-Phase Volume Fraction	0.75	0.15	0.047	0.014	0.013	0.010	0.002	0.007	0.00005

The Case 3 approach assigns the primary particulate density of the solid phase compounds (i.e., crystal density) to the particulate, independent of particle size. As such, it does not account for solids particle density reduction (by agglomeration) below the primary crystal density. As discussed in Wells et al. (2007), this approach does not represent the actual phenomenon of Hanford particulate agglomeration, but it was selected because it provides an upper-bound for possible particle size and density, and it removes the significant uncertainty of quantifying the fractal dimension relating the agglomeration size and density. PSDDs developed using this approach are thus representations of the UDS particulate.

The PSDDs in Table 3.1 and Table 3.2 are three-dimensional matrices of the volume-based probability of each solid-phase compound in a particle-size distribution "bin" and its density in that bin. The PSDD bins represent the upper and lower size limit of the particles in each bin. For example, in Table 3.2 for AY-102, it can be seen that gibbsite [Al(OH)3] comprises 75% of the solids particulate by volume, and gibbsite particles >7.74 μm and ≤ 10 μm have a density of 2.42 g/mL and make up 3.6% of the solids by volume.

The Case 3 PSDD of Wells et al. (2007), representing the total sludge UDS inventory at Hanford (and including the AY-102 and AZ-101 UDS), is presented in Table 3.3. The PSD percentiles for the AY-102, AZ-101, and Hanford sludge from their respective PSDDs are compared in Table 3.4. The smallest 5% by volume of the AZ-101 particulate is shown to be smaller than that of AY-102. The smallest 5% by volume of the AY-102 particulate is similar to Hanford sludge. Nominally, the 25^{th} to 75^{th} volume percentiles of the UDS particulate of AY-102 and AZ-101 are similar and about half that of the Hanford sludge as a whole. There is increasingly significant disparity in the largest 5% by volume of the particulate with the Hanford sludge shown to be larger, that of AY-102 a factor of approximately 4 smaller at the 100^{th} percentile, and that of AZ-101 almost 30 times smaller.

Comparison of the solid phase compounds from the respective PSDDs is made in Table 3.5. Gibbsite is 75% by volume in AZ-101 and 53% and 52% in AY-102 and Hanford sludge, respectively. Iron oxide is the next most significant solid phase compound by volume in AY-102 and AZ-101. Boehmite is not present in any significant quantity in either AY-102 or AZ-101.

These UDS size and composition (representing density and shape) comparisons illustrate that the solids uniformity and mobilization during jet mixing may potentially be dissimilar between feed tanks. This concept is considered further in relation to the settling velocity of the particulate in Section 3.1.2.

3.1.2 Settling Rate Data

The gravity settling behavior of Hanford UDS has been investigated. Both laboratory experiments (summary provided in Poloski et al. 2007) and *in situ* data (Gauglitz et al. 2009) indicate relatively rapid UDS settling. Particulate settling velocity may also be computed from the PSDDs. *In situ*, laboratory, and PSDD-computed settling rates are compared along with variation between tanks in the discussion below.

Table 3.3. Case 3 PSDD (Wells et al. 2007)

	Solid-Phase Compounds and Density (g/mL)																
Particle Size (μm)	$Al(OH)_3$ 2.42	$(NaAlSiO_4)_6 \cdot (NaNO_3)_{1.6} \cdot 2H_2O$ 2.365	AlOOH 3.01	$NaAlCO_3(OH)_2$ 2.42	Fe_2O_3 5.24	$Ca_5OH(PO_4)_3$ 3.14	$Na_2U_2O_7$ 5.617	ZrO_2 5.68	Bi_2O_3 8.9	SiO_2 2.6	$Ni(OH)_2$ 4.1	MnO_2 5.026	CaF_2 3.18	$LaPO_4 \cdot 2H_2O$ 6.51	Ag_2CO_3 6.077	PuO_2 11.43	Total Volume Fraction
	Solid Volume Fraction																
0.22	1E-04	5E-05	3E-05	3E-05	1E-05	6E-06	5E-06	3E-06	2E-06	2E-06	2E-06	2E-06	7E-07	4E-07	3E-08	4E-09	2E-04
0.28	3E-04	1E-04	6E-05	6E-05	2E-05	1E-05	9E-06	6E-06	5E-06	4E-06	3E-06	3E-06	1E-06	8E-07	5E-08	8E-09	6E-04
0.36	6E-04	2E-04	1E-04	1E-04	5E-05	2E-05	2E-05	1E-05	1E-05	8E-06	7E-06	7E-06	3E-06	2E-06	1E-07	2E-08	1E-03
0.46	5E-05	2E-05	1E-05	1E-05	4E-06	2E-06	2E-06	1E-06	9E-07	7E-07	6E-07	6E-07	2E-07	1E-07	1E-08	1E-09	1E-04
0.60	2E-03	5E-04	3E-04	3E-04	1E-04	6E-05	5E-05	3E-05	2E-05	2E-05	2E-05	2E-05	7E-06	4E-06	3E-07	4E-08	3E-03
0.77	8E-03	3E-03	2E-03	1E-03	6E-04	3E-04	2E-04	2E-04	1E-04	1E-04	8E-05	8E-05	3E-05	2E-05	1E-06	2E-07	2E-02
1.0	2E-02	5E-03	3E-03	3E-03	1E-03	6E-04	5E-04	3E-04	2E-04	2E-04	2E-04	2E-04	7E-05	4E-05	3E-06	4E-07	3E-02
1.3	2E-02	6E-03	4E-03	4E-03	2E-03	8E-04	6E-04	4E-04	3E-04	3E-04	2E-04	2E-04	9E-05	5E-05	4E-06	5E-07	4E-02
1.7	3E-02	1E-02	7E-03	6E-03	3E-03	1E-03	1E-03	7E-04	5E-04	4E-04	4E-04	3E-04	1E-04	8E-05	6E-06	8E-07	6E-02
2.2	1E-02	5E-03	3E-03	3E-03	1E-03	5E-04	4E-04	3E-04	2E-04	2E-04	1E-04	1E-04	6E-05	4E-05	3E-06	4E-07	2E-02
2.8	4E-02	1E-02	7E-03	6E-03	3E-03	1E-03	1E-03	7E-04	6E-04	5E-04	4E-04	4E-04	2E-04	9E-05	6E-06	9E-07	7E-02
3.6	5E-02	2E-02	1E-02	9E-03	4E-03	2E-03	1E-03	1E-03	7E-04	6E-04	5E-04	5E-04	2E-04	1E-04	9E-06	1E-06	1E-01
4.6	3E-02	1E-02	6E-03	6E-03	3E-03	1E-03	1E-03	7E-04	5E-04	4E-04	3E-04	3E-04	1E-04	8E-05	6E-06	8E-07	6E-02
6.0	4E-02	1E-02	9E-03	8E-03	3E-03	2E-03	1E-03	9E-04	7E-04	6E-04	5E-04	4E-04	2E-04	1E-04	8E-06	1E-06	8E-02
7.7	5E-02	2E-02	1E-02	9E-03	4E-03	2E-03	2E-03	1E-03	8E-04	7E-04	5E-04	5E-04	2E-04	1E-04	9E-06	1E-06	1E-01
10	4E-02	1E-02	8E-03	7E-03	3E-03	2E-03	1E-03	9E-04	6E-04	5E-04	4E-04	4E-04	2E-04	1E-04	7E-06	1E-06	7E-02
13	4E-02	1E-02	8E-03	7E-03	3E-03	1E-03	1E-03	8E-04	6E-04	5E-04	4E-04	4E-04	2E-04	9E-05	7E-06	9E-07	7E-02
17	4E-02	1E-02	8E-03	7E-03	3E-03	2E-03	1E-03	8E-04	6E-04	5E-04	4E-04	4E-04	2E-04	1E-04	7E-06	1E-06	7E-02
22	3E-02	1E-02	6E-03	6E-03	2E-03	1E-03	9E-04	6E-04	5E-04	4E-04	3E-04	3E-04	1E-04	8E-05	5E-06	8E-07	6E-02
28	1E-02	5E-03	3E-03	3E-03	1E-03	6E-04	4E-04	3E-04	2E-04	2E-04	2E-04	2E-04	6E-05	4E-05	3E-06	4E-07	2E-02
36	2E-02	6E-03	4E-03	4E-03	2E-03	8E-04	6E-04	4E-04	3E-04	3E-04	2E-04	2E-04	9E-05	5E-05	4E-06	5E-07	4E-02
46	7E-03	2E-03	1E-03	1E-03	6E-04	3E-04	2E-04	1E-04	1E-04	9E-05	7E-05	7E-05	3E-05	2E-05	1E-06	2E-07	1E-02
60	5E-03	1E-03	9E-04	8E-04	4E-04	2E-04	1E-04	1E-04	7E-05	6E-05	5E-05	5E-05	2E-05	1E-05	8E-07	1E-07	9E-03
77	4E-03	1E-03	9E-04	8E-04	3E-04	2E-04	1E-04	9E-05	7E-05	6E-05	5E-05	4E-05	2E-05	1E-05	8E-07	1E-07	8E-03
100	3E-03	9E-04	5E-04	5E-04	2E-04	1E-04	8E-05	6E-05	4E-05	4E-05	3E-05	3E-05	1E-05	7E-06	5E-07	7E-08	5E-03
129	2E-03	6E-04	4E-04	3E-04	1E-04	7E-05	5E-05	4E-05	3E-05	2E-05	2E-05	2E-05	8E-06	4E-06	3E-07	4E-08	4E-03
167	7E-03	2E-03	1E-03	1E-03	5E-04	3E-04	2E-04	1E-04	1E-04	9E-05	7E-05	7E-05	3E-05	2E-05	1E-06	2E-07	1E-02
215	4E-03	1E-03	7E-04	7E-04	3E-04	1E-04	1E-04	8E-05	6E-05	5E-05	4E-05	4E-05	2E-05	9E-06	7E-07	9E-08	7E-03
278	2E-03	7E-04	4E-04	4E-04	2E-04	8E-05	6E-05	4E-05	3E-05	3E-05	2E-05	2E-05	9E-06	5E-06	4E-07	5E-08	4E-03
359	3E-03	1E-03	6E-04	5E-04	2E-04	1E-04	9E-05	6E-05	5E-05	4E-05	3E-05	3E-05	1E-05	7E-06	5E-07	8E-08	6E-03
464	6E-04	2E-04	1E-04	1E-04	5E-05	2E-05	2E-05	1E-05	1E-05	9E-06	7E-06	7E-06	3E-06	2E-06	1E-07	2E-08	1E-03
599	4E-04	1E-04	8E-05	7E-05	3E-05	1E-05	1E-05	8E-06	6E-06	5E-06	4E-06	4E-06	2E-06	1E-06	7E-08	1E-08	7E-04
774	4E-04	1E-04	9E-05	8E-05	3E-05	2E-05	1E-05	9E-06	7E-06	6E-06	4E-06	4E-06	2E-06	1E-06	8E-08	1E-08	8E-04
1000	3E-05	9E-06	6E-06	5E-06	2E-06	1E-06	8E-07	6E-07	4E-07	4E-07	3E-07	3E-07	1E-07	7E-08	5E-09	7E-10	6E-05
Total Volume Fraction	0.515	0.166	0.106	0.095	0.041	0.02	0.016	0.011	0.0081	0.0069	0.0055	0.0054	0.0023	0.0013	0.000094	0.000013	1.0

Table 3.4. PSD Volume Percentiles (μm)

Percentiles	1%	5%	25%	50%	75%	95%	99%	100%
AY-102	0.62	0.86	1.5	3	7	49	160	278
AZ-101	0.26	0.5	1.4	3.3	6.9	19	27	36
Hanford Sludge	0.65	1.0	2.8	6.3	14	59	256	1000

Table 3.5. UDS Solid Phase Compounds

		AY-102	AZ-101	Hanford Sludge
Solid Phase Compound	Density (g/mL)	UDS Volume Fraction	UDS Volume Fraction	UDS Volume Fraction
$Al(OH)_3$ - gibbsite	2.42	0.53	0.75	0.515
$(NaAlSiO_4)_6 \bullet (NaNO_3)_{1.6} \bullet 2H_2O$	2.365			0.166
AlOOH - boehmite	3.01			0.106
$NaAlCO_3(OH)_2$	2.42			0.095
Fe_2O_3 - iron oxide	5.24	0.34	0.15	0.041
$Ca_5OH(PO_4)_3$	3.14	0.053	0.014	0.02
$Na_2U_2O_7$	5.617	0.01	0.01	0.016
ZrO_2	5.68	0.00006	0.047	0.011
Bi_2O_3	8.9	0.0002		0.0081
SiO_2	2.6			0.0069
$Ni(OH)_2$	4.1	0.012	0.013	0.0055
MnO_2	5.026	0.052	0.002	0.0054
CaF_2	3.18			0.0023
$LaPO_4 \bullet 2H_2O$	6.51	0.005	0.007	0.0013
Ag_2CO_3	6.077	0.00009		0.000094
PuO_2	11.43	0.00004	0.00005	0.000013

In situ solid-to-liquid interface gravity settling-rate data are available from two Hanford sludge tanks, AZ-101 and AY-102. As summarized in Wells et al. (2010), the initial conditions of the vessels for the settling rate determinations are different (mixer pump operation in AZ-101 [Carlson et al. 2001], and slurry transfer from C-106 in AY-102 [Cuta et al. 2000]). Approximately 85% of the sediment by volume in AY-102 is from C-106. The computed settling rate data are also from different measurement and evaluation techniques. Fully mixed conditions in AZ-101 result in a UDS mass fraction of approximately 0. 04 (Section 3.2), and the actual UDS concentration of the mixed layer was approximately 0.01 (Wells and Ressler 2009). For AY-102, a fully mixed condition results in a UDS fraction of approximately 0.10 (Section 3.2; however, the actual settling conditions had much lower concentrations due to the batch-wise retrieval (Cuta et al. 2000). The *in situ* solid-to-liquid interface settling rates from the respective documents are 6E-4 m/s for AZ-101 and 5E-5 to 6E-6 m/s for AY-102.

Laboratory-scale solid-to-liquid interface gravity settling data for waste samples from these tanks indicate maximum settling rates of 2.8E-5 m/s for AZ-101 (Callaway 2000) and 4.2E-6 m/s for AY-102

(Warrant 2001). The averaged laboratory-scale solid-to-liquid interface gravity settling rates from Poloski et al. (2007) for waste samples representing eight waste types range from 3.5E-6 to 1.9E-5 m/s.

Gauglitz et al. (2009) noted the differences in laboratory and *in situ* settling data. The evaluation by Poloski et al. (2007) of laboratory settling data suggests that *in situ* settling in the Hanford tanks would require about 50 times as long to settle as the laboratory tests. In fact, both the laboratory and *in situ* data show, summarized approximately here, the volume percent of slurry in a vessel (i.e., the portion of the vessel with a UDS fraction) as opposed to UDS-free liquid, from a well-mixed initial state at 100%, reduces to approximately 30% in less than 24 hours. Gauglitz et al. (2009) noted this inconsistency by stating:

> "Scaling behavior, including the role of vessel size, of the settling dynamics and the buildup of strength in the settled layer, with a particular emphasis on shorter settling times and strength increase with depth into a layer is not well quantified with existing data and analysis. The best current estimates are presented in this report, but these estimates have uncertainty. Accurate predictions of the settling behavior and strength formation are needed, so the mixing system is designed to prevent settled layers that will exceed remobilization capabilities. Tank-farm studies of full-scale settling have shown substantially faster settling than expected based on laboratory tests. This inconsistency needs to be understood."

The particle sizes and densities of the PSDDs of Section 3.1.1 can be used in the settling velocity (U_T) equation from Camenen (2008)

$$U_T = \frac{\nu}{d}\left(\sqrt{15+\sqrt{Ga/0.3}}-\sqrt{15}\right)^2 \tag{3.1}$$

where Ga is the Galileo number defined by

$$Ga = \frac{\left(\frac{\rho_S}{\rho_L}-1\right)gd^3}{\nu^2} \tag{3.2}$$

where ρ_S is the UDS density, ρ_L is the liquid density, ν is the kinematic viscosity of the fluid, g is the gravitational constant, and d is the particle diameter.

The cumulative volume-based probability of the settling velocity of the UDS particulate, shown in Figure 3.1, for AY-102, AZ-101 and Hanford, is created using the settling velocities (Equation 3.1) and the respective PSDD volume fractions. In Figure 3.1, the 50th percentile (median) and 95th percentile by volume of settling velocity for AY-102 are approximately 4.6E-6 and 8.8E-4 m/s, for AZ-101, approximately 6.4E-6 and 2.3E-4 m/s, and for Hanford sludge, approximately 4.6E-5 and 3.8E-3 m/s, respectively.

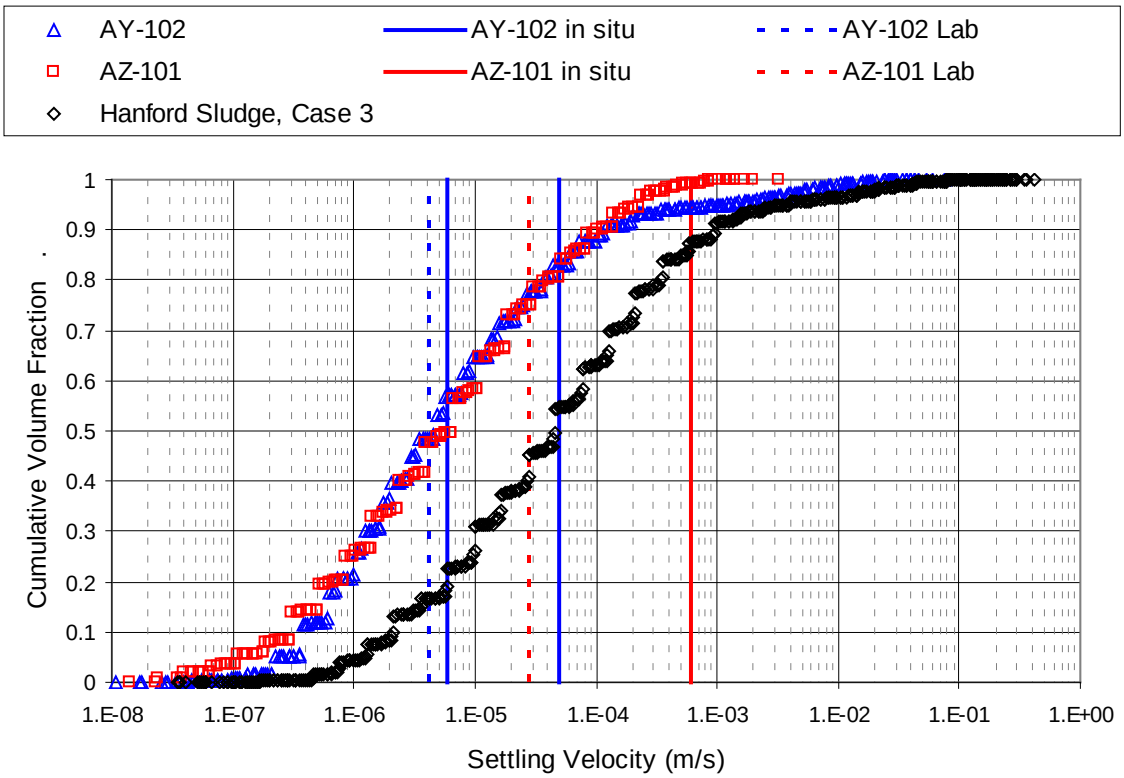

Figure 3.1. Cumulative UDS Volume Fraction as Function of Settling Velocity. AY-102: Wells and Ressler (2009), Cuta et al. (2000), Warrant (2001). AZ-101: Wells and Ressler (2009), Carlson et al. (2001), Callaway (2000). Hanford Sludge Case 3: Wells et al. (2007), Wells and Ressler (2009).

Also shown in Figure 3.1 are the *in situ* and laboratory solid-to-liquid interface gravity settling rates. The span of the *in situ* and laboratory rates from 0 to 1 cumulative volume fraction has no physical meaning and is solely for clarity. The two lines for AY-102 *in situ* represent the spread of calculated rates. The *in situ* settling rates for AY-102 correspond approximately to the 55th to 85th percentile of the PSDD settling velocity and exceed the laboratory-measured settling rate, which corresponds to approximately the 50th percentile of the settling velocity of the PSDD. The *in situ* and laboratory settling rates for AZ-101 are greater than the 99th percentile and approximately the 77th percentile by volume respectively of the PSDD settling velocity.

For AZ-101, it is significant to note that the settling followed particle suspension by the mixer pump operation. As estimated in Wells and Ressler (2009), only 32% of the UDS was suspended above 38 in. in AZ-101 at the commencement of the settling test. Thus it is reasonable to assume that the suspended UDS particulate was the "lighter" material; i.e., the particulate with lower settling velocities. Section 4.1.2 describes scaled laboratory tests with simulants where this behavior of the lighter (smaller diameter and therefore slower settling) particles being preferentially suspended was observed. Further, the settling velocity is determined from the solid-liquid interface, or the slowest settling particulate. Therefore, the apparent discrepancy between the *in situ*, laboratory, and PSDD-based settling rates may be even more pronounced.

The *in situ* and laboratory UDS settling velocity for AZ-101 exceeds that of AY-102. Acknowledging the uncertainty (see settling rate discussion above) in the representativeness of the PSDDs, the difference in the PSDD calculated settling rates, given that the PSDDs are on the same basis (i.e., same measuring technique [Wells et al. 2007]), further illustrate the point made in Section 3.1.1 that the solids uniformity and mobilization during jet mixing may potentially be dissimilar between feed tanks.

3.2 Undissolved Solids Concentration

The rheology of both cohesive and non-cohesive solid-liquid system is affected by the UDS concentration of that system (see Section 2). Hanford wastes are in a liquid, liquid over sediment, or sediment configuration (Barker and Lechelt 2000, Barker et al. 1999). The UDS concentration in a tank, or region of a tank, is dependent on the UDS inventory, the quantity of that UDS inventory in the region of interest, and the quantity of liquid in that region. Expected UDS concentrations for Hanford sediment are presented together with a methodology to estimate the concentration in a region of interest.

The average UDS concentration in the sediment, representing the UDS inventory in a tank,[1] may be expressed on a mass basis and can be determined from the conservation of mass as

$$w_S = \frac{\frac{1}{\rho_B} - \frac{1}{\rho_L}}{\frac{1}{\rho_S} - \frac{1}{\rho_L}} \tag{3.3}$$

where ρ_B is the bulk sediment density, ρ_S is the UDS density, and ρ_L is the liquid density.

The UDS mass fractions are approximated for the sediments in Hanford tanks. With the tank-specific UDS densities from the Environmental Simulation Program (ESP)[2] chemical thermodynamic model results used by Wells et al. (2007),[3] and sediment and liquid densities from Weber (2008),[4] the cumulative probabilities of the mass UDS fractions for Hanford sediment are as indicated in Figure 3.2. Also included in Figure 3.2 is the cumulative probability for the sediment of the Hanford sludge tanks. The probabilities are strictly based on tank count. The median and 95th percentile for the UDS mass fraction are approximately 0.58 and 0.74 and 0.53 and 0.73 for the Hanford sediment and sludge sediment (81 tanks, Weber [2008]), respectively.

The sediment UDS mass concentration of sludge tanks AY-102 and AZ-101, 0.46 and 0.48, respectively (Wells and Ressler 2009), is specifically considered in comparison to the current sediment for all other DSTs (28 total tanks) and those DSTs specified as sludge (11 tanks, Weber 2008) computed as above, Figure 3.3. The median and 95th percentile for the UDS mass fraction are approximately 0.31

[1] Floating crust layers do exist in some of the saltcake Hanford tanks (Weber 2008) but are not considered herein.
[2] ESP was supplied and developed by OLI Systems, Inc., Morris Plains, New Jersey.
[3] Sodium salts are included in the current analysis. Densities are on a dry-solid, crystal density basis.
[4] Sediment densities are assumed to be degassed (e.g., Stewart et al. 2005).

and 0.65 and 0.48 and 0.63 for the Hanford sediment and sludge sediment, respectively. The span of the AY-102 and AZ-101 mass fraction from 0 to 1 cumulative probability has no physical meaning and is solely for clarity.

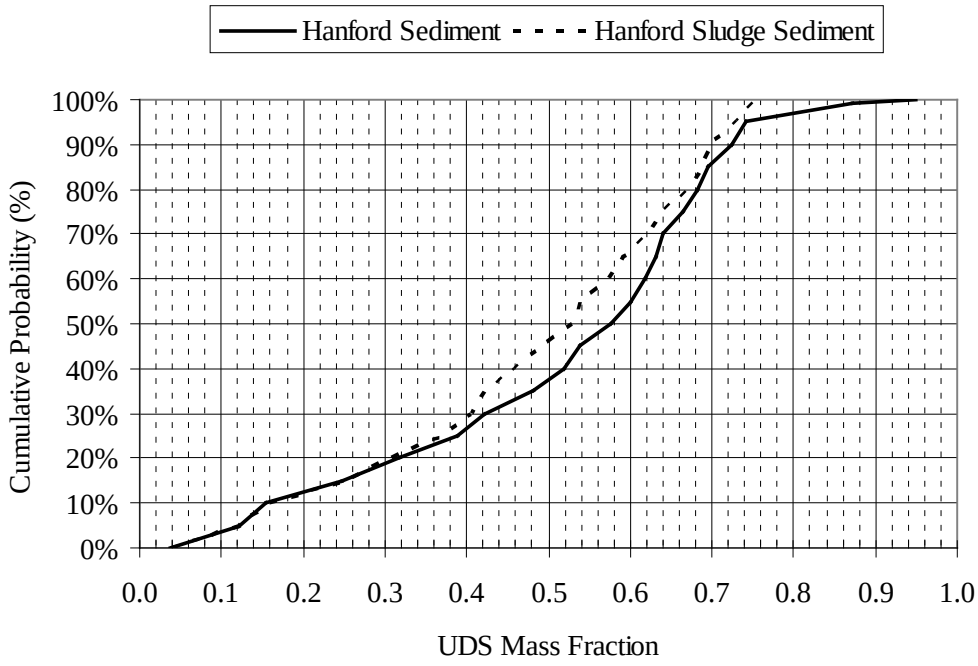

Figure 3.2. Hanford Sediment UDS Mass Fraction

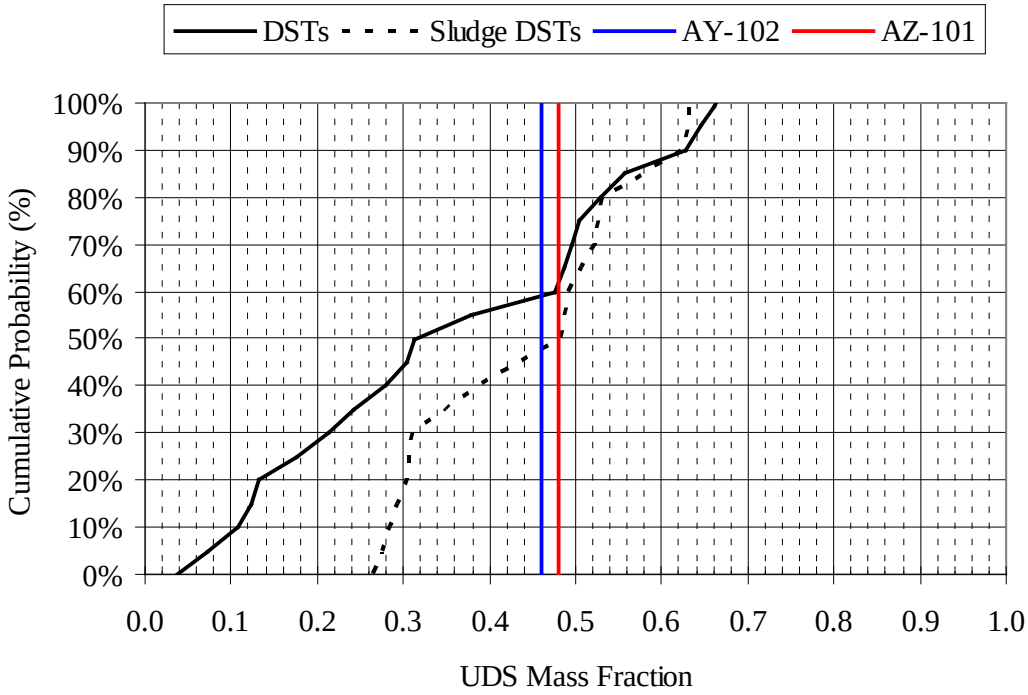

Figure 3.3. Hanford DST Sediment UDS Mass Fraction

When the single-shell tanks are included (Figure 3.2 in comparison to Figure 3.3) the mass fractions are increased. For both Figure 3.2 and Figure 3.3, when solely the sludge tanks are considered, the mass fractions are shown to increase. This is an expected result given the increased concentration of dissolved solids in the saltcake tank liquids. The UDS mass concentrations in the sediment of AY-102 and AZ-101 are shown to be representative of the DST sludge at approximately the 50th percentile of the cumulative probability.

The UDS concentration in a sediment can be treated as the maximum concentration in the tank (the estimated sediment concentrations are average in the sediment; vertical and horizontal gradients are present in the Hanford sediments). If the tank is perfectly homogenized (the supernatant liquid is assumed to be in equilibrium with the interstitial liquid in the sediment; no dissolution occurs), the resultant UDS mass fraction (w_M) can be computed via conservation of mass as

$$w_M = \frac{w_S}{1 + \frac{\rho_L}{\rho_B}\left(\frac{h_T}{h_B} - 1\right)} \tag{3.4}$$

where w_S is the sediment UDS mass fraction, h_T is the liquid surface level, and h_B is the sediment depth. Waste parameters for AY-102 and AZ-101 are reported in Table 3.6, and the homogenized tank UDS mass fractions from Equation 3.4 are 0.10 and 0.04 respectively.

If a portion of the sediment is mixed into a portion of the liquid, Equation 3.4 is still applicable, but the sediment UDS mass fraction, w_S, can be adjusted to account of the sediment "portion" that is mixed, and the liquid surface level can be likewise adjusted. In this discretized approach the concentrations are additive. The mixer pump operation in AZ-101 (Carlson et al. 2001) and resultant UDS concentration with elevation is used for an example.

Table 3.6. AY-102 and AZ-101 Waste Parameters and UDS Concentration

	ρ_L (g/mL)[(a)]	ρ_B (g/mL)[(a)]	h_T (m)[(b)]	h_B (m)[(b)]	w_S[(a)]	w_M
AY-102	1.17	1.55	8.99	1.54	0.46	0.10
AZ-101	1.24	1.62	7.74	0.53	0.48	0.04

(a) Wells and Ressler (2009).
(b) Weber (2008).

Wells and Ressler (2009) estimated that 32% of the UDS by mass was homogenously suspended in AZ-101 from 0.97 to 7.74 m. Holding the sediment depth constant and multiplying the UDS mass fraction in the sediment, 0.48, by 32%, the mixed UDS mass fraction over the entire waste depth is approximately 0.01 from Equation 3.4. The remaining UDS mass is accounted for by again holding the sediment depth constant, multiplying the UDS mass fraction in the sediment, 0.48, by 68%, and the mixed UDS mass fraction up to 0.97 (h_T in this case) is computed as 0.20 from Equation 3.4. This result is

summed with the previously computed 0.01 over the waste depth, resulting in a discrete UDS mass concentration vertical profile of 0.213 from 0 to 0.97 m and 0.01 from 0.97 to 7.74 m.[5]

The AZ-101 example can be presented graphically as well. The layer density ratio, ρ_L/ρ_B, from Equation 3.4 for AZ-101 is approximately 0.75 (Table 3.6). The ratio of the total waste height to sediment depth, h_T/h_B, is 14.6, and the ratio of the second waste height, 0.97 m, to sediment depth is $h_T/h_B = 1.8$. Figure 3.4 shows lines of constant h_T/h_B at $\rho_L/\rho_B = 0.75$. Going from high to low h_T/h_B results from increasing h_B or decreasing h_T and is shown to increase the mixed UDS concentration for a given initial concentration.

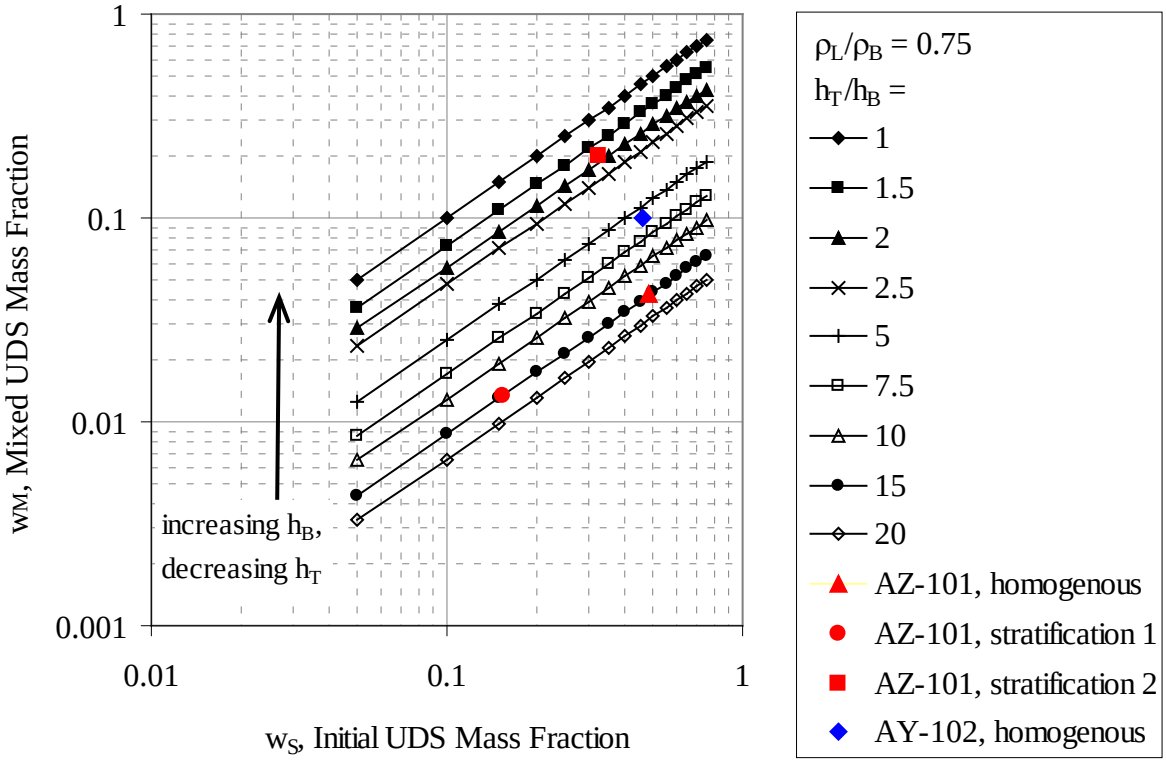

Figure 3.4. UDS Concentration as a Function of Initial Conditions, Density Ratio 0.75

From Figure 3.4, the homogenous mixed UDS mass fraction for AZ-101 is determined from Figure 3.4 by starting at the initial UDS mass fraction in the sediment, $w_S = 0.48$, and going vertically up to $h_T/h_B \sim 15$, which results in a mixed UDS mass fraction of $w_M = 0.04$. The actual mixer pump estimates can be replicated as well. For "stratification 1", at $w_S = 0.48 \times 0.32 = 0.15$, reading vertically up to $h_T/h_B \sim 15$ results in a mixed UDS mass fraction of approximately 0.01. Similarly for "stratification 2", at $w_S = 0.48 \times 0.68 = 0.33$, reading vertically up to $h_T/h_B \sim 2$ results in a mixed UDS mass fraction of approximately 0.20 for a total of 0.01 + 0.20 = 0.21 mass fraction UDS in this region. Again, the result is a discrete UDS mass concentration vertical profile of 0.21 from 0 to 0.97 m and 0.01 from 0.97 to 7.74 m.

[5] The as-mixed UDS concentration in AZ-101 was homogenous, i.e., vertically uniform, above 0.97 m. Below 0.97 m, the UDS concentration increased with depth.

Figure 3.4 allows determination of the determination of the mixed UDS mass fraction for any vessel with a density ratio of 0.75. AY-102 has $\rho_L/\rho_B = 0.75$, and $h_T/h_B = 5.8$, so the homogenously mixed UDS mass fraction, depicted in Figure 3.4, is 0.10. The potential impact on particulate suspension by mixer pump operation of the increased UDS loading in AY-102 as compared to AZ-101 can be neglected, and it is thereby assumed that the similarity in the lower settling rate particulate (Figure 3.1) will result in the same stratification during mixing in AY-102 as AZ-101 (32% of the UDS mass above h_B x 1.8, 68% below). Thus, from Figure 3.4, a "best-mixed case" UDS mass concentration vertical profile of 0.24 from 0 to 2.77 m and 0.03 from 0.97 to 8.99 m can be determined for AY-102.

As computed from Weber (2008), the 5th, 50th, and 95th percentiles (based on tank count) for ρ_L/ρ_B of Hanford sludge are 0.60, 0.75, and 0.93 respectively and 0.67, 0.78, and 0.83 for sludge DSTs. The sediment depth in feed staging tanks may be up to 200 in., and the maximum waste liquid level ranges from 364 in. (AY and AZ farms), to 409 in. (AW-102), to 422 in. (AN and SY farms, AW-101, and AW-103 through AW-106), to a maximum of 454 in. (AP farm) (Rast 2009). As indicated, Figure 3.4 can be used for any tank with a density ratio of 0.75. For example, if a tank in the AP farm is filled to the maximum liquid waste level (454 in.) and has 200 in. of solids ($h_T/h_B = 2.3$) at the median DST sludge $\rho_L/\rho_B = 0.75$ and the median UDS mass fraction in the sediment, $w_S \sim 0.48$ (Figure 3.3), the homogenously mixed UDS mass fraction is approximately $w_M = 0.24$. Varying the density ratio from 0.60 to 0.90 is shown to decrease the resultant mixed UDS mass fraction when all other inputs are held constant, Figure 3.5 and Figure 3.6.

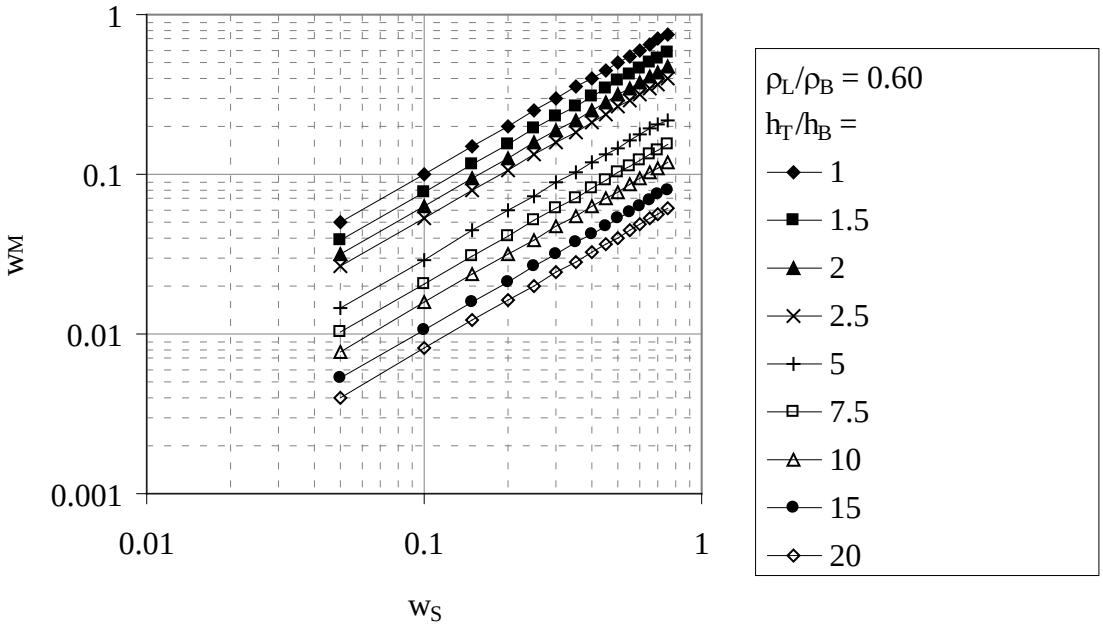

Figure 3.5. UDS Concentration as a Function of Initial Conditions, Density Ratio 0.60

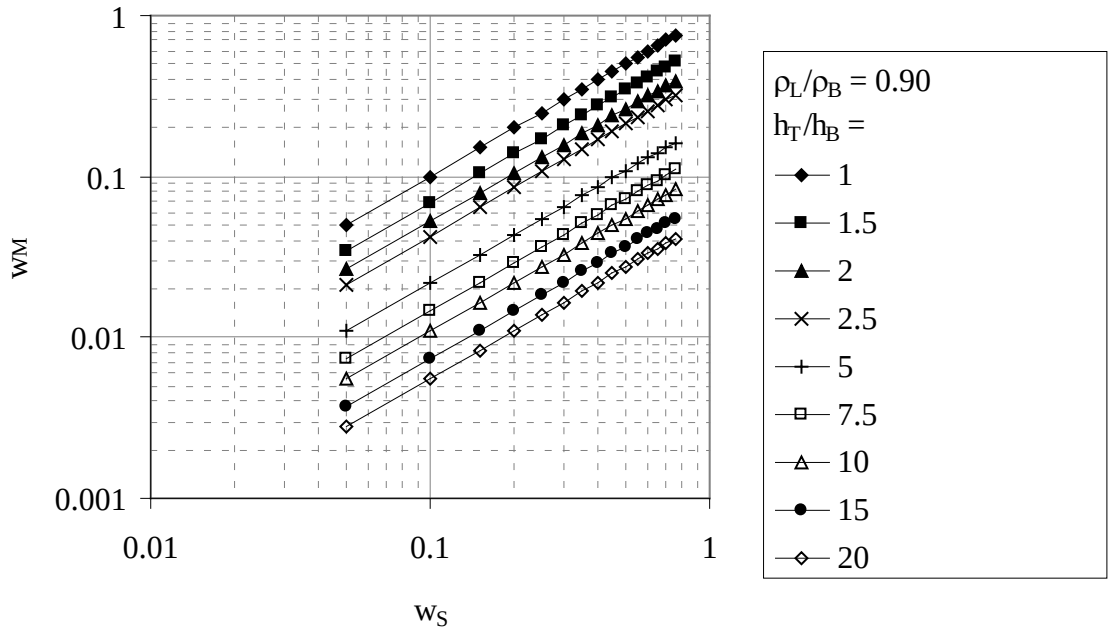

Figure 3.6. UDS Concentration as a Function of Initial Conditions, Density Ratio 0.90

The lower settling rate particulate for Hanford sludge Case 3 PSDD can be seen in Figure 3.1 to have a higher settling rate than the estimates for AY-102 and AZ-101. Thus, as suggested in Wells and Ressler (2009), particulate suspension of the bulk Hanford sludge UDS may be a significant challenge. Solids uniformity and mobilization during jet mixing may potentially be dissimilar between feed tanks. The relationship between UDS concentration and waste rheology, and hence the impact of cohesive particle interactions for Hanford sludge waste, is discussed in Section 3.3.

3.3 High-level Waste Rheology

Rheology data are available for a limited number of sludge tanks. The Bingham rheological model data, yield stress and consistency (viscosity), provided in Poloski et al. (2007) for slurries from 18 sludge tanks are presented in Figure 3.7 and Figure 3.8, respectively, as functions of the approximated UDS mass fraction. The samples are typically sludge sediment diluted to various concentrations with supernatant liquid from the same sludge tank. All measurements are taken ex-tank, and the measurement temperature range is 25 to 95ºC.

The 95% empirical limits for the Bingham rheological model data from Wells et al. (2010) are also provided in Figure 3.7 and Figure 3.8. Partitions in the UDS mass fraction are taken, and the 2.5%, 50% (median), and 97.5 % probabilities of the partitions are determined. The resultant 95% empirical limit and median are represented at the average mass fraction UDS of the partitions. The lack of clear functionality of the Bingham model parameters with the UDS concentration may be expected because of the varied waste and sample conditions represented. The general expected trend of increased Bingham yield stress and consistency with increased UDS concentration (e.g., Gauglitz et al. 2009; Poloski et al. 2007; Shatzmann et al. 2003; Turian et al. 2002; Ancey and Jorrot 2001; Zhou et al. 1999; Channell and Zukoski 1997; and Buscall et al. 1987) is observable for the medians.

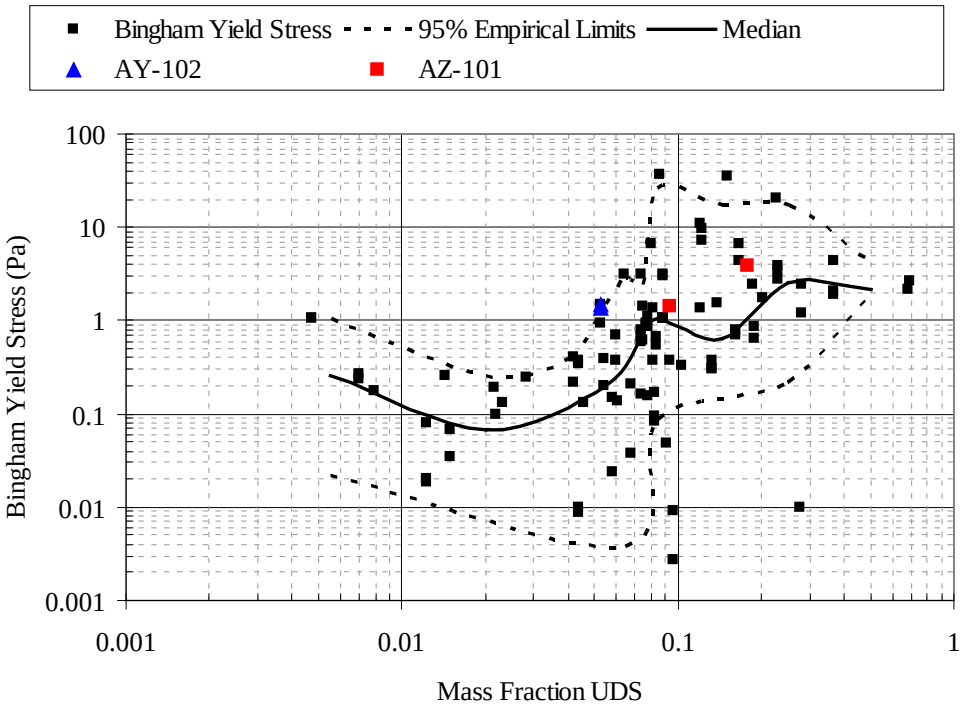

Figure 3.7. Probabilities for Bingham Yield Stress for Slurries from 18 Hanford Sludge Tanks, Mass Fraction UDS. Wells et al. (2010), data from Poloski et al. (2007).

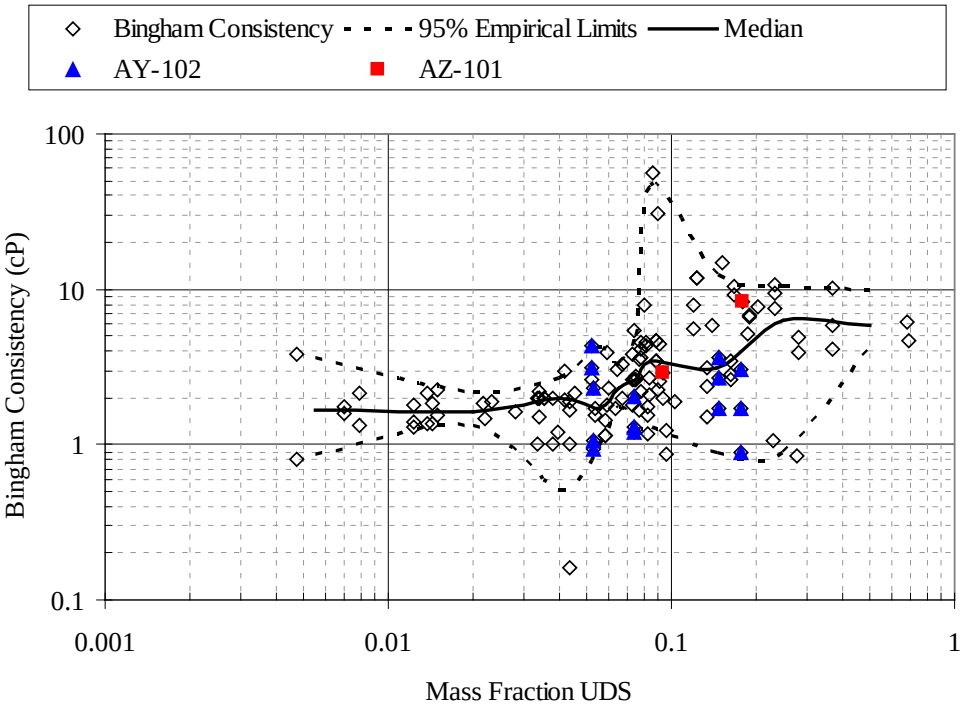

Figure 3.8. Probabilities for Bingham Consistency for Slurries from 18 Hanford Sludge Tanks, Mass Fraction UDS. Wells et al. (2010), data from Poloski et al. (2007).

The Bingham rheology data from Poloski et al. (2007) for AY-102 and AZ-101 is highlighted in Figure 3.7 and Figure 3.8. The AY-102 Bingham yield stress data reported in Poloski et al. (2007) from Coleman et al. (2003) indicate that the AY-102 waste at a UDS concentration of approximately 0.05, half of that if the tank is homogenously mixed (Section 3.2), is at the upper 95% empirical limit. This indicates that the AY-102 waste at that concentration is more cohesive in nature than the other measured Hanford wastes, and at about 1.4 Pa Bingham yield stress it is non-Newtonian with cohesive interactions affecting the rheology (see Section 2 for a further discussion of rheology). The Poloski et al. (2007) reported data from Warrant (2001) shows no Bingham yield stress for AY-102 waste samples up to UDS mass fractions approaching 0.25 (different estimates for the UDS concentration of the reported data exist), indicating that the AY-102 is non-cohesive at those UDS concentrations. Thus, one set of data suggests that AY-102 is somewhat non-Newtonian (cohesive effect important) when homogenously mixed, and another indicates that, even when stratified as approximated in Section 3.2, the waste will be weakly non-Newtonian (cohesive particle interaction are minor).

In addition to the Geeting et al.(2002) rheology data for AZ-101 provided in Poloski et al. (2007), rheology data are also available from Urie et al. (2002), Callaway (2000), Gray et al. (1993), and Peterson et al. (1989), and as with AY-102, different estimates of the UDS concentration for some of the reported data exist. The AZ-101 Bingham yield stress data reported in Poloski et al. (2007) are shown to be above the median Bingham yield stress for the Hanford sludge, suggesting that it may typically be cohesive in relation to Hanford waste. Thus, for the as-mixed concentrations reported in Section 3.2 for the two-layer stratification, AZ-101 was nearly Newtonian (UDS mass fraction 0.01, Bingham yield stress less than 1 Pa) above 0.97 m, and non-Newtonian with cohesive interactions playing a role below 0.97 m (UDS mass fraction 0.21).

Homogenous mixing of the "full" AP farm example in Section 3.2 at typical Hanford sludge conditions resulted in a UDS mass fraction of 0.24 from Figure 3.4, which is indicated by the data of Figure 3.7 to be cohesive. The interface control document for waste feed from the feed staging tanks to the WTP, Hall (2008), lists the maximum UDS content in the HLW feed as 200 g/L. For typical Hanford sludge properties, this concentration corresponds to a UDS mass fraction of approximately 0.15 (Wells et al. 2007). The available data indicate that feed at this concentration will most likely be impacted by cohesive particle interactions.

Per the System Plan (Rev. 4, Certa and Wells 2009), the DST storage space for UDS is limited. Thus, it is reasonable to expect that the feed staging tanks will contain large volumes of sediment. At typical UDS concentrations and sediment and liquid layer properties (Section 3.2), homogenous mixing in the feed vessels may result in a cohesive slurry unless the ratio of sediment to liquid layer heights is above approximately 7.5.[6] For a feed tank with a 454-in. liquid surface level, this layer height ratio limit for cohesive behavior limits the sediment depth to approximately 60 in. to ensure non-cohesive behavior, assuming that homogenous mixing can be achieved.

The apparent viscosity at the estimated strain rate within the baseline mixer pump head (1000 s^{-1}, Section 4.2) as determined from the Bingham parameters is provided in Figure 3.9 as a function of the UDS mass fraction. The apparent viscosity in the mixer pump head is shown to be approximately 2 cP,

[6] From Figure 3.7, a reasonable UDS mass fraction limit for probable cohesive behavior is 0.08. From Figure 3.4 at an initial UDS mass fraction in the sediment of approximately 0.45, $h_T/h_B \geq 7.5$ is required to result in a homogenously mixed tank of less than 0.08 UDS mass fraction.

corresponding approximately to the typical Hanford sludge tank liquid viscosity (Wells et al. 2010), and typically increases after a UDS mass fraction of approximately 0.05.

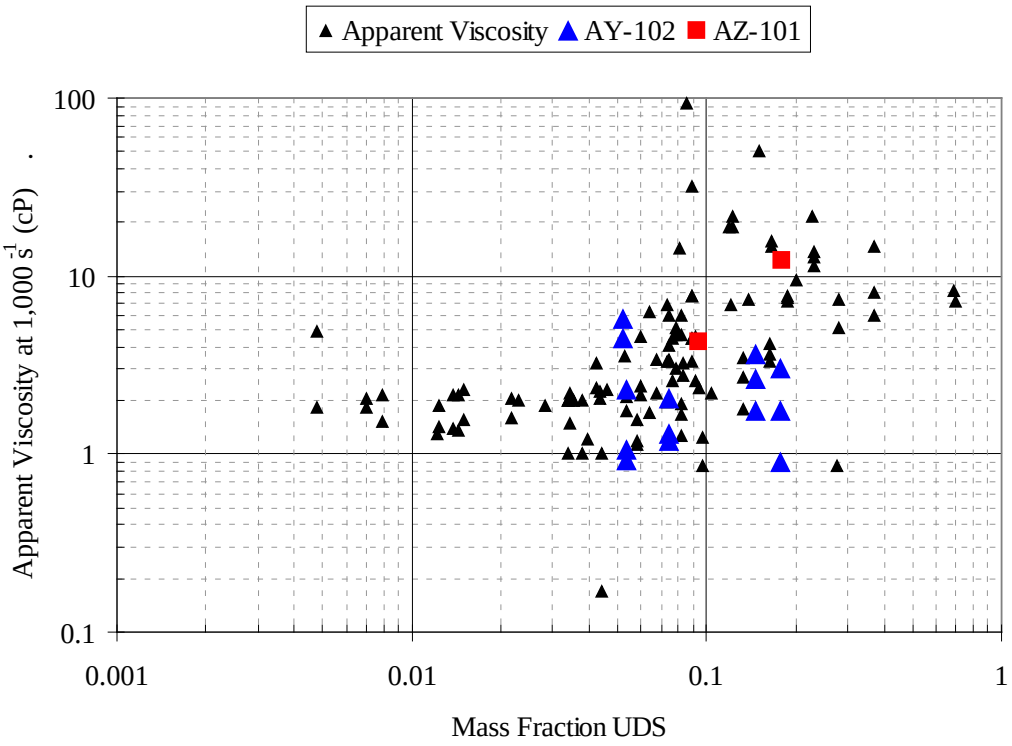

Figure 3.9. Apparent Viscosity at 1000 s^{-1} from Bingham Parameters for Slurries from 18 Hanford Sludge Tanks as a Function of Mass Fraction UDS. Bingham Parameters from Poloski et al. (2007), Figure 3.7 and Figure 3.8.

The preceding discussions relating the UDS suspension observed in AZ-101 to other Hanford tanks do not address the mobilization of the UDS from the original sediment layer. As presented in Section 1 and Section 4.4, the extent of sediment mobilization is a function of the shear strength of the sediment and the jet force applied by the mixer. For constant jet properties, less UDS suspension will occur for a sediment with sufficiently high shear strength as compared to a low shear strength sediment. To summarize, differences in sediment shear strength will change the mobilization of that layer. This in turn will change the suspended UDS concentration, which then affects the cohesiveness of the slurry.

The sediment shear strength data provided in Gauglitz et al. (2009) for 15 sludge tanks is presented in Figure 3.10 as a function of the approximated UDS mass fraction. The data presented are from the shear vane technique on ex-tank waste sludge sediment samples. As for the Bingham rheological model data of Figure 3.7 and Figure 3.8, the 95% empirical limits from Wells et al. (2010) are also provided. Hanford sediment has varied shear strength, so mobilization and thereby UDS suspension may be affected.

The shear strength data from Gauglitz et al. (2009) for AY-102 and AZ-101 is also indicated in Figure 3.10. As specified in Section 3.2, the approximated UDS mass fraction is computed using the dry-solid crystal density. Thus there are differences in the sediment UDS fractions for AY-102 and AZ-101 between Figure 3.10 and Table 3.6. Regardless, the significance of the data in Figure 3.10 is clear.

Sediments with widely divergent UDS concentrations may have similar shear strengths; the median shear strength in Figure 3.9 is shown to be nominally 1000 Pa independent of UDS concentration. Conversely, sediments with similar UDS concentrations (i.e., AY-102 and AZ-101, see Table 3.6) may have dissimilar shear strength (median AY-102, 510 Pa, median AZ-101, 1770).

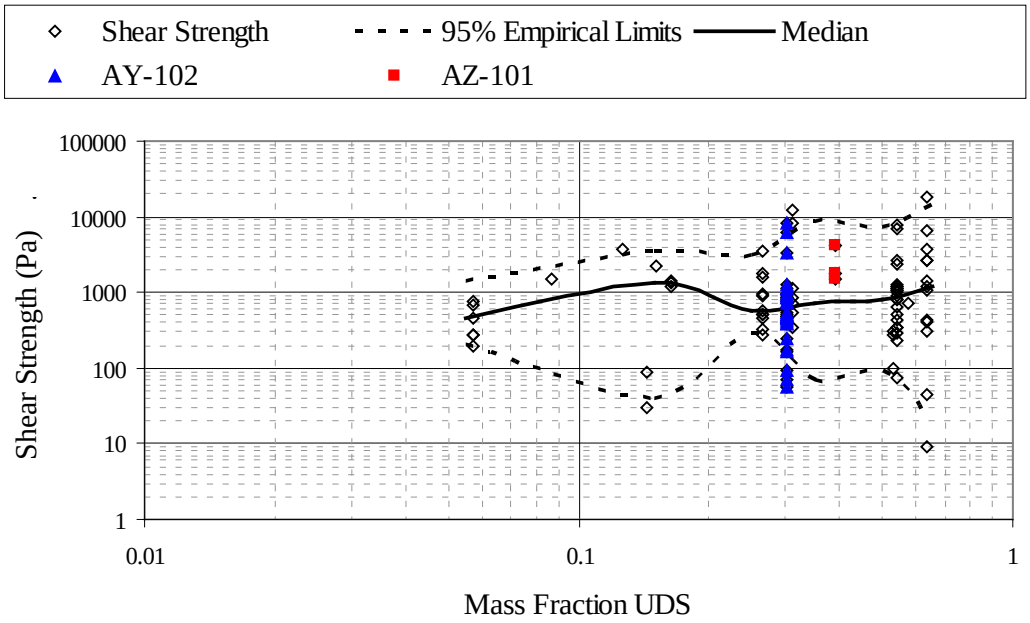

Figure 3.10. Probabilities for Shear Strength for Sediment from 15 Hanford Sludge Tanks. Wells et al. (2010), shear strength data from Gauglitz et al. (2007), UDS mass fractions estimated from Wells et al. (2007), Weber (2008) (see Section 3.2).

Following the preceding discussion relating shear strength and mobilization and assuming all other parameters are equivalent,[7] it could be concluded from the shear strength difference in AY-102 and AZ-101 that more UDS would be suspended in AY-102 than in AZ-101. However, as concluded by Carlson et al. (2001), 95 to 100% of the sediment in AZ-101 was mobilized, thus indicating that the same would be true for a weaker sediment. More suspension may initially occur in a weaker sediment as less of the jet energy would be required for mobilization, but once 100% mobilization is achieved, suspension will be equivalent for identical systems.

[7] As discussed in Wells and Ressler (2009), both the increased UDS loading in AY-102 (see Section 3.2) and the increased particulate settling velocities (see Section 3.1.2) would be expected to reduce UDS suspension in AY-102 relative to AZ-101 for the same pump operating conditions.

4.0 Evaluation of Cohesive Effects in Each Region

To evaluate the role of cohesive particle interactions in tank mixing systems, the tank has been divided into seven mixing regions based on the jet mobilization and suspension that are defined in Section 1.2. In some regions, the effects of cohesive particles are favorable and enhance mixing; in some regions cohesive particles do not affect mixing; and in some regions, the effects of cohesive particles are unfavorable to mixing. The primary focus of this report is to evaluate the impact of cohesive particle interactions on the distribution of solid particles in the upper mixed region of the tank, so Region 7 will be evaluated first followed by Regions 1-6 near the bottom of the tank, which will be evaluated in order.

4.1 Region 7: Mixing (Lifting and Settling) of Suspended Particles

The particle lifting and settling that occur in Region 7 are the critical behaviors affecting the overall uniformity in the mixed region. The turbulent jet carries the more particle-loaded and dense slurry at the bottom of the tank outward to the wall where the jet spreads and carries some of the particles upward. Depending on the density and velocity (inertia) of the jet, the particles carried by the jet will move inward after moving upward at the wall of the tank. As discussed in Sections 4.4 and 4.5, the settled material may or may not be fully mobilized; hence, the total solids loading in Region 7 may be less than the total tank inventory. Accordingly, changes in operational and waste parameters that affect mobilization of the settled material will also change the amount of suspended material, and this will be seen in the data presented below.

4.1.1 General Description

While mixing and uniformity of suspended solids have been studied extensively in mechanically agitated vessels, there are relatively few studies that have focused on solids uniformity in jet-mixed vessels. None of these studies, even in mechanically agitated vessels, has quantified the relative amounts of different particles in the mixed region, and none of these studies has sought to quantify the role of cohesive particle interactions on the uniformity of the suspended solids. Accordingly, in the absence of any studies focusing on the two key issues of the relative amounts of different particles and the impact of cohesive particle interactions, it is difficult to address the primary objective of this report, which is evaluating whether cohesive particle interactions will have a significant influence on uniformity of suspended solids.

4.1.2 Effect of Cohesive Properties

While specific studies on the role of cohesive particle interactions are not available, there are a number of studies that give insight into the problem. These studies include uniformity (particle concentration profiles) in jet mixed vessels with simulants, jet mixing studies in Hanford DSTs, and previous modeling studies of jet mixing in DSTs. Key results from selected studies are discussed in the remainder of this section. In a number of the discussions below, the analyses have focused on determining if the uniformity of suspended solids is affected by the viscosity of the suspending liquid because this might indicate how a cohesive non-Newtonian slurry might behave.

In the section below, selected test results data are presented from both scaled laboratory tests with simulants and full-scale tests. The first two studies used a 1/12-scale test vessel with a single jet mixer

pump. The next two studies are for AZ-101, both the full-scale test and then 1/22-scale laboratory tests that also used test conditions appropriate for AY-102. Selected results are then summarized from full-scale testing in SY-101. The next two studies are for AP-102, both full-scale and 1/19-scale. Finally, the results from PJM testing in three scaled vessels are summarized.

4.1.2.1 1/12-Scale Uniformity Study

One of the most extensive data sets on the uniformity of suspended solids in jet mixed vessels is given by Bamberger et al. (2007). These tests used non-cohesive particles in aqueous solutions of sugar and water, so the data do not directly address the role of cohesive particle forces on the uniformity of suspended solids. These tests did, however, use simulants that had different sugar concentrations to vary the viscosity of the suspending liquid. As discussed previously in Section 2, one consequence of having cohesive particle interactions in a suspension is that the viscosity of the suspension will be increased. In the figures below, we will show a portion of the data from Bamberger et al. (2007) that highlights the role of increased viscosity on three key indications of uniformity. The two simulants specifically highlighted below are S2, which was the low viscosity material with water as the suspending liquid, and S4, which was the high-viscosity material in a 22 wt% sugar water solution. Both of these simulants used the same particle, Minusil-40, at 18 wt%. Minusil-40 had a reported mean particle size of 27.4 μm. A particle size distribution for this material was not reported in Bamberger et al. (2007), but current product information for Minusil-40 shows the majority of the particles ranging from about 2 to 40 μm (US Silica 2010). In these tests, the jet diameter was 0.5 in. (1/12 of the full-scale 6-in. jet). The jet velocity was varied over a range, with the highest velocity (the 100% U_0D_0 condition) being 17.04 ft/s, which is (1/12)^1/2 of the full-scale velocity of 58.8 ft/s (Bamberger et al. 2007, 1990b).

For evaluation of uniformity, the first measure is the total solids concentration at any location in the tank in comparison to the initial total concentration in the tank. The second measure is the relative concentration of different particles (species concentration) in comparison to the initial relative concentration in the tank. In the experiments with Minusil-40, if the median particle size differed from the initial value, this is equivalent to the relative concentration of different particles (species concentration) being different from the initial value. As we will see below, a third measure that is useful is how the concentrations vary from point-to-point in the mixed region because the concentrations can be essentially identical throughout the mixed region even though they differ significantly from the initial values.

Figure 4.1 shows how the total concentration varies with elevation for U_0D_0 varying from >100% to 25%. The two plots show the data separately for S2 (low viscosity) and S4 (high viscosity). The first observation is that for a given simulant and % U_0D_0, the concentrations values at different elevations are essentially identical. This is very striking uniformity in terms of point-to-point uniformity. The second key observation is that the total concentration at the sample points decreases substantially as the % U_0D_0 is decreased. The data for >100% U_0D_0, which was an intensely mixed condition done at the beginning of the testing, gives normalized concentrations very near unity. This indicates almost perfectly uniform total solids distribution at this condition. For the lower U_0D_0 test conditions, the normalized total concentrations were much below unity. In these tests, a large fraction of the solids were below the bottom sampling location. The tests did not determine if the solids below the bottom sampling location were completely stagnant or moving but they were not being suspended into the upper region of the tank. Profiles measured of the solids elevation along the floor of the tank indicated that much of the solids were settled.

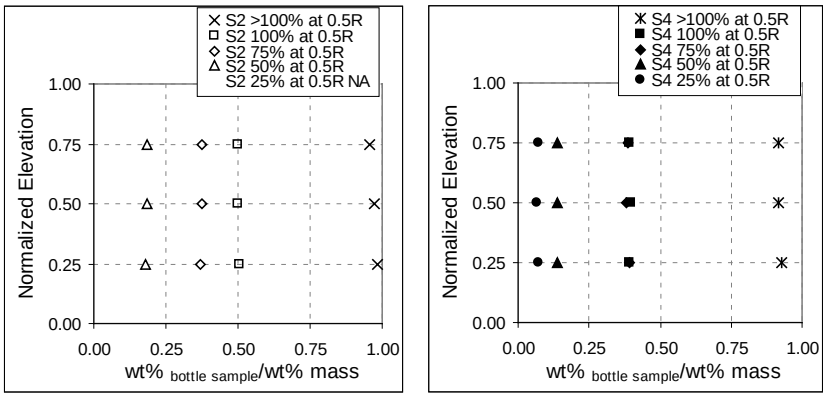

Figure 4.1. Comparison of Normalized Total Concentration as a Function of Elevation for Simulants S2 (low-viscosity) and S4 (high-viscosity) Based on Bottle Sample Measurements with U_0D_0 Varying from >100% to 25%.

Figure 4.2 shows comparisons between the low-viscosity (S2) and high-viscosity (S4) simulants at three different U_0D_0 values. The higher-viscosity simulant (S4) had slightly lower total solids concentrations in comparison to the low-viscosity simulant, but the concentrations were essentially uniform at the different elevations. This result suggests that if cohesive particles interactions only changed the viscosity of a slurry, there would be only a small change in the solids total solids distribution.

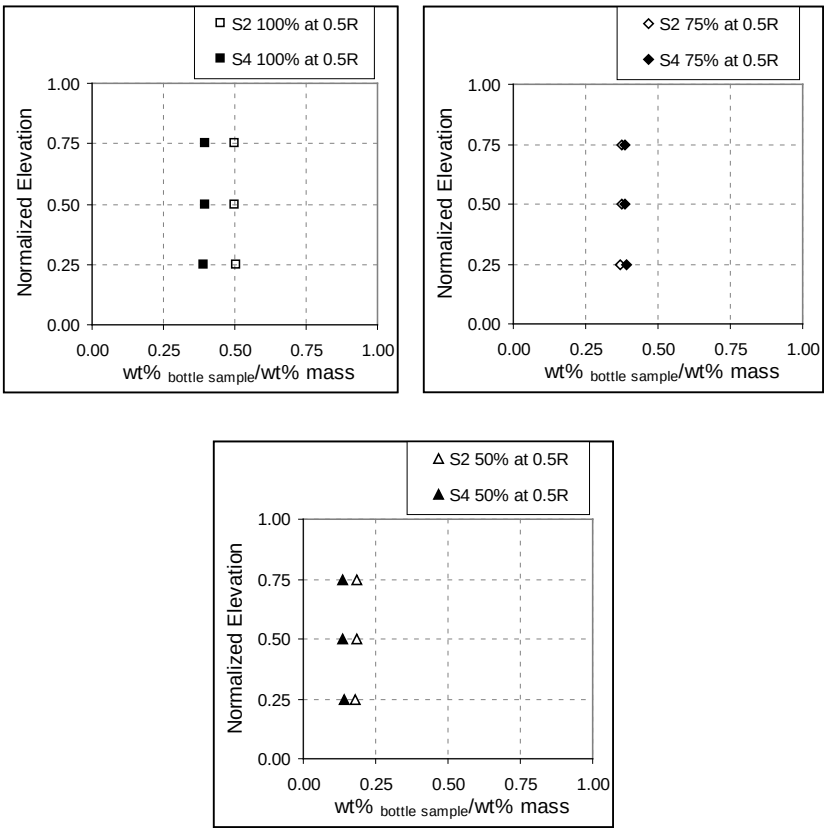

Figure 4.2. Comparison of Concentration as a Function of Elevation for S2 and S4 Based Bottle Sample Measurements for 100%, 75%, and 50% of U_0D_0

Figure 4.3 shows how the normalized particle size varies with elevation for U_0D_0 ranging from 100% to 25%. In these tests, the median volume-based particle size was reported by Bamberger et al. (2007) for bottle samples taken at the different test conditions and elevations. The normalized particle size shown in the plots is the measured median size of a specific sample divided by 27.4 μm, which was mean size reported by Bamberger et al. (2007) for the Minusil-40 used in the tests. The two plots show the data separately for S2 (low-viscosity) and S4 (high-viscosity) simulants. Similar to the total concentration data, the first thing to note is that for a given simulant and % U_0D_0, the normalized particle sizes at different elevations are essentially identical. This is very striking uniformity in terms of point-to-point uniformity for relative particle concentrations (species concentration). The second key observation is that the normalized particle sizes at the sample points decrease substantially as the % U_0D_0 is decreased and values are much less than unity. In these tests, a large fraction of the solids were below the bottom sampling location. The data show that the smaller particles in the Minusil-40 were suspended in the upper region of the tank and the larger particles remained at the bottom. This segregation of particles became progressively more pronounced as the % U_0D_0 was decreased.

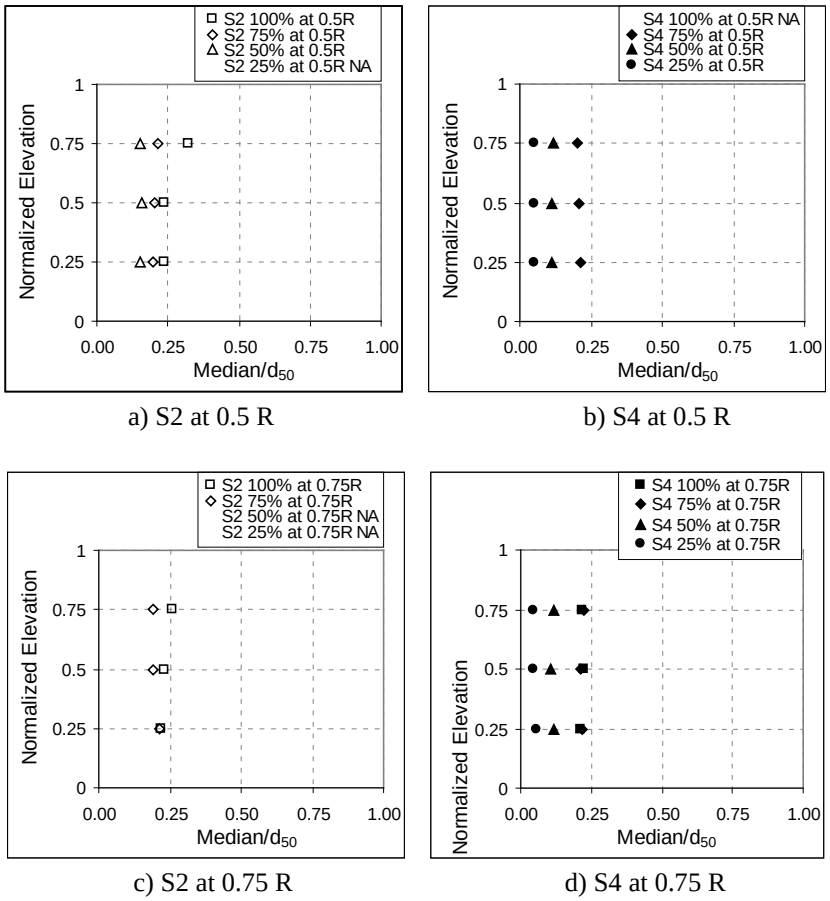

a) S2 at 0.5 R

b) S4 at 0.5 R

c) S2 at 0.75 R

d) S4 at 0.75 R

Figure 4.3. Comparison of Normalized Particle Size at U_0D_0 Conditions 100%, 75%, 50%, 25% at Two Radii for Simulants S2 (large diameter, low-viscosity) and S4 (large diameter, high-viscosity)

Figure 4.4 shows comparisons between the low-viscosity (S2) and high-viscosity (S4) simulants at two different U_0D_0 values. There is very little difference in the median particle sizes between the low- and high-viscosity simulants. Similar to the total concentration data, the median particles sizes were

essentially the same at the different elevations for a specific test. This result again suggests that if cohesive particles interactions only changed the viscosity of a slurry, there would be only a small change in the relative concentration of different particles.

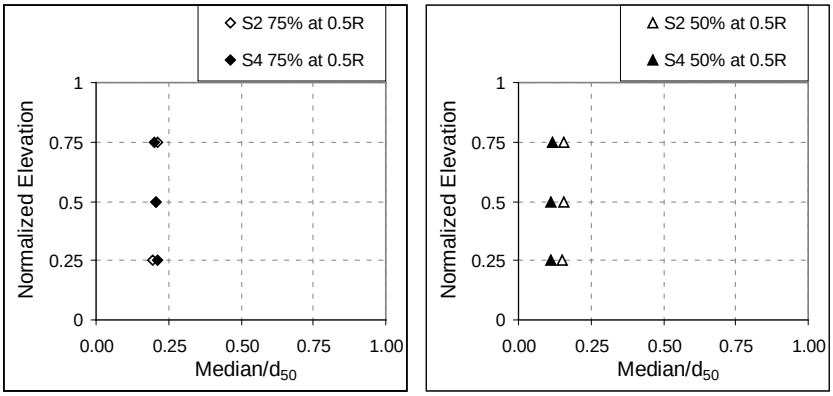

Figure 4.4. Comparison of Normalized Particle Size as a Function of Elevation for S2 and S4 at 75% and 50% U_0D_0

The quantified segregation of particles with respect to size for the 1/12-scale uniformity study is postulated to have occurred during the full-scale testing in AZ-101. Although the *in situ* settling velocity of the AZ-101 particulate is shown in Section 3.1.2 to greater than the 99th percentile by volume of the AZ-101 UDS PSDD settling velocity, it is argued in that the PSDD under-represents the UDS particulate given that the *in situ* measured settling velocity was a result of suspension due to mixer pump operation. Given that only a fraction of the UDS mass in AZ-101 was suspended (Section 3.1.2), it is reasonable to expect that this suspended UDS particulate was the "lighter" or easier-to-suspend material, i.e., the particulate with lower settling velocities. This expectation is supported by the *in situ* PSD data from the AZ-101 mixer pump test (see Section 4.1.2.3.1).

Because the total concentrations and the median particle sizes are essentially the same at all elevations for a specific test, it is useful and reasonable to calculate the average value at each test condition and then plot how these average values vary with tests conditions. In the plots below, data are shown for all four simulants used in the testing reported by Bamberger et al. (2007). The two simulants not previously discussed are S1 and S3. These simulants used Minusil-10, which had a mean particle size of 6.3 μm, which is smaller than Minusil-40, and the same low- and high-viscosity suspending liquids.

Figure 4.5 shows how the normalized total solids concentration increased with increasing U_0D_0. The data show that the smaller particle simulants, S1 and S3, have a higher normalized solids concentration in the mixed region of the tank in comparison to larger particle S2 and S4 simulants. For the S1 and S3 simulants, the normalized concentrations are nearly unity at 100% U_0D_0. For both the small particle and larger particle simulants, the effect of viscosity on the total solids concentration is very small. Figure 4.5 also shows how the normalized particles size increases with increasing U_0D_0. Again, the normalized particles size is equivalent to the relative concentration of different size particles (species concentration), and approaching unity means that the particle size is approaching the initial value for the particles. Similar to the total concentration result, the smaller particles are closer to a normalized size of unity and the effect of viscosity is very small.

Overall, these results show that increasing the suspending liquid viscosity has a minor effect on the total solids and median particle size in the upper region of the tank where the solids are uniform. This result suggests that if cohesive particles interactions only change the viscosity of a slurry, there would be only a small impact on the overall particle uniformity

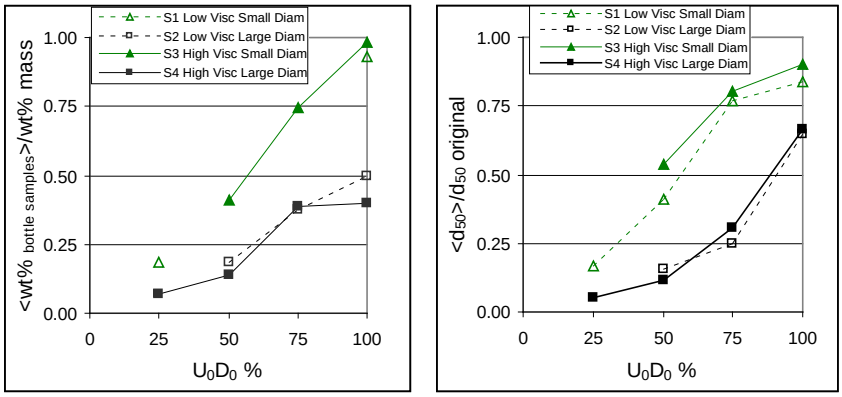

Figure 4.5. Comparison of Normalized Solids Concentration and Normalized Particle Size as a Function of U_0D_0. Values are based on bottle sample measurements of density and are averages of three elevations at each test condition.

4.1.2.2 1/12-Scale SY-101 Mixer Pump Test

Fort et al. (1993) measured fluid velocities and solids concentrations profiles in a 1/12-scale test using turbulent jets to mobilize and mix a settled slurry. The velocity data are discussed in Section 4.3, and the concentration profiles data are discussed here. These tests used non-cohesive particles in aqueous solutions of sugar and water, so the data do not directly address the role of cohesive particle interaction, which is the primary object of this report These tests did, however, use simulants that had different sugar concentrations to vary the viscosity of the suspending liquid. As discussed previously in Section 2, one consequence of having cohesive particle interactions in a suspension is that the viscosity of the suspension will be increased. In Figures 4.6 - 4.9 below, we will highlight data that show the roles of particles in general and the role of increased viscosity on measured fluid velocities. Two simulants were used in the study. A low viscosity simulant that used a 2 wt% sugar water solution and a high-viscosity simulant that used a 20 wt% sugar water solution. Both of these simulants used the same particle, Minusil-30, at 33 wt%. Minusil-30 was described as having a mean particle size of about 10 μm. A particle size distribution for this material was not reported in Fort et al. (1993), but current product information for the particle size distribution for Minusil-30 is available (US Silica 2010). The jet diameter was 0.224 in., which was 1/12 of the full-scale nozzle.

Figure 4.6 to Figure 4.8 show the normalized concentration as a function of elevation for the three different tests where the mixer pump was indexed (rotated to specific angles for a period of time then rotated to the next position). The slurry concentration is shown as mass fraction of particles normalized by the overall average mass fraction. The profiles show the transient mobilization and mixing of the initial settled bed. The results show that the profiles become more uniform with time. Similar to the 1/12-scale uniformity tests described above, the profiles are quite uniform over the elevations measured. Figure 4.9 shows a comparison of the three profiles that were essentially at steady state. The concentrations were all below the average value in the tanks, and the high-viscosity tests (Ops 1) had a

profile that was closer to the tank average (normalized value of one) in comparison to the low-viscosity test (OpsL 1). Figure 4.9 also shows that increasing the jet velocity improves the uniformity as expected.

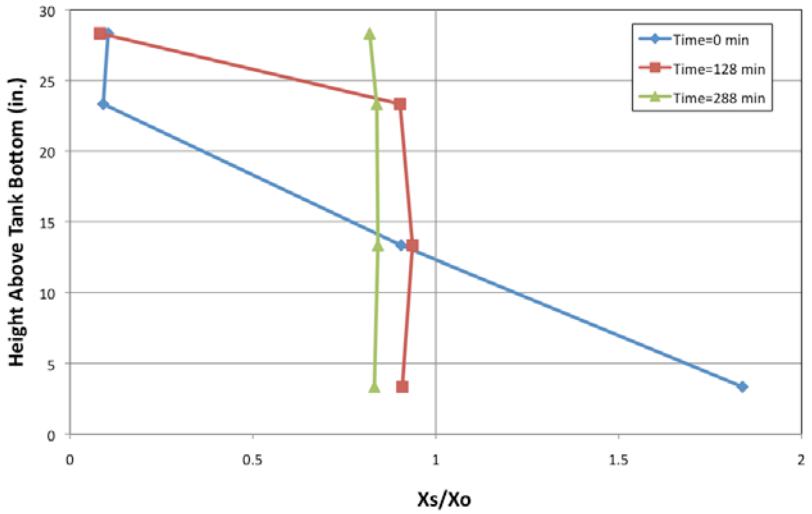

Figure 4.6. Operations Parameter Test 1 (Ops 1)-High-viscosity, V=25.4 ft/s. Ratio of local and tank average solids mass fraction as a function of height above tank bottom. Data from Table B-14, Fort et al. (1993).

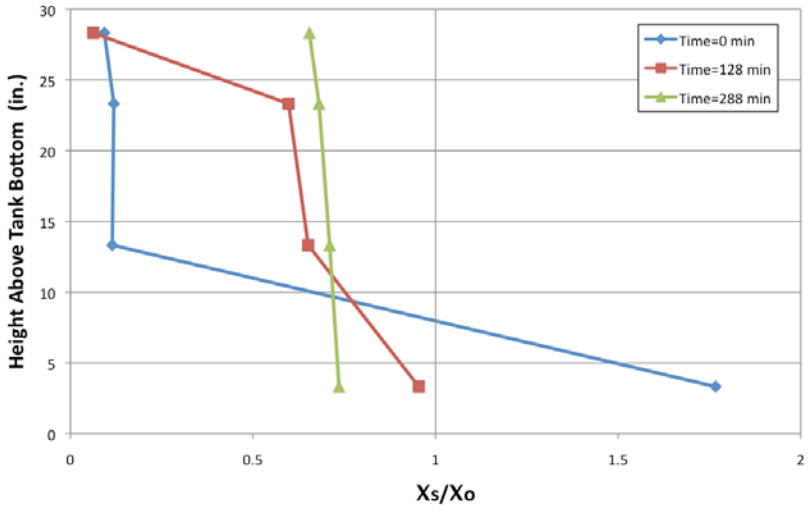

Figure 4.7. Operations Parameter Test 1-Lo (OPLS 1) Viscosity, V=25.4 ft/s. Ratio of local and tank average solids mass fraction as a function of height above tank bottom. Data from Table B-16, Fort et al. (1993).

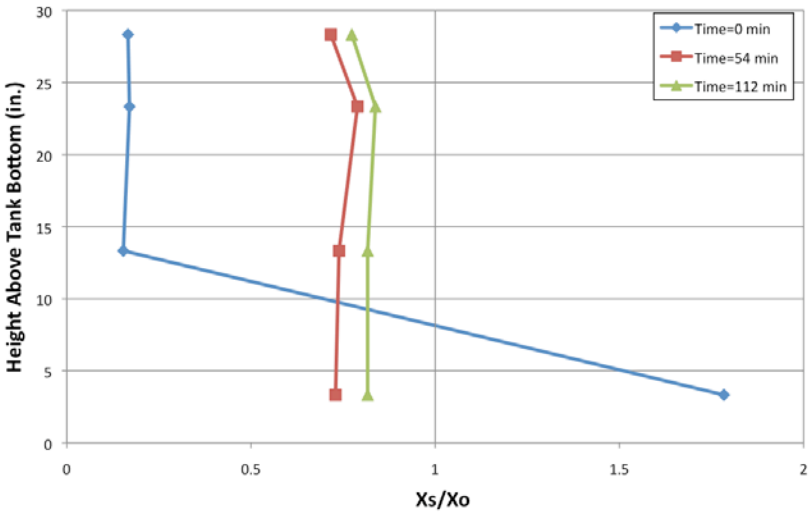

Figure 4.8. Operations Parameter Test 2-Lo (OPLS 2) Viscosity, V=50 ft/s. Ratio of local and tank average solids mass fraction as a function of height above tank bottom. Data from Table B-18, Fort et al. (1993)

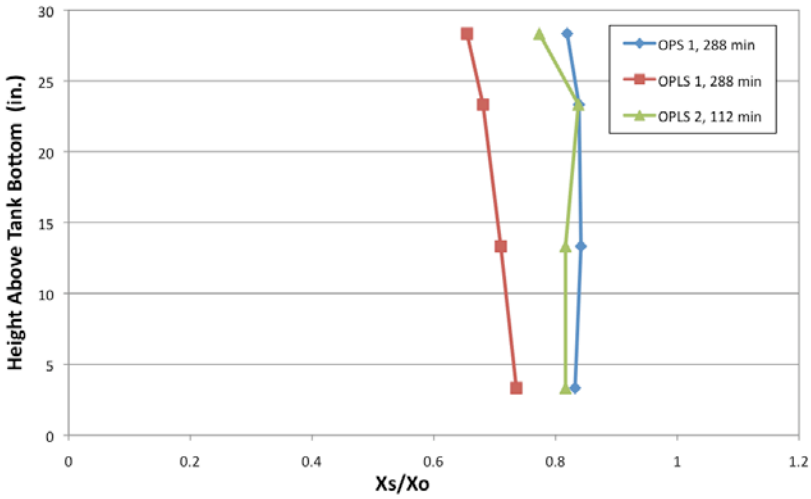

Figure 4.9. Ratio of Local and Tank Average Solids Mass Fraction as a Function of Height Above Tank Bottom for Ops 1, OPLS 1 and OPLS 2

4.1.2.3 Hanford Full-Scale Mixing and Comparisons to Scaled Tests

As referenced in Section 1, centrifugal jet mixer pumps have been used in Hanford tanks AZ-101 (baseline configuration mixer pump test, Carlson et al. 2001), SY-101 (mitigation of sediment gas retention, e.g., Allemann et al. 1994, Stewart et al. 1994), and AP-102 (mixing efficiency, Hunter 1987). Data from these mixer pump operations are considered with regard to the distribution of mobilized solids in the tank during mixing operations.

AZ-101 Full-Scale Test

The baseline mixer pump operation tests in AZ-101 are described in Carlson et al. (2001). Two 300-hp Lawrence mixer pumps take fluid in from approximately 12 in. above the tank bottom and discharge it horizontally from two opposed 6-in.-diameter nozzles at nominally 18 in. above the tank bottom. Mixer pump 1 was initially operated with the horizontal nozzle discharge at five fixed radial directions through a series of tests typically incrementally increasing in pump discharge speeds of nominally 725, 1,000, and 1,150 rpm. The pump was operated at each speed for approximately 3 hours.

Mixer pump 1 was then operated in oscillation mode (horizontal nozzle discharge, 180º pump rotation at 0.05 and 0.2 rpm) at each of the three nominal velocities totaling an operating period of almost 3.5 days. Mixer pumps 1 and 2 subsequently operated at equivalent rates, again ramping up at nominally 725, 1,000, and 1,150 rpm over a total operating period of approximately 11 days. The nominal operation rates approximately correspond to 7,100, 9,200, and 10,500 gallons per minute (gpm) total flow, or 12.3, 15.9, and 18.2 m/s for each nozzle (Wells and Ressler 2009).

Two specific test sequences were conducted to evaluate UDS suspension as a function of pump operation as reported in Carlson et al. (2001). In the initial sequence, both mixer pumps were simultaneously operated in oscillatory mode for 19 hours at nozzle velocities of approximately 12.3, 15.9, and 18.2 m/s. The operating time of 19 hours was selected as it represents the time required to transfer 600,000 L of HLW at a nominal flow rate of 530 L/min (140 gpm). The second test sequence was similar except that only mixer pump 1 was operated.

Gamma profiles and Suspended Solids Profiler (SSP) readings were taken after the mixer pumps were shut off at the end of the 19-hour period. A gamma profile is produced by the gamma-monitoring systems which detect radionuclides, and the SSP uses light reflectance to determine turbidity. Both instruments can therefore be used to evaluate UDS concentration.

The SSP data collected nominally 40 minutes after cessation of mixing were qualitatively examined by Carlson et al. (2001) to determine the effect of pump operation on UDS suspension quantities and profile, Figure 4.10. Each SSP profile required 6 to 12 minutes to traverse from 33 to 300 in. above the tank bottom. Carlson et al. (2001) note that the UDS concentration profiles throughout the range of pump operation are relatively similar in that the suspended UDS is uniformly distributed with lesser concentrations in the top 2 to 3 ft of the measurement range. More UDS appears to be suspended at higher pump speeds and with both mixer pumps operating. It is emphasized that the SSP data can only be used as relative values for comparison between different test conditions due to lack of instrument calibration.

Carlson et al. (2001) used the SSP data to compute the mass of UDS suspended by the range of mixer pump operations (Table 4.1). As indicated with respect to Figure 4.10, more UDS mass is computed to be suspended at higher pump speeds and with both mixer pumps operating (mixer pump 1 at 1,000 rpm does not follow the trend). Carlson et al. (2001) note that the estimated mass of UDS suspended determined from the SSP data appears to be consistent with that based on grab sample data for concurrent pump operation at maximum speed.

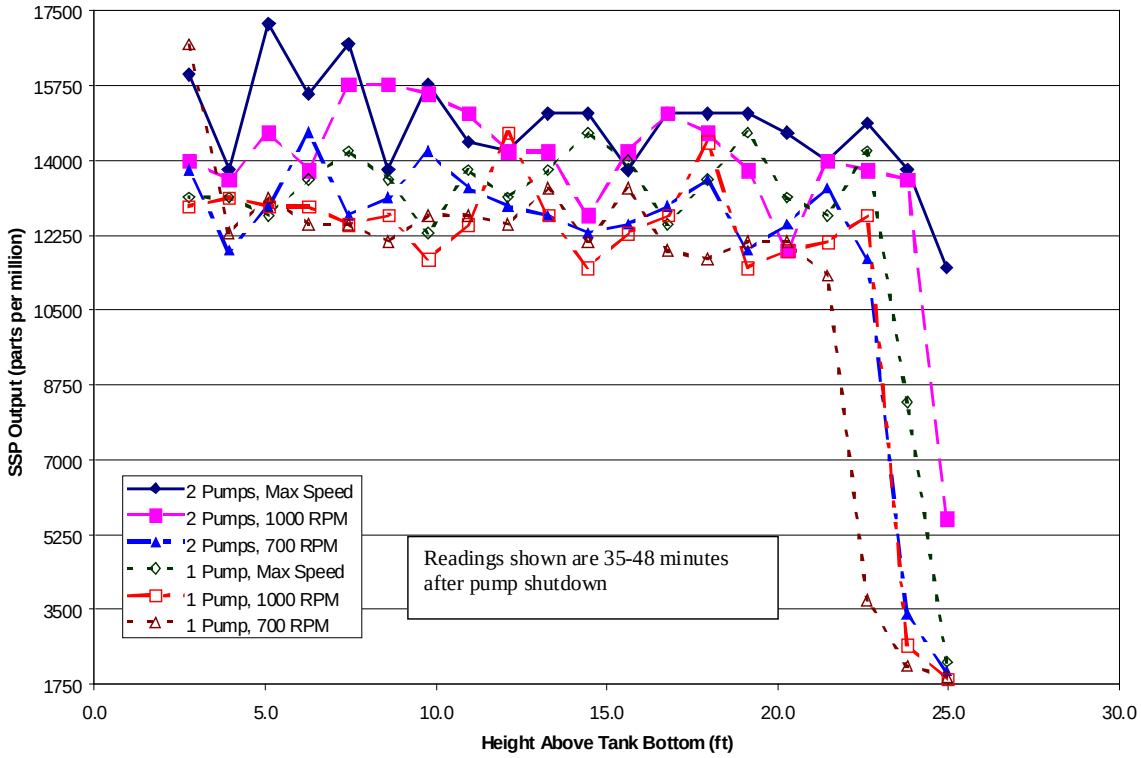

Figure 4.10. SSP Data from Suspension Testing at Various Pump Conditions (Figure 5-20 of Carlson et al. 2001)

Table 4.1. UDS Mass Suspended Computed from SSP Data as a Function of Mixer Pump Operating Conditions (data from Table 5-9 of Carlson et al. 2001)

Pumps Operating	Operating Speed (r/min)	Solids Suspended (kg)[(a)]
1 and 2	Maximum	40,100
1 and 2	1,000	36,100
1 and 2	700	32,800
1	Maximum	32,300
1	1,000	29,400
1	700	31,100

(a) Values based on shop test calibration curve of a different probe using simulated waste.

As reported in Wells and Ressler (2009) from analysis of the gamma data, only 32% of the UDS waste inventory was suspended at concurrent pump operation at maximum speed. The suspension of 32% of the total UDS mass above 38 in. represents 45,300 kg, and this is in close agreement with the suspended mass above 33 in. of 40,100 kg estimated from the SSP data as listed in Table 4.1. As discussed in Section 3, the waste in AZ-101 was non-cohesive (uniform as indicted by the data, UDS mass fraction of 0.01) above 38 in. (0.97 m), and cohesive below 38 in. (assuming uniform distribution, UDS mass fraction is 0.21).

The mass fraction of UDS suspended in AZ-101 above 30 in. as a function of the pump operating conditions can be estimated by assuming that concurrent pump operation at maximum speed from the SSP data of Table 4.1 is equivalent to that estimated in Wells and Ressler (2009). The effect of pump operation speed and number of pumps operated is shown to be minimal (Figure 4.11). Although the previously discussed trends of increased suspension with pump speed and number are apparent, the uniform UDS mass fraction is essentially constant at 0.01 (non-cohesive, see Section 3). It is possible to argue that the rate of increased UDS mass suspended with increasing nozzle velocity is greater for concurrent mixer pump operation, but if the displayed trend continues, extremely high nozzle velocities are indicated to achieve homogenous mixing of the full tank contents (UDS mass fraction of 0.04, Section 3).

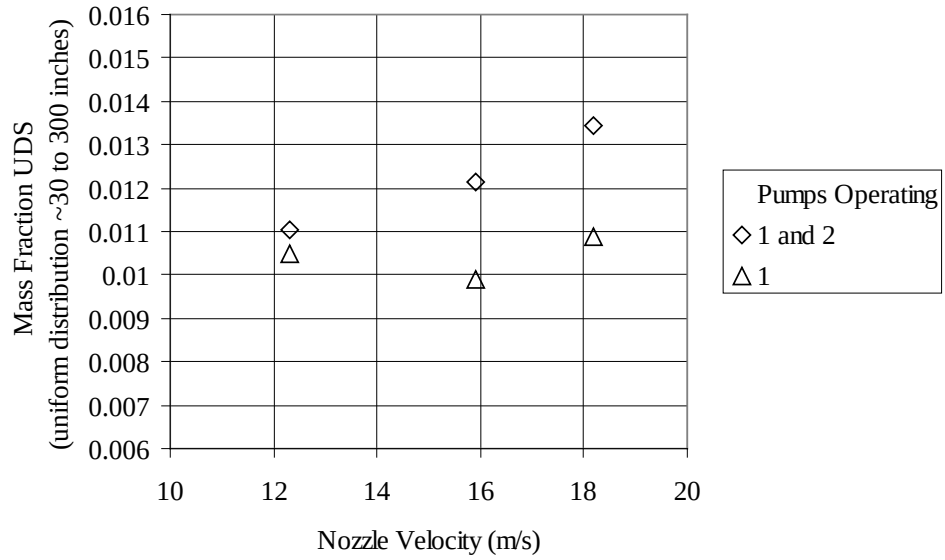

Figure 4.11. AZ-101 Uniform Mass Fraction UDS above 30 in. as a Function of Nozzle Velocity. The tank average wt fraction UDS is 0.04.

The mean particle diameters of the UDS suspended during the time period immediately following the final operation of the mixer pumps (the "settling test," Carlson et al. 2001) are reported in Bell (2001). Grab samples were taken at the elevation and time after the cessation of mixing as specified in Table 4.2. It is noted in Bell (2001) that at the time of the particle size analysis, the samples had evaporated to dryness and were stored in that condition for an extended period of time. It is further noted that the particle size "...results should be treated as suspect as related to their representation of the PSDs of the originally sampled materials." Regardless, all samples underwent similar processes, so sample result comparison is of interest.

As shown in Table 4.2, the mean particle size of the samples in the homogenously suspended region of the tank (i.e., above 38 in., see Section 3) was nominally a factor of 10 less than that at the 6-in. elevation. This result–smaller, more slowly settling particles homogenously suspended in the upper region of the tank with larger, slowly settling particles stratified at or near the tank bottom–agrees with the results of the 1/12-scale uniformity study as reported in Section 4.1.2.1. The result also supports the postulation that, given only a fraction of the UDS mass in AZ-101 was suspended (Section 3.1.2), it is reasonable to expect that this suspended UDS particulate was the "lighter" or easier-to-suspend material; i.e., the particulate with lower settling velocities. The data for composition of the centrifuged solids

reported by Bell (2001) (data also briefly summarized in Carlson et al. [2001]) showed only minor differences between grab samples taken at elevations of 6, 48, and 132 in., suggesting that for this particular tank the particles suspended into the upper region (generally smaller) had a similar composition to the larger particles that remained in the lower region.

Table 4.2. AZ-101 Grab Sample PSD Data (from Bell [2001] and Carlson et al. [2001])

Grab Sample Identification	Time After Mixer Pump Stopped (min)	Elevation (in.)	Mean Particle Size (μm) [1 standard deviation]
1AZ-00-35	11	6	482 [240]
1AZ-00-36	20	48	11.7 [5.9]
1AZ-00-37	44	90	53.1 [37.6]
1AZ-00-38	56	132	10.9 [6.2]
1AZ-00-39	81	174	27.6 [20.2]
1AZ-00-40	104	216	48.8 [33.7]

AZ-101/AY-102 1/22-Scale Tests

Laboratory geometrically scaled testing in a 40.5-in. flat-bottomed tank with two rotating dual-horizontal opposed jets has been conducted (Adamson et al. 2009). A two-component UDS simulant was used that consisted of gibbsite (up to 30 μm maximum particle size) at approximately 90% of the total UDS mass and SiC (particle size ranging from 50 to 165 μm) comprising the remaining 10%. The liquid simulant had a density of 1.289 g/mL and a viscosity of 2.55 cP. At particle densities of 2.42 g/mL (Wells et al. 2007) and 3.22 g/mL (Weast 1985) respectively, the settling velocity of the maximum size gibbsite corresponds to approximately one-third the *in situ* measured AZ-101 settling rate (see Section 3) and the SiC settles approximately 2 to 18 times faster.

With a UDS quantity in the test vessel approximating the scaled sediment depth in AZ-101, it can be inferred for nozzle velocities from approximately 3.4 m/s (two tests) to the maximum operated velocity of 8.5 m/s that the suspended gibbsite may be relatively homogenously distributed over the tank depth but the SiC is only suspended when directly impacted by the jets, thus creating an approximate two-layer stratification if the pumps were stopped. This stratification condition is qualitatively similar to that of the full-scale AZ-101 mixer pump test as discussed previously.

When the UDS loading was increased to the scaled sediment depth in AY-102, a nozzle velocity of approximately 4.3 m/s to 5 m/s (two tests) was required to suspend the gibbsite to the liquid surface. The increased UDS loading is therefore indicated to require an increased nozzle velocity to distribute the gibbsite over the tank depth homogenously. The effect of increased loading on UDS suspension is referenced in Section 3, as Wells and Ressler (2009) postulated that the increased UDS loading in AY-102 (and also the increased particulate settling velocities, see Section 3.1.2) would be expected to reduce UDS suspension in AY-102 relative to AZ-101 for the same pump operating conditions.

SY-101 Full-Scale Test

A jet mixer pump was installed in SY-101 to mitigate gas retention and release (Johnson et al. 2000). Full-scale testing results from the mixer pump operation are provided in Allemann et al. (1994) and Stewart et al. (1994). At the time the mixer pump was installed, SY-101 was experiencing large buoyant displacement gas release events. SY-101 is a saltcake tank (greater than 85% by mass of the UDS are soluble salt species) (Weber 2008). The sediment layer was approximately 5.33 m thick (0.26 UDS mass fraction) with a total waste depth of 10.2 m, and the crust layer was approximately 1.3 m thick (Stewart et al. 1994, 2005).

The submersible mixer pump in SY-101 was a modified Barrett, Haentjens & Co. Model 10-in. GN, Hazelton Type "SSB" mixer pump from the Hanford Grout Program. The pump inlet is nominally 20 ft above the tank bottom with two horizontal-discharge, 2.6-in.-diameter nozzles at nominally 28 in. above the tank bottom. Full-scale testing was conducted at typical pump speeds 360, 750, 920, and 1,000 rpm, with corresponding nozzle velocities of approximately 7, 15, 18, and 21 m/s. The pump was operated at fixed radial directions for time intervals ranging from 5 minutes ("bumps") and longer (maximum time of pump operation was limited by the maximum pump motor oil temperature; 40 minutes at 920 rpm, 20 minutes at 1,000 rpm, etc.).

Given that the purpose of the mixer pump operation in SY-101 was to mitigate gas retention in the sediment, the focus of the data analysis of Allemann et al. (1994) and Stewart et al. (1994) was gas retention and release due to the mixer pump. However, the following qualitative information regarding solids mobilization and suspension is provided:

- The initial, low-speed bumping (seconds to minutes of operation at 340 to 380 rpm, approximately 7 m/s nozzle velocity) did very little to disturb the waste.
- More powerful bumps (5 minutes at 1,000 rpm, 21 m/s) increased the hydrogen concentration in the tank headspace, "...indicating that the 'canyon' around the nozzles was being excavated...hot material [i.e., sediment] had been injected into the convective [i.e., liquid] layer..." (Allemann et al. 1994).
- After a series of 30 incremental rotations, where the nozzle velocities ranged up to 21 m/s with operation times limited by the oil temperature (operations typically daily or multiple times per day over an approximate 2-month period), the waste was mixed to a "...nearly isothermal state..." (Allemann et al. 1994). Stewart et al. (1994) states that the waste at this point was "quite well mixed" with a settled layer (excavated when the pump was directed at it) approximately 1.3 m deep, and a mixed slurry layer at uniform temperature (i.e., it is a convective liquid) from 1.3 m to approximately 8.9 m.
- The pump is able to excavate more of the bottom sludge if run at maximum power. The behavior of the waste observed to date indicates that "...once the bottom sludge is excavated and mixed by the pump, it will tend to remain suspended" Stewart et al. (1994).

For the bulk of the operation of the SY-101 mixer pump, 1994 through 2000, the mixer pump was typically operated on a tri-weekly schedule and was incrementally rotated by approximately 30º (mixer pump rotated incrementally for approximately 180º, then reversed incremental rotation back to starting position; "return" rotation offset by 15º) for each operation. Thus, regions away from the orientation of the mixer pump were "undisturbed" for nominal 30-day periods.

As summarized in Gauglitz et al. (2009), the thermocouple profiles during the bulk of the mixer pump operation time period clearly illustrate the mobilization and resettling of a fraction of the sediment within a few days; the periodic mixer pump operations (and solids accumulation in the floating crust layer) resulted in a settled layer of approximately 50 in. in the "undisturbed" regions (Rassat et al. 2000). The yield stress of this settled layer, as measured with the ball rheometer, approximately 10 days after the mixer pump was directed at that location, was about 10 Pa at 24 in. above the tank bottom and 30 Pa at 6 in. (Stewart et al. 1996). The ball apparently did not reach the tank bottom, indicating that it was fully supported by the waste, which thus has a shear strength of at least 900 Pa (Meyer et al. 1997).

The mixed slurry layer between the floating crust layer and settled sediment layer was "...clearly a fluid as evidenced by its uniform temperature profile, the operation of the mixer pump, and the fact that particles and bubbles can move within it....ball rheometer data...showed no yield stress..." (Rassat et al. 2000). Rassat et al. (2000) estimated the *in situ* UDS volume fraction to be 0.15 (UDS mass fraction 0.21). Core sample segments taken from this slurry region had to be "...stirred with a spatula for the material to be transferred..." to an alternative container.[1] This apparent inconsistency, *in situ* fluid to ex-tank "solid," can be attributed to the precipitation of solids from the liquid as the sample cooled upon removal from the tank.

From Figure 3.7 in Section 3, a slurry with a UDS mass fraction of 0.21 may be expected to be non-Newtonian with cohesive particle interactions having an impact. This result is inconsistent with the *in situ* behavior of the SY-101 slurry as a convective liquid, thus indicating, as may be reasonably be expected (see Section 2), that different waste types have different rheology as a function of UDS content.

Although the long-term intermittent, short duration, operation of the SY-101 mixer pump and the apparent slow settling of the bulk of the suspended particulate (relative to that of AZ-101) make direct comparison to the baseline mixer pump operation in AZ-101 challenging, the data from SY-101 indicate that the bulk of the UDS was suspended above 1.3 m with mixer pump operation at nozzle velocities of approximately 21 m/s. The available data indicate that the suspended UDS was uniformly distributed.

Two qualitative results from the full-scale SY-101 mixing can be compared to the scaled experiments described in Section 4.1.2.2. These key results are 1) the bulk of the UDS that is suspended, and 2) the suspended UDS is uniformly distributed. The fraction of UDS suspended in the full-scale test was larger than in the small-scale tests (full-scale mixer pump operation was at a higher velocity than at small scale but had intermittent operation). In both the full-scale and scaled tests, the suspended UDS is uniformly distributed.

AP-102 Full-Scale Test

AP-102 was constructed to be the feed tank for the Grout Treatment Facility (De Lorenzo et al. 1994). An in-tank test of the 102-AP Mixer Pump (APMP) was conducted from 10/19/1987 to 10/24/1987 with the objective to develop a mixing efficiency curve (Hunter 1987). Mixing efficiency was investigated via tests in which the vertical and radial concentrations of liquid tracers and UDS were tracked with time.

[1] Numatec Hanford Corporation Internal Memo 82100-99-017, Process Chemistry, JF O'Rourke, to JC Person, May 3, 1999. Subject: *Results of Viscosity Measurements of Tank 241-SY-101 Samples.*

The pump is a 150-hp submersible mixer pump from the Hanford Grout Program (Carlstrom 1994), presumably an unmodified version of the SY-101 mixer pump described in Section 4.1.2.3.3. The pump inlet is nominally 6 in. above the tank bottom and it has two horizontal-discharge, 2.5-in.-diameter nozzles at nominally 18 in. above the tank bottom (Hanford Drawings H-2-76503 and H-2-76504).

One reading per-day pump data are provided in Hunter (1987). Limited inference can be made from the reported data regarding nozzle velocity during the tests. From the start of the test at 13:26, 10/19/87 through 14:13, 10/20/87, the "total pressure to nozzle" was 9 psig, and after 13:45 on 10/21/87 through the remainder of the test, 45 psig. However, the relatively constant "mixer pump amperage" with increased "total pressure to nozzle" may suggest that a restriction was added (e.g., partial plugging, restricted valve, etc.) to the pump system between 14:13, 10/20/87, and 13:45, 10/21/87, which would reduce the flow rate. For lack of more definitive data, the "total pressure to nozzle" in the initial portion of the test, 9 psig, is translated to nozzle velocity via the pump speed to nozzle pressure and pump speed to flow rate relations for the SY-101 pump from Allemann et al. (1994). A pump speed of approximately 450 rpm can be determined, which corresponds to a flow rate of approximately 1,050 gpm or nozzle velocity of 10 m/s. The pump was rotating during the test, but the rotation rate is not specified in Hunter (1987).

For the test, AP-102 was filled with approximately 350 in. (approximately 965 kgal) of raw (i.e., process) water, 0.6 kgal of 19M NaOH, 12 kgal of Na_2SO_4 at 130 g/L in water, 1 kg disodium fluorescein in 10 gal of water, and 50 tons of crushed-aggregate quarried limestone as UDS. The homogenous mass fraction of UDS is approximately 0.012 (1.2 wt%, Hunter 1987).

Grab samples were taken while the mixer pump was operating at three radial locations, which were risers specified as 1, 16, and 22 in Hunter (1987), and by comparing the configuration to the Tank 241-AP-102 TCR plan view, these risers are assumed to correspond to risers 3, 19, and 22 in Figure 4.12.[1] Samples were taken at each riser representing 12-ft vertical regions. Vertical sample locations within each vertical region were randomly chosen for each sampling event.

[1] TWINS: Tank Waste Information System database. http://twins.pnl.gov/twins3/twins.htm.

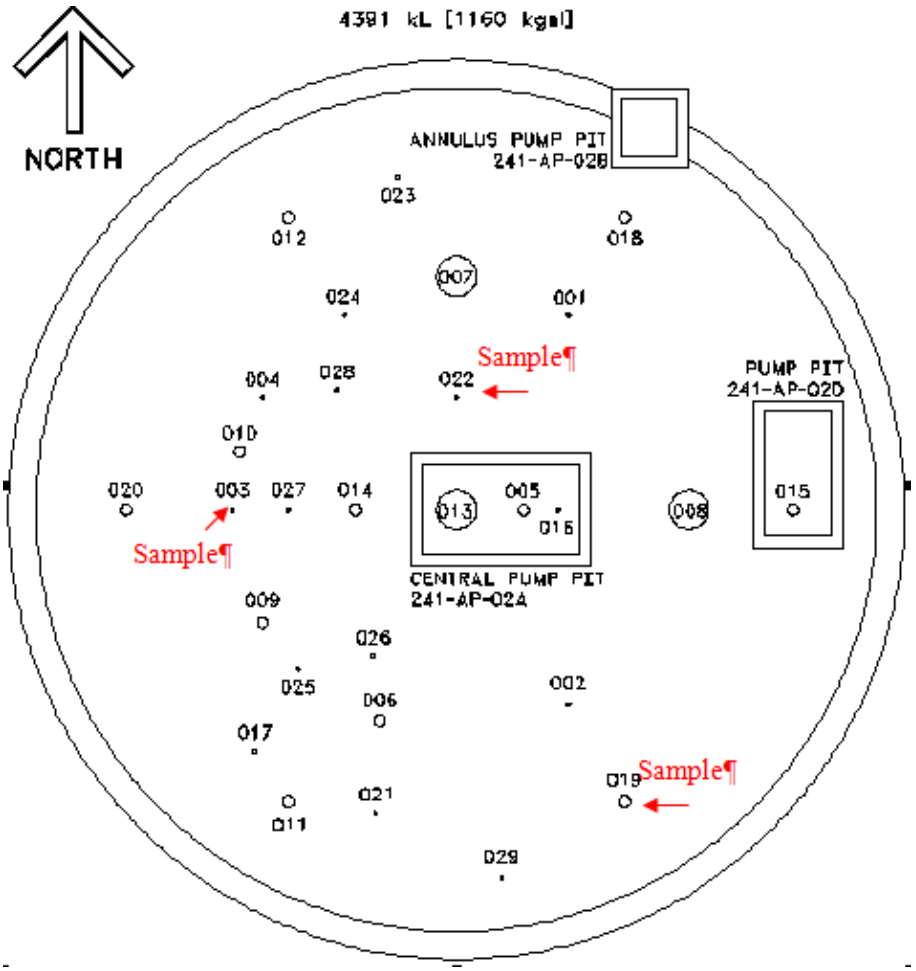

Figure 4.12. AP-102 Plan View With Grab Sample Risers Denoted

Hunter (1987) reports the following:

- Liquid concentrations approach well-mixed conditions rapidly. Fairly constant disodium fluorescein concentrations are attained at the three depths sampled after about 1 hour of pump operation in risers 1 and 16 and for sulfate in all three risers. The concentrations are very near the homogenous values.
- There is very little suspended material when the pump is off, and the suspended UDS concentration increases "significantly" when the pump is on. Measured UDS concentrations are an order of magnitude less than the homogenous 1.2 wt% value. Only about 10% by mass of the UDS are suspended. It is noted that the sampling methodology may bias the suspended UDS results low.

UDS mass concentrations in wt% with mixing time for risers 1, 16, and 22 (3, 19, and 22, Figure 4.12) are provided in Figure 4.13 through Figure 4.15, respectively. The concentrations at mixing time 0.01 hours correspond to the start of mixing and are essentially zero. The three vertical regions are represented by bottom, middle, and top, and two samples for each region at each time are shown. The data shown do not encompass the entire test period because mixer pump failure was reported before the 120 hour samples were completed (the mixer pump was off and had to be re-started).

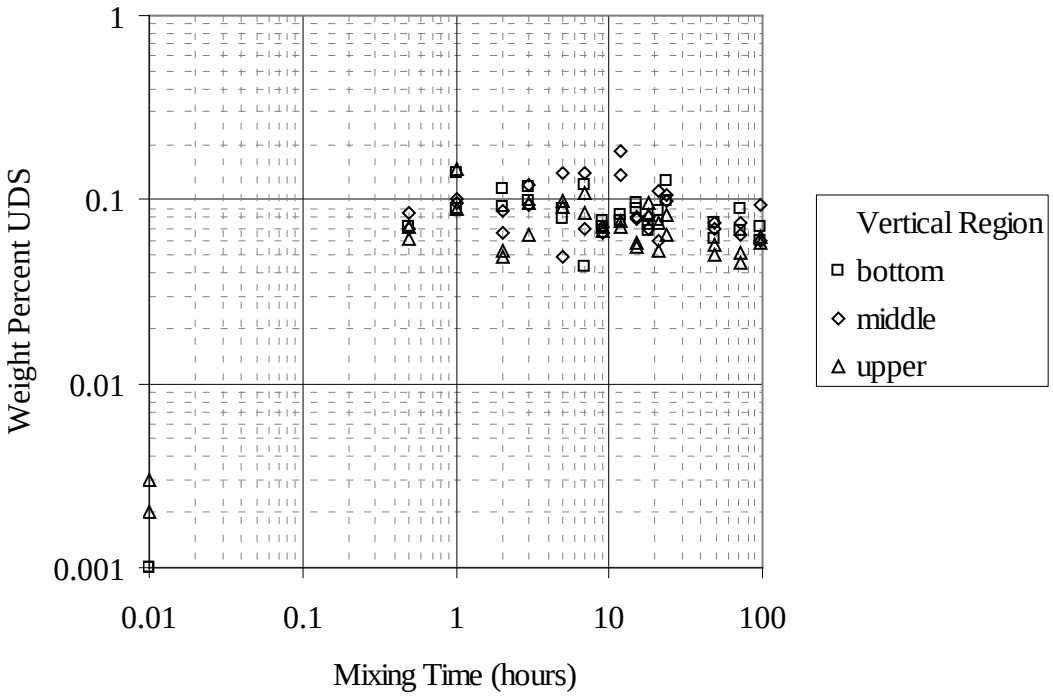

Figure 4.13. Riser 1 (3) UDS wt% as a Function of Mixing Time (Data from Hunter 1987)

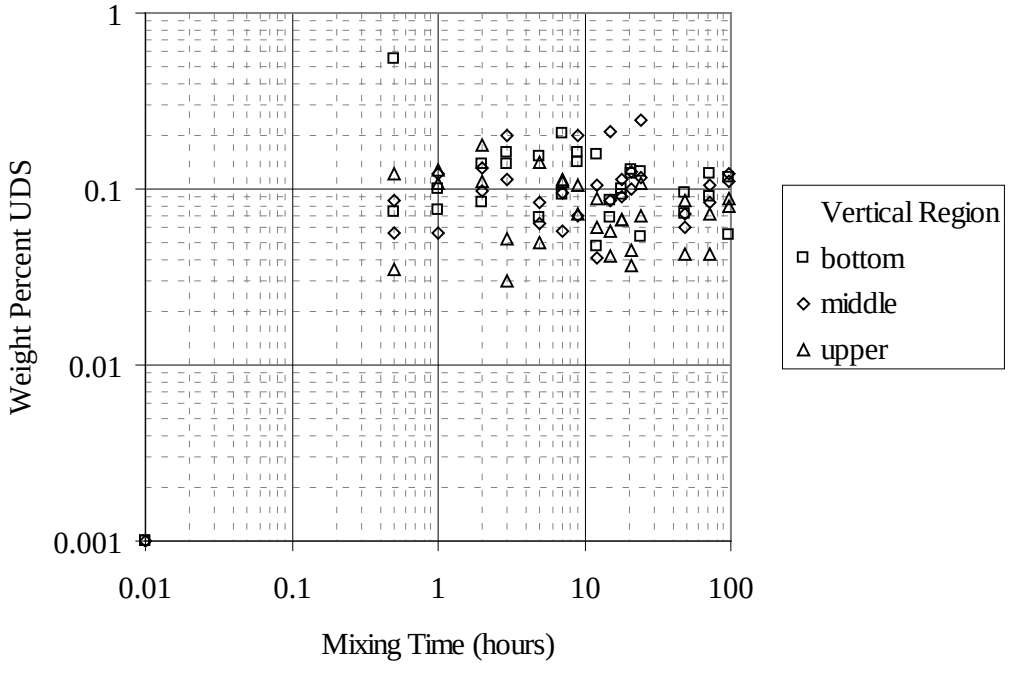

Figure 4.14. Riser 16 (19) UDS wt% as a Function of Mixing Time (Data from Hunter 1987)

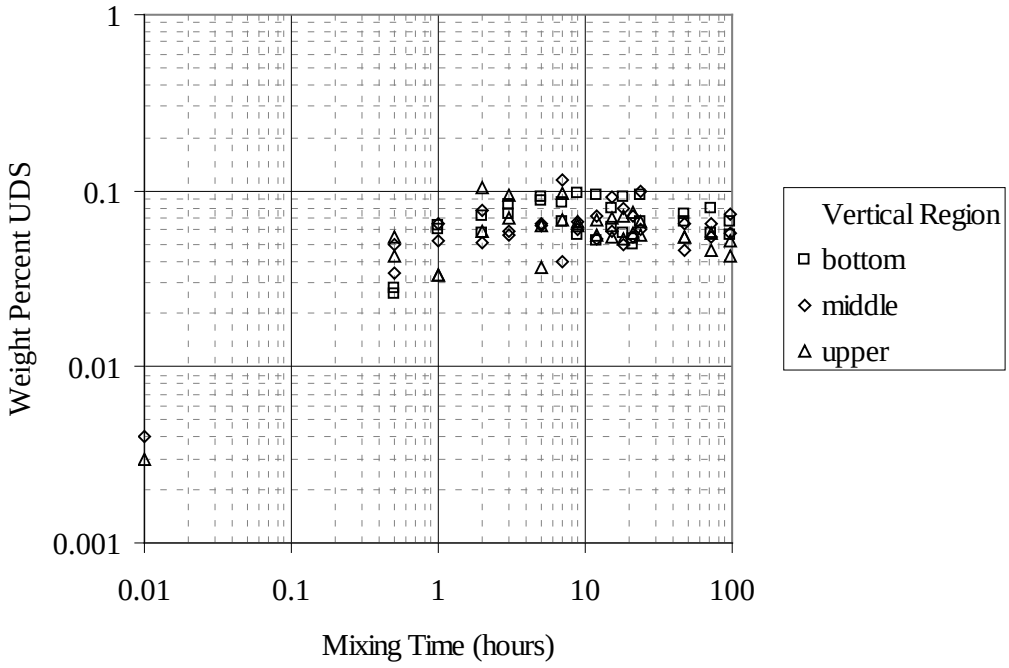

Figure 4.15. Riser 22 (22) UDS wt% as a Function of Mixing Time (Data from Hunter 1987)

At one-half hour of mixing time, the highest (~0.07 wt%) and most uniform distribution of suspended UDS was measured for the mid-radius riser 1 (3), although in the data scatter, there is no pronounced vertical stratification in any of the risers. The maximum uniform UDS wt% is approximately 0.1, which, as reported above, is an order of magnitude less than the homogenously mixed concentration. The nominally highest and most uniform concentration was achieved in the mid-radius riser 1 (3) at 1 hour mixing time, nearest-to-the-wall riser 16 (19) at 2 hours, and closest-to-the-pump riser 22 at 3 hours. The reductions in concentration observed after 24 hours of mixing time support the hypothesis described above that the relatively constant "mixer pump amperage" with increased "total pressure to nozzle" after 24 hours may suggest that a restriction reduced the mixer pump flow rate. The mixer pump "failure" is reported in Hunter (1987) after the 96 hour samples.

AP-102 Scaled Test

Laboratory-scale testing of the AP-102 mixing efficiency test was conducted in a 48-in. (about 1/19-scale) test tank (Hunter 1987). Limited information regarding the test parameters is available. The mixer is referred to as the "agitator," so it is uncertain that the mixing was due to fluid jets or a turbine agitator. However, sodium sulfate and disodium fluorescein were used as the liquid tracers, and limestone was used as the UDS. It can be estimated that the bulk mass fraction UDS is approximately 0.012, the same as the full-scale AP-102 test. Samples were taken for three vertical regions in the tank (lower, middle, and upper), but no radial location for the sampling is specified.

Hunter (1987) report the following for the laboratory-scale tests:

- "Bumping" the agitator "a few times" resulted in near uniform mixing of the sulfate tracer and some increase and layering of smaller diameter suspended UDS.

- Samples taken during "vigorous agitation" show that both the liquid tracers are distributed homogenously and that "some" of the limestone is suspended. Even with vigorous agitation, most of the limestone remains on the bottom of the tank.

The measured UDS concentration for the scaled testing relative to the fully mixed condition is shown in Figure 4.16 as a function of the level of agitation and sample elevation. Also shown in Figure 4.16 is the nominal full-scale result. The full-scale result line represents the uncertainty of the differences between the test scales in the actual level mixing and duration.

The UDS concentration in the scaled test is relatively uniform vertically in the test tank and nominally 16% of the UDS mass is suspended. 10% of the UDS mass was suspended relatively uniformly in the full-scale AP-102 test.

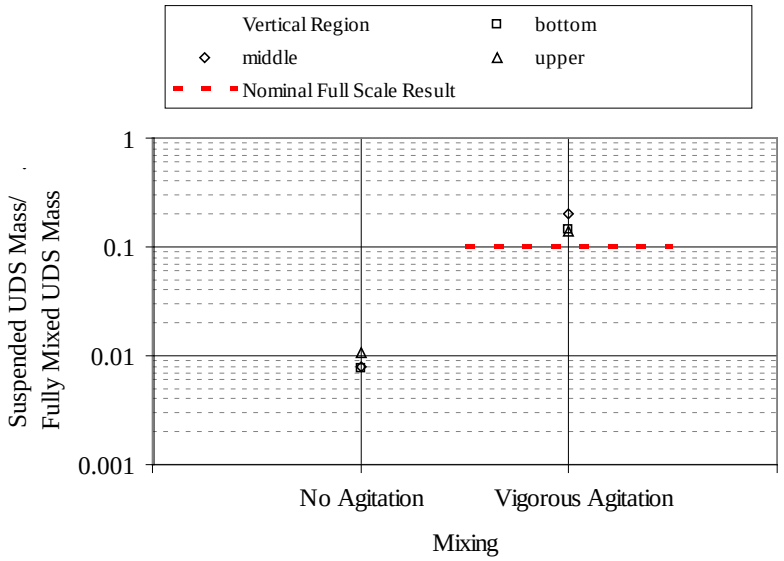

Figure 4.16. Scaled AP-102 Mixing Test UDS Concentration (Data from Hunter 1987)

No solid particle size or density is provided in Hunter (1987) for the limestone UDS. Powell et al. (1999b) report an average particle size by volume of 200 μm for the limestone they used, with 20 wt% of the particles below 90 μm and a maximum particle size of 1,000 μm.[1] If it is assumed that the limestone in the AP-102 tests in Hunter (1987) is the same as that of Powell et al. (1999) and that the suspended UDS is the "lighter" (i.e., slower settling velocity) particulate, it is reasonable to conclude that the suspended UDS particulate had a particle size less than 90 μm (less than 20 wt% of the UDS was suspended in the AP-102 tests). From Weast (1985) the crystal density of limestone ($CaCO_3$) is 2.93 g/mL. A 90-μm limestone particle has a settling velocity of approximately 7E-3 m/s (Equation 3.1, Section 3), which corresponds approximately to the 96th percentile by volume of the Hanford Case 3 PSDD (Section 3). This is an interesting result for understanding the AP-102 test, but the actual AP-102 UDS PSD is unknown. The data from the AZ-101 mixing test discussed throughout this report are a much better source of quantitative results on settling and suspension.

[1] MarbleWhite 30 crushed limestone (Synergistic Performance Corp., Seattle, Washington.

4.1.2.4 WTP PJM Tests

Scaled testing of the WTP PJM mixing systems has been conducted. Pulse jet mixing test results with relatively mono-dispersed noncohesive solids were compared to other mono- and poly-dispersed solids test results in Meyer et al. (2009). Results from these tests pertinent to the mixing of suspended particles are summarized. Mixing results from the cohesive poly-dispersed simulant of Kurath et al. (2009) are considered as well.

M3 Scaled Tests to Evaluate PJM Performance in WTP Mixing Vessels

Tests at three scales were conducted using various non-cohesive solids to evaluate the adequacy of mixing system designs in the solids-containing vessels in WTP (Meyer et al. 2009, Fort et al. 2010). The program addressed the effectiveness of the mixing systems to suspend settled solids off the vessel bottom and distribute the solids vertically. A range of solids loadings and operational parameters was evaluated including jet velocity (U), pulse volume (ϕ_p) and duty cycle (DC). Tests were conducted using 4, 8, and 12 PJMs with a range of nozzle sizes (d) to develop results that could be applied to the broad range of WTP vessels with varied geometrical configurations and planned operating conditions. Data for three metrics were collected, analyzed, and correlated: critical suspension velocity (U_{CS}) – the minimum velocity needed to ensure all solids have been lifted from the floor, solids cloud height (H_C) – the height to which solids will be lifted by the PJM action, and solids concentration vertical profiles (Meyer et al. 2009; Fort et al. 2010).

Correlation models were developed using a physical approach based on hydrodynamic behavior. In the critical suspension model the exponents on pulse volume fraction (ϕ_p=N V_P/V_{REF} = $NV_P/[\pi D^3/4]$)) and jet density (ϕ_J=Nd^2/D) were allowed to vary unconstrained from those in the H_C model. The correlation for U_{CS} is (see Fort et al. 2010, Equation 7)

$$\frac{U_{CS}}{U_{TH}} = 2.302\left[\frac{D^*}{Ga^{0.673}}\right]^{0.261} = 2.302\frac{\left[D^*\right]^{0.261}}{Ga^{0.412}} \tag{4.1}$$

where D* is a nondimensional critical suspension parameter which was written in terms of the hindered terminal settling velocity U_{TH} in place of the settling velocity U_T, and Ga is the Galileo number.

$$D^* = \frac{D(s-1)g\phi_s}{DCU_{TH}^2\phi_p^{0.898}\phi_J^{1,958}},\ U_{TH} = U_T\left(1-\frac{\phi_S}{0.6}\right)^6 \text{ and } Ga = \frac{\left(\frac{\rho_S}{\rho_L}-1\right)gd_S^3}{\nu^2} \tag{4.2}$$

By rearranging, U_{CS} can be written as:

$$U_{CS} = 2.302g^{-0.151}(s-1)^{-0.151}\phi_S^{0.261}D^{0.261}d_S^{2.588}DC^{-1}\phi_p^{-0.637}\phi_J^{-1.697}\nu^{-2.412}U_{TH}^{-0.739} \tag{4.3}$$

When all variables except scale (vessel diameter, D) are constant at two scales, the jet velocity to obtain the critical suspension is given by

$$\frac{U_{CS-LS}}{U_{CS-SS}} = \left(\frac{D_{LS}}{D_{SS}}\right)^{0.261} \tag{4.4}$$

and U_{CS} varies as (system size)^0.26. For constant power per unit volume, the exponent in this scaling relationship would be 1/3 so this result is somewhat similar to constant power per unit volume (see Section 4.1.3).

The cloud height model (H_C) includes the number of PJMs (N) as an independent parameter. As in the critical suspension model the exponents on ϕ_p and ϕ_J were allowed to vary independently. The model includes a jet Reynolds number term to account for geometric scale. The correlation for cloud height is (see Fort et al. 2010, Equation 10):

$$\ln\left[H_C^* \, \mathrm{Re}^{-0.143}\right] = 8.223\left(\frac{U}{U_{TH}}\right)^{0.1364} \tag{4.5}$$

where H_C* is the nondimensional cloud height and Re is the jet Reynolds number:

$$H_C^* = \frac{H_C (s-1) g \phi_S N^{0.658}}{DC \; U_{TH}^2 \phi_p^{0.898} \phi_J^{1.662}} \text{ and } \mathrm{Re} = \frac{dU}{\nu} \tag{4.6}$$

Rearranging shows

$$H_C = g^{-1}(s-1)^{-1} \phi_S^{-1} d^{0.143} DC \; N^{-0.658} \phi_p^{0.898} \phi_J^{1.662} \nu^{-0.143} U^{0.143} U_{TH}^2 \; e^{\left(8.223\left(\frac{U}{U_{TH}}\right)^{0.1364}\right)} \tag{4.7}$$

When all variables (including Reynolds number = dU/ν) except scale are constant at two scales, the cloud height scales as shown below where the ratio of jet diameter (d) is equivalent to the ratio of tank diameter (D).

$$\frac{H_{C-LS}}{H_{C-SS}} = \left(\frac{d_{LS}}{d_{SS}}\right)^{0.143} = \left(\frac{D_{LS}}{D_{SS}}\right)^{0.143} \tag{4.8}$$

For geometric similarity, d varies as D for a given test, thus the cloud height varies as (system size)^(0.14). While cloud height is very important for understanding vertical concentration profiles in PJM mixed vessels (Meyer et al. 2009; Fort et al. 2010), it is difficult to apply this result to the solids profiles in jet-mixed DSTs.

PJM Mixing Tests with AZ-101/102 Filtration Simulant

As reported in Meyer et al. (2009), the PJM mixing tests with AZ-101/102 filtration simulant tests described in Bontha et al. (2000) continue to be referenced frequently as PJM mixing tests with a broad distribution of settling solids. The simulant recipe was initially developed to physically represent the AZ-101/102 solids for cross-flow ultrafiltration equipment tests. To simulate the washed solids, the

aqueous liquid phase was water with 0.01 M NaOH. The recipe is described in full in Golcar et al. (2000), and the simulant PSDD is provided in Table 4.3.

Table 4.3. PSDD for AZ-101/102 Filtration Simulant

Particle Size (μm)	Volume Fraction	UDS Density (g/mL)
0.25	0.05	2.42
0.6	0.10	5
2.5	0.22	5
7.5	0.08	2.42
10	0.07	2.66
14	0.13	2.42
15	0.15	3.25
22	0.13	5
50	0.10	3.01

The vertical concentration profiles in the test vessel at prototypic nozzle velocities (8 m/s) are shown in Figure 4.17 for test Cases 1 through 6 from Meyer et al. (2009). The data are presented as the measured UDS concentration normalized by the total mass fraction of UDS in the vessel as a function of the sample elevation height normalized by the simulant depth. The specifics of the individual test cases are presented in Meyer et al. (2009). Broadly, the time of actual operation of the PJMs during the drive and refill cycle is decreased form Case 1 to 3 and Case 4 to 6. The total mass fraction of UDS for Cases 1 through 3 is 0.176, and 0.283 for Cases 4 through 6. Thus, as indicated in Figure 4.17, it is expected that mixing (fraction of suspended material and vertical homogeneity) will be reduced for lower drive times and at the higher UDS concentration. Well mixed homogenous conditions are shown for Cases 1 and 4.

PJM Mixing Tests with Glass Bead Simulants

Meyer et al. (2009) reported on the Bontha et al. (2003a) 75-μm glass bead PJM tests. These tests (denoted as Case 7) used a single loading of 10 wt% solids in water and four operating PJMs. This particle had a relatively high settling rate and was selected for this test to give incomplete suspension under normal PJM operations. Meyer et al. (2009) also reported on a second set of experiments from Bontha et al. (2003b) that used 35-μm glass beads. The two 35-μm glass bead tests are at 20 wt% solids: one test (denoted as Case 8) had four PJMs operating and the other (denoted as Case 9) at a reduced power level reflected by running just two PJMs. The PJM nozzle velocities are 6.8 m/s for Case 7, 8.3 m/s for Case 8, and 8 m/s for Case 9. Additional specifics of the tests are presented in Meyer et al. (2009).

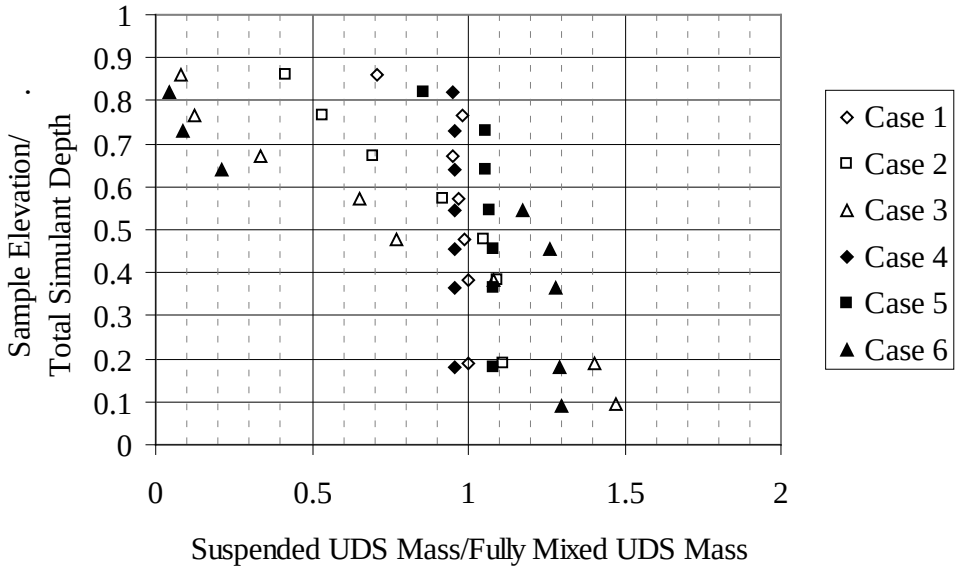

Figure 4.17. Bontha et al. (2000) AZ-101/102 Simulant PJM Mixing Test UDS Concentration (Data from Meyer et al. 2009)

The vertical concentration profiles in the test vessel are shown in Figure 4.18 for the glass bead test Cases 7, 8, and 9. The data are taken from Meyer et al. (2009). The data are presented as the measured UDS concentration normalized by the total mass fraction of UDS in the vessel as a function of the sample elevation height normalized by the simulant depth. Case 7, with the largest particulate and lowest nozzle velocities, shows the most stratification. Case 8 has better mixing than Case 9 as expected given the number of PJMs operating.

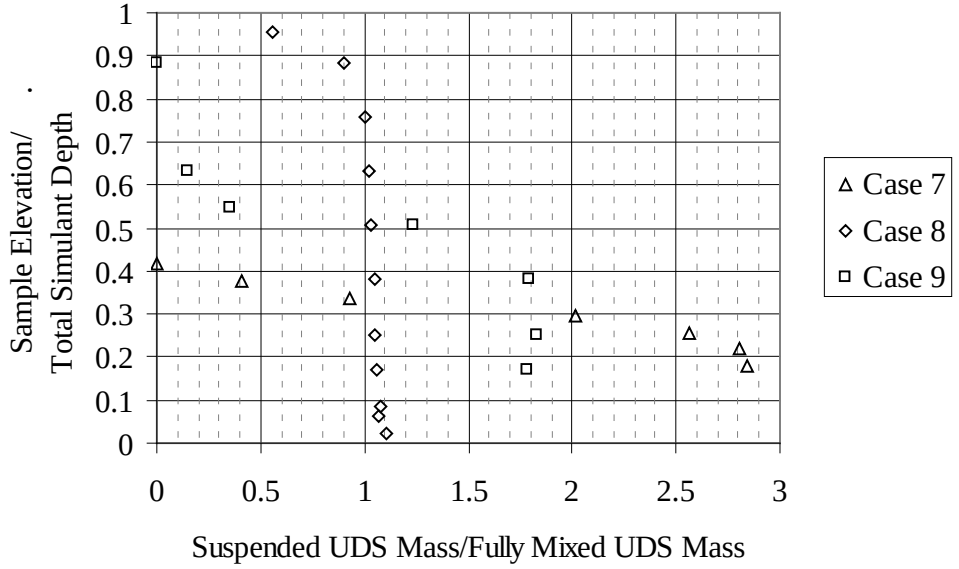

Figure 4.18. Bontha et al. (2003a and 2003b) Glass Bead Simulant PJM Mixing Test UDS Concentration (Data from Meyer et al. 2009)

PJM Mixing Tests with Chemical Simulant

Data were taken in PJM Tanks T01A and T02A of the Pretreatment Engineering Platform to look for evidence of stratification (Kurath et al. 2009). As reported in Kurath et al. (2009), the stratification tests were conducted to determine whether solids stratified or "settled" over an extended period of time (i.e., 36 hours) in Tanks T01A/B. Quadruplicate samples were taken from the inner-low, inner-middle, and inner-high sample locations near the center of the tank at 0, 12, 24, and 36 hours and analyzed for wt% UDS. Two separate, nearly identical tests were conducted. The first test is denoted as "TI-062" (conducted in Tank 01A) and the second as "TI-032" (conducted in Tank 01B). One test in T01A was conducted with PJM nozzle velocities of 7 m/s, and a second 12-hour test was conducted at 4.8 m/s. The stratification test in T01B was conducted with a PJM nozzle velocity of 4.8 m/s. Prototypic mixing was maintained (80% stroke length, 35-s cycle time). The total UDS mass fraction is approximately 0.055.

The vertical concentration profiles in the test vessels T01A and T02B are shown in Figure 4.19 and Figure 4.20, respectively. The data are taken from Kurath et al. (2009). As in the preceding sections, the data are presented as the measured UDS concentration normalized by the total mass fraction of UDS in the vessel as a function of the sample elevation. It is concluded in Kurath et al. (2009) that there is no statistically significant difference in wt% UDS with time or elevation. No effect of the reduction of nozzle velocity in T01A is observed.

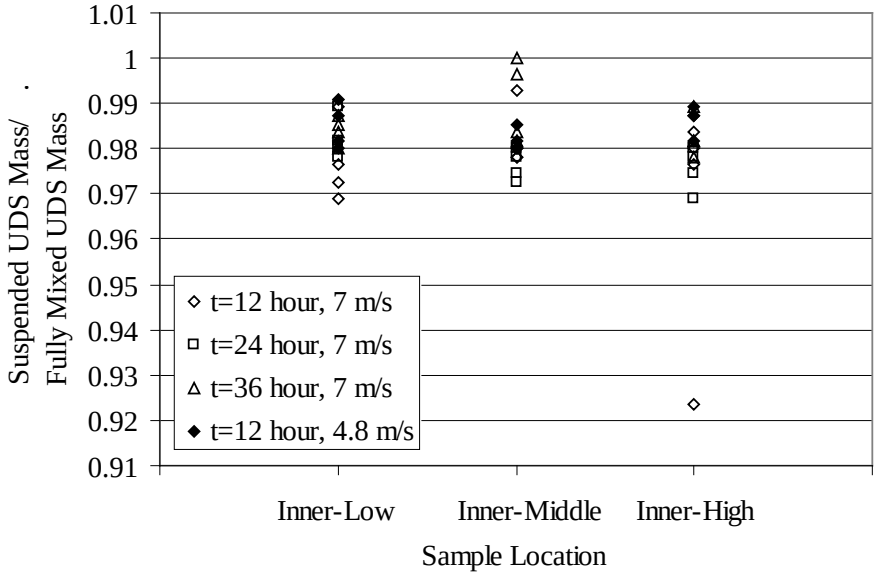

Figure 4.19. T01A Stratification Test Results (Data from Kurath et al. 2009)

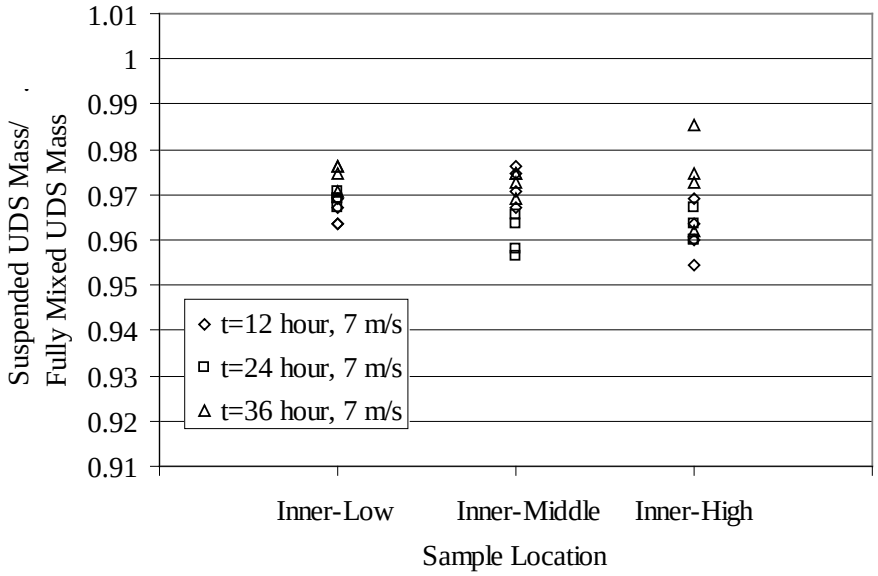

Figure 4.20. T01B Stratification Test Results (Data from Kurath et al. 2009)

4.1.3 Scale-up Relationships

There is very little information that directly shows the scale-up behavior for the concentration of mobilized solids in the upper mixed region of a DST. However, the results presented in Section 4.1.2 above allow three useful comparisons. These comparisons are between laboratory-scale tests and full-scale tank tests for tanks AZ-101, AP-102, and SY-101. For AZ-101 and AP-102, the laboratory- and full-scale tests both show an essentially two-layer stratification with only a fraction of the UDS mass (32% AZ-101 full-scale, 10% AP-102 full-scale, 16% AP-102 laboratory-scale) suspended uniformly to the waste surface while the remaining UDS mass is at or near the bottom of the vessel. Uniform suspension is again indicated for both the laboratory- and full-scale SY-101 tests, but whereas the bulk of the UDS mass is indicated to be suspended at full-scale, only approximately 50 to 75% by volume of the UDS is suspended at laboratory-scale. This result is counter intuitive to the mixer pump operations, but may be attributable to the difference of the UDS characteristics. Rassat et al. (2000) report that the actual SY-101 particulate "...are apparently quite small and/or they are close to neutrally buoyant because they remain in suspension with very little stratification over periods of a few days to over a week between mixer pump runs." Together, these three comparisons give the qualitative result that similar two-layer stratification with uniform concentration of suspended particles in an upper region occurs in both laboratory- and full-scale tests.

A very important series of scale-up studies was conducted for evaluating Flygt mixers for removing waste from tanks at SRS (Poirier et al. 1998a, b; Powell et al. 1999a, 1999b, 1999c). These tests were conducted in different size tanks with rapidly settling particles (zeolite and limestone that are essentially non-cohesive) and with kaolin clay layers for evaluating mobilization of cohesive sludge materials. The tests with rapidly settling particles are discussed here. Flygt mixers are axial flow mixers that were oriented horizontally on the tank floor to produce a horizontal flow along the floor. The Flygt mixers are certainly different from the jet mixer pumps used in Hanford DTSs, which is the focus of this report, but Flygt mixers still create turbulent jets that cause particle mobilization and suspension. The conclusion of the studies with rapidly settling particles is that scale-up of the Flygt mixers follows the constant power-

per-unit-volume relationship for achieving the condition of all-particles-in-motion (the specific relationship for jet velocity at constant power-per-unit-volume in jet mixed tanks is given below in Equation 4.9). Because of the difference between Flygt mixers and Hanford DST jet mixers, this power per unit volume scaling should only be considered as information on the general behavior of smaller scale tests.

As presented above in Section 4.1.2, scaled testing of PJMs also has provided scale-up relationships for non-cohesive particles. As with the Flygt mixers, the PJMs are certainly different from the jet mixer pumps used in Hanford DSTs, but the PJMs still create turbulent jets that cause particle mobilization and suspension. As discussed above (see Equation 4.4 in Section 4.1.2.4 and compare with Equation 4.9 below), the scale-up behavior for off-bottom suspension in vessels with PJMs followed a relationship that was similar to constant power-per-unit-volume. Because of the differences between PJMs and Hanford DST jet mixers, this result is again only an indication of general behavior.

To obtain constant power-per-unit-volume with jets in different size vessels (see for example Section 2.4 of Meyer et al. 2009 for an equation for jet power per volume), the jet velocity at small scale (U_{SS}) is related to the jet velocity at full scale (U_{LS}) and the vessel diameters as follows

$$\frac{U_{SS}}{U_{LS}} = \left(\frac{D_{SS}}{D_{LS}} \right)^{1/3} \tag{4.9}$$

This equation shows how smaller scale tests will need to be conducted at a reduced jet velocity if the goal is to have equal power per unit volume.

In the 1/22-scale tests of mixing for AY-102/AZ-101 conducted by Adamson et al. (2009a, 2009b), the jet velocity was varied but over a range of a reduced jet velocities in comparison to the full-scale velocity of 60 ft/s. Tests were only done in a single-size vessel so these tests did not provide information to compare with Equation 4.9. However, Adamson et al. (2009a) did use a qualitative visual comparison of surface flow in the scaled tests with video of the full-scale AZ-101 mixer pump tests to obtain a rough estimate of the jet velocity when the small tests visually matched the full-scale test. This comparison suggested that a jet velocity of ~14 ft/s[1] in the small-scale test approximates the surface flow at full-scale. Similar surface flows do not readily correspond to a similar distribution of solids, but this is an interesting result. For comparison with the jet velocity to have constant power per unit volume, Equation 4.9 gives a velocity of 21 ft/s for a 1/22-scale test with a full-scale velocity of 60 ft/s.

Overall, the results show that at all scales there is essentially no vertical variation in the concentration of particles at any specific test condition (jet velocity) in the upper mixed region. The actual particle concentration does, of course, depend strongly on the test condition. The results also show that the scaling relationship will probably be roughly similar to constant power-per-unit-volume for the suspension of particles and thus the particle concentration in the upper mixed region. Unfortunately, there is nothing that can be inferred from any of these studies on role of cohesive inter-particles forces on the scale-up behavior of particle concentration within the upper mixed region when the particles are both settling and cohesive. Finally, with any non-Newtonian fluid the shear rate will be higher in smaller tests.

[1] In Adamson et al. (2009a), the condition for equal surface flow was specified as 5 gpm, which we assumed is total flow for a pump with two nozzles. Using this flow and the information in Table 2 gives a jet velocity of 14 ft/s.

If the smaller tests are conducted at the full-scale velocity, the viscosity will be affected by the scale of the test through the shear thinning behavior of a non-Newtonian fluid.

4.2 Region 1: Pump Discharge Velocity

For a specific pump, the performance is typically determined by the manufacturer using water. If the pump is used with fluids other than water, changes in pump performance and power will occur if the fluid has a viscosity or density that are different from water. Charts showing correction factors for the role of viscosity and density are available (Hydraulic Institute 2000). In general, at a given rpm, an increase in fluid density will require more power, but the pump will still transport the fluid at the same flow and head. Increasing the fluid viscosity results in more frictional losses within the pump and a lower discharge flow at a given rpm, but the reduction in flow does not occur until the viscosity is moderately high. As described in Section 2, one effect of cohesive particle interactions is to increase the apparent viscosity of the suspension. In comparing suspensions where the only difference is whether the particles are non-cohesive or cohesive, the density of the suspension will be the same. Accordingly, the primary role of cohesive particle interactions will be an increase in viscosity and also shear thinning.

4.2.1 Effect of Cohesive Properties

Given the apparent viscosity and known pump performance with water, correction factors accounting for an increased viscosity on pump performance can be found. Figure 4.21 shows the correction factors for viscous liquids determined from the more general corrections given by the Hydraulic Institute (2000) that are based on empirical data for several single-stage centrifugal pumps. The data in this figure are for a pump capacity of 10,000 gpm for a rated head of 65 ft. Figure 4.21 shows that for a fixed rpm, the pump discharge velocity will not be degraded until the viscosity exceeds at least 100 cP. At lower viscosities, the pump performance is dominated by the fluid density.

When viscous losses become important, the majority of the viscous loss can be attributed to friction on the pump impeller. To determine the apparent viscosity of the non-Newtonian (shear thinning) waste, the shear rate in the pump must be estimated. Two different methods are used to estimate the shear rate. For the first estimate, the shear rate is estimated based on the flow between each vane in the pump. Assuming the flow between each vane can be modeled as laminar in a pipe, the shear rate, $\dot{\gamma}$, is estimated as (Munson et al. 2002)

$$\dot{\gamma} = \frac{8V}{d} \tag{4.10}$$

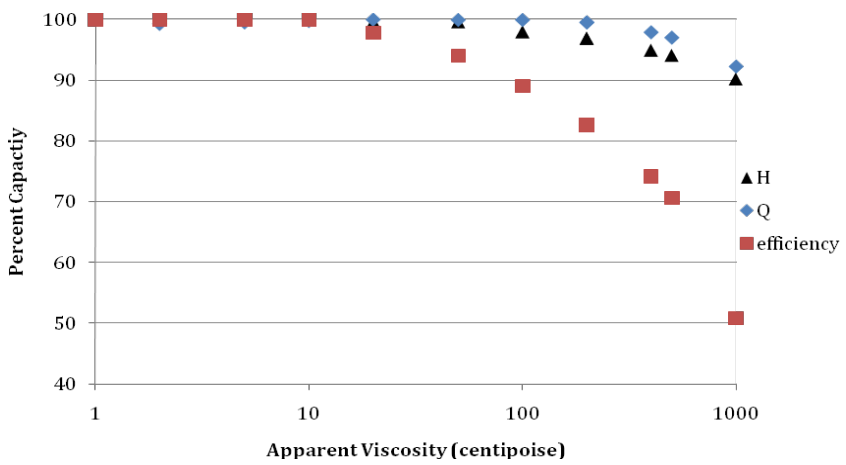

Figure 4.21. Pump Operating Capacity as a Function of Apparent Viscosity (rpm=1200)

In Equation 4.10, *d* is the average spacing between vanes and *V* is the apparent velocity determined from the total flow:

$$V = \frac{Q}{n_v A_v} \tag{4.11}$$

where n_v and A_v are the number of vanes and the flow area between a vane, respectively. The shear rate between the vanes for a centrifugal pump is estimated to be 1000 s^{-1} using Equation 4.10 and assuming $n_v = 7$ and $A_v \approx 1.7 \cdot 10^{-2}$ (m^2) between vanes.

A second estimating for the shear rate can be made by considering the distance between the tip of a vane and the impeller housing as shown in Figure 4.22. The tip velocity is the fluid velocity at given distance from the wall:

$$\dot{\gamma} = \frac{V_{tip}}{d} \tag{4.12}$$

where d is now the gap between the vane and the pump housing as shown in Figure 4.22, and V_{tip} is the tip velocity.

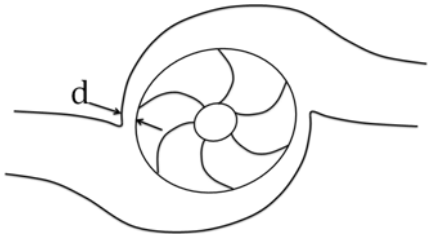

Figure 4.22. Centrifugal Pump Housing/Impeller Spacing

Using equation 4.12 with a gap of 1/4 in. and an impeller diameter of 18 in. rotating at 1200 rpm, the shear rate is 2200 s^{-1}. Both Figure 3.9 and Figure 2.3 give viscosity data for Hanford waste at 1000 s^{-1}.

These data show that the viscosity at this shear rate is less than 100 cP even at relatively high solids fractions, therefore pump discharge velocity should not be affected by the magnitude of cohesive inter-particle forces.

4.3 Region 2: Turbulent Jet Velocity Decay

For a turbulent jet in a Newtonian fluid, the velocity varies across the jet, decays with distance from the nozzle, and will be influenced by the presence of walls. For a Newtonian turbulent circular free jet, the maximum time averaged velocity u(z) , which is typically called the centerline velocity, at a distance z from the jet decays as

$$u(z) = c_J \frac{U_0 D_0}{z} \tag{4.13}$$

where U_0 is the nozzle exit velocity, D_0 is the nozzle diameter, and the coefficient c_J is a constant (see for example Equation 3.8 of Bamberger et al. [2005] or Rajaratnam [1976]). The primary objective of this report is to evaluate the difference between cohesive and non-cohesive materials in jet mixing, so the key question for Region 2 on jet velocity decay is whether turbulent jet studies have identified any significant difference between cohesive and non-cohesive materials. As described in Section 2, a primary effect of cohesive particle interactions is to make a slurry non-Newtonian with shear thinning behavior and potentially a yield stress.

4.3.1 Effect of Cohesive Properties

There are two studies that are particularly useful in evaluating the role of non-Newtonian fluid properties on the decay of a turbulent jet. One series of studies specifically measured the velocity and behavior of turbulent jet in yield stress fluids (Shekarriz et al. 1995, 1996, 1997a; Powell et al. 1997). In these studies, jets were studied in carbopol solutions that had a yield stress of about 1 Pa. The second study is by Fort et al. (1993), where velocity measurements were taken of a turbulent jet in series of 1/12-scale DST jet mixer tests.

The key finding from the studies with jets in yield stress fluids is that at a sufficient distance from the jet the presence of a yield stress dramatically reduces the jet velocity (Shekarriz et al. 1995, 1996, 1997a; Powell et at 1997). As shown in Figure 3.7, a 1 Pa yield stress is quite common in waste slurries, and if a jet mixed tank has a lower stratified region with a high solids concentration (see discussion in Section 3) , it is reasonable to expect a yield stress will be present and that this would dramatically reduce the jet velocity. Although there are no specific studies, it is expected that any significant shear thinning behavior in a non-Newtonian fluid will have the same effect as a fluid having a yield stress, which is simply a specific type of shear thinning fluid.

The second study useful in evaluating the jet velocity decay is the work by Fort et al. (1993). In this study, fluid velocities and solids concentrations profiles were measured in a 1/12-scale test of Hanford Tank 101-SY using a single, centrally located pump with opposed jets to mobilize and mix a settled slurry. The velocity data from this study will be discussed here, and the concentration profiles were discussed in Section 4.1. These tests used non-cohesive particles in aqueous solutions of sugar and water, so the data do not directly address the role of cohesive particle interactions, which is the primary object of this report. These tests did, however, use simulants that had different sugar concentrations to vary the viscosity of the

suspending liquid. As discussed previously in Section 2, one consequence of having cohesive particle interactions in a suspension is that the viscosity of the suspension will be increased. In Figure 4.23 and Figure 4.24 below, we will highlight data that show the roles of particles in general and the role of increased viscosity on measured fluid velocities. Two simulants were used in the study. A low-viscosity simulant that used a 2 wt% sugar water solution and a high-viscosity simulant that used a 20 wt% sugar water solution. Both of these simulants used the same particle, Minusil-30, at 33 wt%. Minusil-30 was described as having a mean particle size of about 10 μm. A particle size distribution for this material was not reported in Fort et al. (1993), but current product information for the particle size distribution for Minusil-30 is available (US Silica 2010). The jet diameter was 0.224 in., which was 1/12 of the full-scale nozzle.

Velocity measurements were made at a number of locations that are particularly useful for addressing the role of cohesive particle forces on the decay of a turbulent jet. Fort et al. (1993) made measurements for the jet velocity profile at different distances from the jet along the tank floor and also measured the vertical velocity as a function of elevation very near the tank wall. These velocity measurements were made for the three fluids tested: water, the low-viscosity slurry simulant, and the high-viscosity slurry simulant. For the jet velocity near the tank bottom, the key conclusion was that there was no difference that could be distinguished between the three fluids (see Section 5.3.1 of Fort et al. 1993). This result suggests that if cohesive particle interactions only changed the viscosity of a slurry, there would be only a small change in the solids total solids distribution.

Figure 4.23 shows the vertical velocity measured near the tank wall for water jets with different velocities. The vertical velocity is important because of its dominant role on lifting and suspending particles. The vertical velocity increases with increasing jet velocity as expected, but the magnitude of the increase is somewhat surprising. While the 42.5 ft/s jet has a vertical velocity that is approximately double that of the 24 ft/s jet, the vertical velocity for a 52.6 ft/s jet is ~4 fold larger that the vertical velocity for a the 24 ft/s jet. It is believed that the observed jet attachment to the floor causes this behavior, but this effect could not be quantified. The shift in the jet downward to the floor was observed to occur between the 42.5 and 52.6 ft/s jet velocity (see Figure 5.2 in Fort et al. 1993). The possible explanation for the increased vertical velocity at the wall for the highest jet velocity is that the rate of entrainment of surrounding fluid is lessened for the attached jet, and when reaching the wall it retains a higher peak velocity.

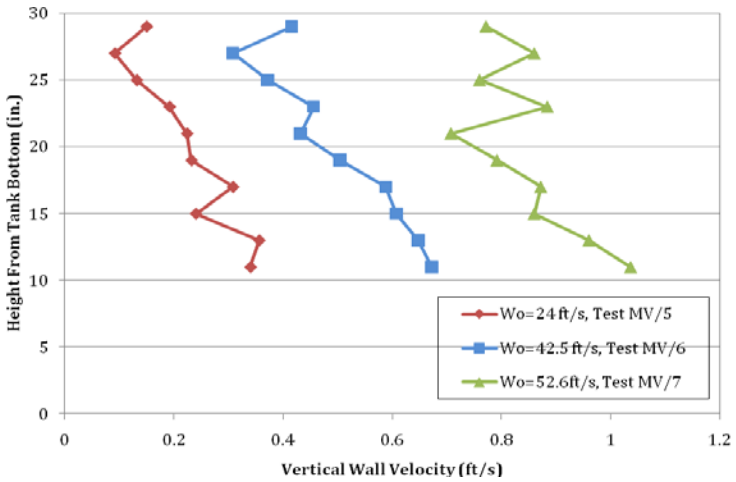

Figure 4.23. Vertical Velocity near the Tank Wall as a Function of Height from Tank Bottom for Water. Data from Figure 5.4, Fort et al. (1993).

Figure 4.24 compares the vertical jet velocity between tests with water and the two slurry simulants. The comparison in Figure 4.24(a) shows the difference between water and the low-viscosity slurry simulant at a jet velocity of about 40 ft/s. The slurry clearly has a reduced vertical velocity at the wall. In Figure 4.24(b), vertical velocities at the wall are compared for water and the high-viscosity slurry simulant at a jet velocity of 24.1 ft/s. For these conditions, the vertical velocity with the slurry is actually a bit higher than the water test. As described previously, a useful comparison for indirectly inferring the potential role of cohesive particle interactions is to determine the impact of increasing the slurry viscosity. The two tests with different viscosity slurry simulants were conducted at different jet velocities. To make a direct comparison, the vertical velocity for the high-viscosity simulant corresponding to a jet velocity of 40.9 ft/s was estimated by increasing the vertical velocity at 24.1 ft/s by the ratio of jet velocities (40.9/24.1). This comparison is shown in Figure 4.24(c). Based on this analysis, the vertical velocity is higher with the higher-viscosity slurry simulant, which seems counter-intuitive if the increased viscosity caused a faster decay of the jet velocity. One possible explanation is that with the higher-viscosity slurry there was less particle settling so the bulk slurry density was more uniform, and the vertical jet velocity was not reduced by vertical density variation.

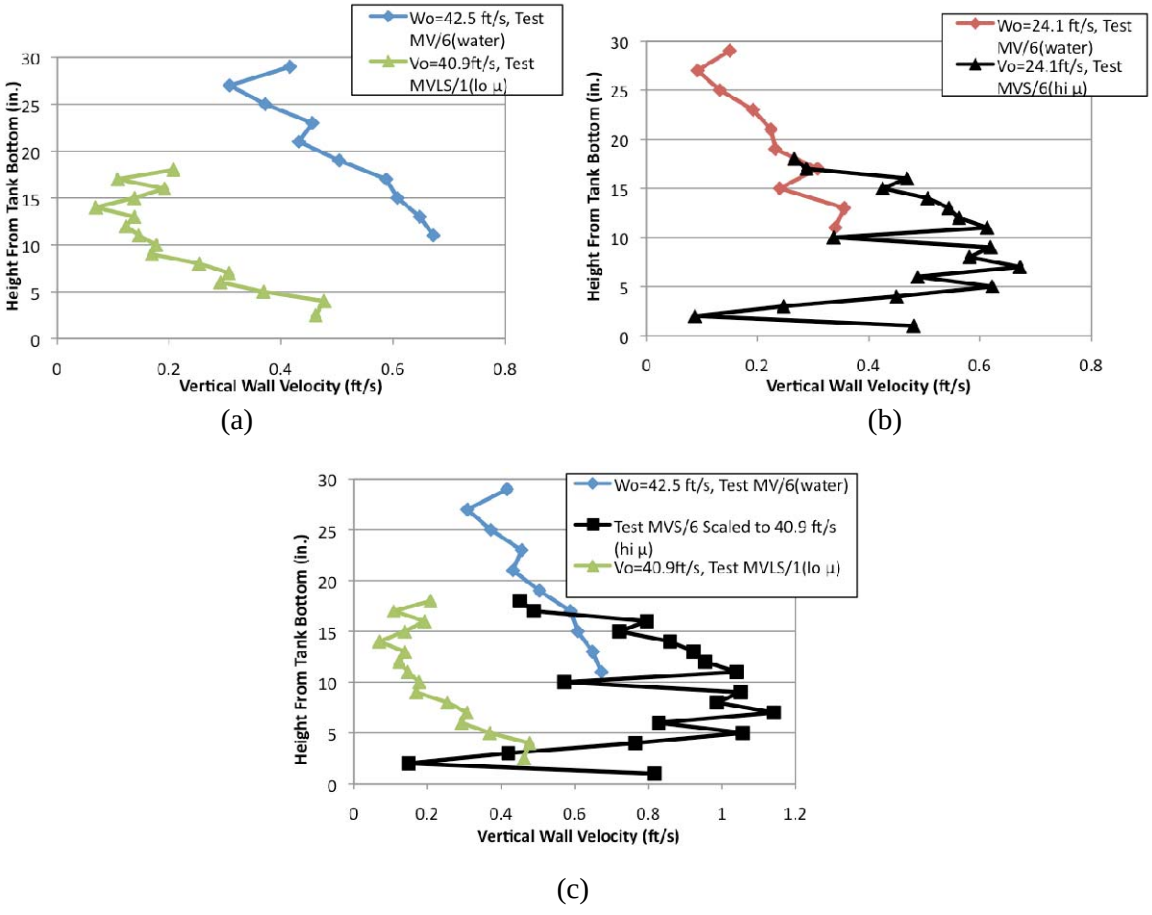

Figure 4.24. Vertical Velocity near the Wall as a Function Height from Tank Bottom for Various Simulants and Jet Velocities: (a) water and low-viscosity simulant, (b) water and high-viscosity simulant, and (c) water, low-viscosity simulant, and high-viscosity simulant scaled to 40.9 ft/s. Data from Figure 5.4, B.15, B.22, and B.25, Fort et al. (1993).

4.3.2 Scale-up Relationships

The centerline velocity decay of a circular turbulent free jet in a Newtonian fluid is well established and given by Equation 4.13. Equation 4.13 shows that the maximum velocity should increase proportional to the initial jet velocity and decrease with dimensionless distance from the jet (z/D_o). As described in the section above, the water velocity data in Figure 4.23 differ from this simple expectation. One possible explanation is associated with the jet attachment behavior. Because of this added complexity, it is difficult to estimate how an attaching jet will behave in different scale vessels.

4.4 Regions 3 and 4: Surface and Mass Erosion of Original Solids Bed

Erosion of solids by liquid flow occurs by many mechanisms. As summarized in Wells et al. (2009), surface erosion is the basic mode of erosion and occurs when individual particles are removed from the sediment surface. The rate of particulate removal can be faster than the rate at which the removed particulate mixes with the overlying fluid. The removal of a particle from the surface is accompanied by the replacement of an equal volume of liquid, which creates a resulting flow of liquid into and out of the pores at the surface of the sediment. The flow induced at the sediment surface by the removal of a particle can have the effect of increasing the sediment porosity at the surface. In instances where the sediment porosity at the surface is affected, the sediment swells as a result of hydrodynamic pressure fluctuation increasing the sediment porosity, which reduces the shear strength at the sediment surface. In cohesive materials, surface erosion occurs when the shear stress applied by the fluid to the surface is at or above the sediment's critical shear stress for surface erosion. For non-cohesive materials, erosion is expected to occur when the viscous drag force exceeds the submerged weight of the particle. Additional factors that influence whether the applied shear stress can remove the particle from the bed is the packing or interlocking of the particle relative to the adjacent particles. A detailed analysis of the particle would take into account the moments created by the drag and lift forces about a pinning point representing the particle's contact with a downstream stationary particle.

Mass erosion is described in Wells et al. (2009) as being independent of particle action at the surface of the sediment. It occurs when the shear stress applied to the surface of the sediment creates failure along a plane below the sediment surface. This phenomenon occurs when the applied shear stress exceeds a minimal macroscopic yield stress along a plane of the sediment and results in large portions of the sediment material being removed. These portions of material are intact as they leave the sediment and are not the result of rapid, localized surface erosion. The depths of the removed portions are significantly greater than the depth of any gradient in porosity resulting from surface erosion effects.

The ECR is the distance between the exit of the mixer pump nozzle and the base of the sediment eroded by the mixer pump via mass or surface erosion. As discussed in the section below, the ECR is expected to correlate linearly with scale based on an evaluation of numerous studies (Powell et al. 1997) and may also depend on the strength of the sediment. Powell et al. (1995b) identified that changing slurry rheology in the jet from Newtonian to non-Newtonian caused a significant reduction in the mobilization (erosion) of a clay layer, with a non-Newtonian jet requiring a 40% higher flow rate to achieve the same ECR as a Newtonian slurry jet. Thus, ECR scaling may be expected to be different for cohesive and non-cohesive slurries when the particle concentration in the slurry is high enough to create a non-Newtonian yield stress material.

4.4.1 General Description

In the late 1970s, studies at SRS were initiated to determine the key parameters affecting the ECR. The site conducted scaled tests with a clay simulant in a full-scale half-tank model and confirmed theoretical predictions that jets with the same momentum produce the same sludge-slurrying patterns. The ECR was proportional to the product of the nozzle velocity (U_0) and nozzle diameter (D_0). At the maximum U_0D_0 developed by the pump (~14 ft^2/s), the effective cleaning radius was ~20 ft (Bradley et al. 1977). SRNL also stated that reversing the direction of pump rotation increased the rate at which sludge was removed from behind larger obstructions.

Results of testing at SRNL in full-scale, half- and full-tank models developed the following effective cleaning radius relationship to predict the slurry pump requirements for sludge removal during waste mobilization, which relates sludge and pump characteristics to cleaning radius (Churnetski 1981, 1982):

$$ECR = KD_0U_0\left(\frac{\rho}{2\tau_0 g_c}\right)^{1/2} \tag{4.14}$$

where: D_0 = jet diameter
U_0 = jet velocity
g_c = constant
K = $C_1 \exp\{-C_2[\tan\theta]^2\}$
ρ = density
θ = jet half angle
τ_0 = yield stress.

4.4.2 Effect of Cohesive Properties

Powell et al. (1995b) conducted a particularly significant jet erosion test that quantified the effect of the jet and fluid causing the erosion having a yield stress and changing the effectiveness of the jet to erode a 640 Pa kaolin clay layer (see the discussion in Section 4.3.1 of Powell et al. 1995b). In this test, a xanthan gum solution with a yield stress of about 1.2 Pa was found to require a 40% higher flow to achieve the same ECR in comparison to a Newtonian (water) jet. One possible explanation, given later by Powell et al. (1997), was that the non-Newtonian xanthan solution formed a high-viscosity layer near the eroding surface that resisted the penetration of turbulent eddy bursts from the jet. This behavior of a non-Newtonian jet with a yield stress being less effective than a Newtonian jet is a significant finding in terms of the impact of cohesive particle interactions. Specifically, if the UDS concentration and particle cohesion are sufficiently high to create a non-Newtonian yield stress slurry, the effectiveness of a jet is expected to be diminished.

4.4.3 Scale-up Relationships

Powell et al. (1997) reviewed a wide range of ECR data and correlations from a number of studies that used cohesive sediments and concluded that the ECR scales with U_0D_0 as given in Equation 4.14 and also depends on the shear strength of the sediment being mobilized but not always by the relationship given by Equation 4.14. This scaling shows that for a given material the same velocity is needed at all scales to achieve the same dimensionless cleaning radius (ECR/D_0). This is an important scaling result that is specifically for the mobilization of a sediment layer. There are complications (see Powell et al. 1997 for the discussion) but there was rough agreement between tests at different scales and conducted by

different researchers that support this scaling. A more recent large-scale test by Enderlin et al. (2003) with a kaolin simulant and also a mixture of sand, zeolite, and kaolin provide additional ECR data. For the kaolin tests, Enderlin et al. (2003) noted the approximate value of 0.06 s/cm for ECR/U_0D_0 from previous studies of Powell et al (1995b). The ECR data from Enderlin et al. (2003) was somewhat smaller than this result but generally similar considering the more shallow geometry of their tests. None of the previous studies have specifically compared the laboratory ECR data with the limited Hanford tank mobilization data collected for AZ-101 and SY-101, and this comparison is given below. The comparison shows remarkable agreement between the laboratory tests with clay-based simulants, which are described as cohesive, and the full-scale tank behavior.

Another important behavior associated with scale up is the time scale for the transient growth of the ECR to a steady state value. Shekarriz et al. (1997a) addressed this specific topic, including reviewing previous data, and noted that the ECR should grow faster at smaller scale. They presented a limited amount of data comparing ECR growth rates in 1/50- and 1/25-scale experiments with kaolin clay that support the faster approach to a steady state ECR at smaller scale. Recognizing and accounting for this effect in small scale experiments is important. With any shear thinning fluid such as a cohesive slurry, tests done at reduced scale but with same velocity as full scale will have higher shear rates and therefore lower viscosities. This also needs to be considered in conducting small-scale experiments.

The effective cleaning radius for the full-scale mixer pump operations in Hanford DSTs AZ-101 and SY-101 are reported in Carlson et al. (2001) and Stewart et al. (1994). A summary of the mixer pump operations is provided in Section 4.1. The salient differences specific to the mixer pump operations are included in Table 4.4 together with the reported ECRs. The sediment in AZ-101 at the time of the mixer pump operations was approximately 17.5 in. deep at 0.48 UDS mass fraction (Wells and Ressler 2009) and 210 in. at UDS mass fraction 0.26 in SY-101 (Stewart et al. 1994, Stewart et al. 1995).

The relation of nozzle velocity and ECR from Table 4.4 is shown in Figure 4.25. Carlson et al. (2001) state "...the ECR for mixer pump 1 is significantly larger than for mixer pump 2...because the material [sediment] closer to mixer pump 1 had been disturbed during [prior] testing, and subsequent remobilization of that material was easier...". The difference between the ECR/$\mathbf{U_0D_0}$ of AZ-101 and SY-101 may be attributed to the difference in nozzle diameter, pump operation time (see Table 4.4), sediment depth, UDS concentration, and shear strength (shear strength discussed below). Also, as noted in Table 4.4, the SY-101 ECR may be a minimum distance. Further, the ECRs were not determined at a steady-state condition, they were the observed distance at the end of the mixer pump operation time.

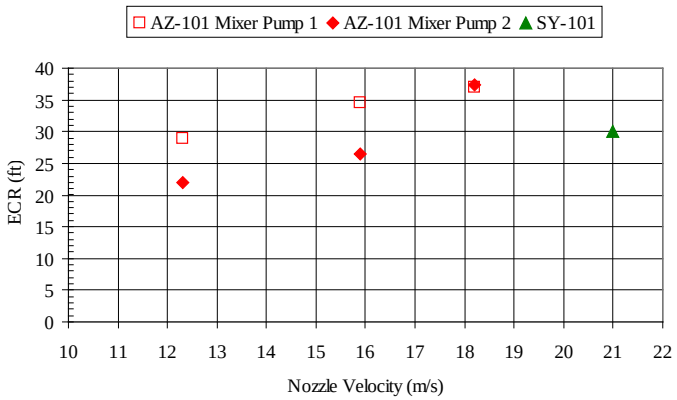

Figure 4.25. ECR as a Function of Nozzle Velocity, AZ-101 and SY-101 Full-Scale Mixer Pump Operation

As discussed previously, Powell et al. (1997) summarized scaled ECR tests. The ECR data from Powell et al. (1997) are provided in Figure 4.26 together with the full-scale ECR data from AZ-101 and SY-101 (Table 4.4). The median shear vane shear strength is 1770 Pa for AZ-101 and 730 Pa for SY-101 (Gauglitz et al. 2009).[1] These ECR data show remarkable agreement between the scaled clay testing and the full-scale *in situ* Hanford waste mobilization. This suggests that that the AZ-101 sludge sediment and the SY-101 saltcake sediment behave similar to clay simulants that are generally thought to be cohesive.

Table 4.4. ECR and Mixer Pump Operating Conditions (AZ-101: Carlson et al. 2001 and Wells and Ressler 2009; SY-101: Stewart et al. 1994)

Tank	Mixer Pump[(a)]	Nozzle Diameter (D_0) (in.)	Nozzle Velocity (U_0) (m/s)	ECR (ft)	ECR/U_0D_0
AZ-101	Mixer Pump 1	6	12.3	28.9	0.047
	Mixer Pump 1	6	15.9	34.5	0.043
	Mixer Pump 1	6	18.2	37[(b)]	0.041
	Mixer Pump 2[(c)]	6	12.3	21.9	0.036
	Mixer Pump 2[(c)]	6	15.9	26.4	0.033
	Mixer pump 2[(c)]	6	18.2	37.4	0.041
SY-101	Single Mixer Pump	2.6	21[(d)]	30[(e)]	0.066

(a) See Section 4.1. AZ-101 has two 300-hp mixer pumps. Reported ECR data for AZ-101 at mixer pump oscillation rate of 0.05 rpm; oscillation rates of 0.2 rpm were used in intermediary pump operations; see note b. 24-hours of operation was conducted at each nozzle velocity. SY-101 has one 150-hp mixer pump. ECR data for SY-101 at fixed nozzle direction.
(b) Longer operation of mixer pump 1 as part of the concurrent mixer pump operation extended the ECR to 37.4 ft.
(c) Prior and concurrent operation of mixer pump 1. The ECRs of the two mixer pumps overlap. Nozzle velocities of 12.3 m/s for mixer pump 2 could not be exceeded for 60º of the rotation. At higher speeds, mixer pump 2 was rotated manually; fixed orientation for nominally 1 to 2 hours, then manually rotated to the next fixed position, typically 10º from the prior position excepting the 60º at 12.3 m/s (pump speed was turned down for this region).
(d) Two once-per-day 40-minute mixer pump operations were conducted at approximately 18 m/s followed 3 days later by once-per-day 9 and 20 minute operations at 21 m/s.
(e) Distance at which a thermocouple tree response to mixer pump operation was observed. Thermocouple tree location may thus influence result, i.e., 30 ft may be the minimum ECR. See also note c.

[1] As shown in Gauglitz and Aiken (1997) and Weber (2008), *in situ* shear strength measurements and estimates for saltcake wastes are significantly lower than shear vane measurements for those wastes. No *in situ* shear strength measurements for the sediment in SY-101 prior to mixer pump operation exist.

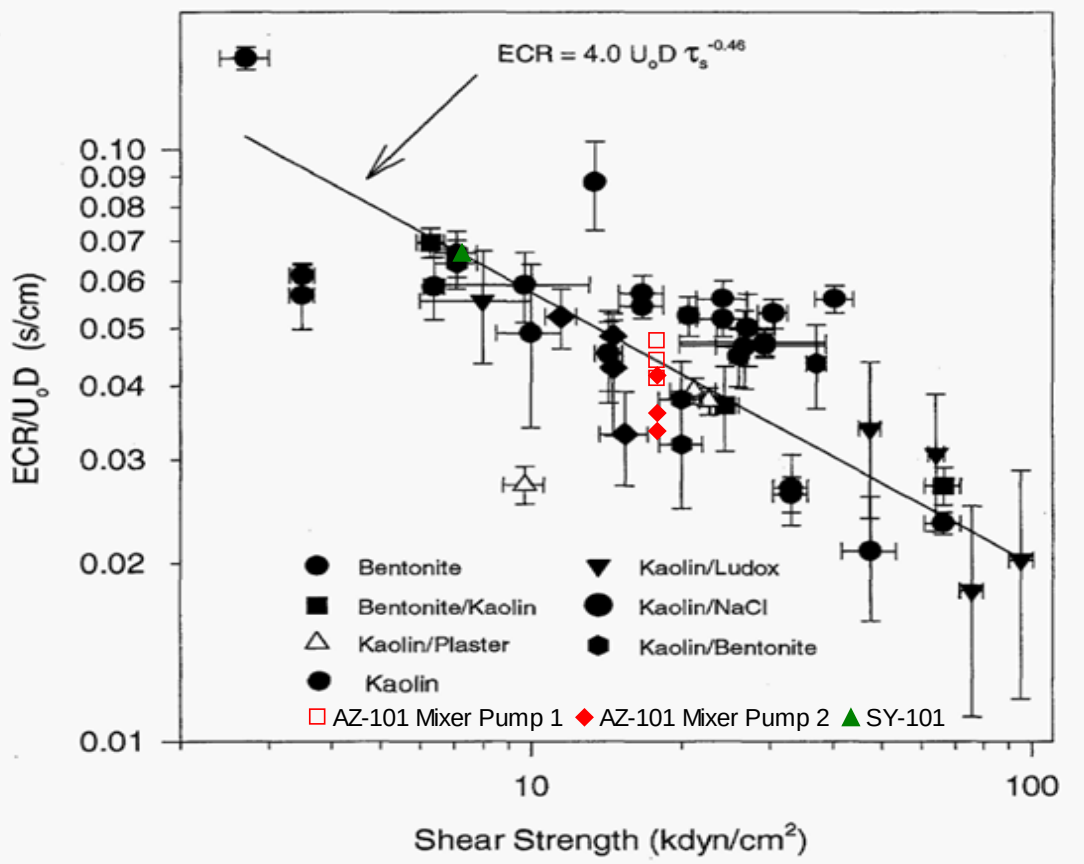

Figure 4.26. Mobilization Data (primary figure is Figure 4.5, Powell et al. [1997])

Adamson et al. (2009) reported the ECR for the laboratory geometrically scaled testing in a 40.5-in. flat-bottomed tank with two rotating dual-horizontal opposed jets (operated at approximate 0.7 rpm rotation rate). As summarized in Section 4.1, a two-component UDS simulant was used that consisted of gibbsite at approximately 90% of the total UDS mass and SiC comprising the remaining 10% in a liquid at 1.289 g/mL and 2.55 cP. No information for the rheology of the simulant sediment is available.

ECR data from the scaled experiments of Adamson et al. (2009) are provided in Table 4.5 together with operational parameters. As reported in Adamson et al. (2009), there was "very little difference" in the ECR data with or without obstructions (representing air lift circulators) in the test vessel. The ECR data provided in Table 4.5 are the average reported with and without obstructions. Tests were conducted with scaled sediment depths approximating AZ-101 and AY-102. Additional tests were performed with an intermediary UDS loading with one-half of the gibbsite mass as in the "AY-102" tests; gibbsite comprised approximately 84 wt% of the UDS, and SiC comprised 16 wt%. The ECR is listed as "MAX" in each test case for nozzle velocities above those reported in Table 4.5 (maximum nozzle velocities up to approximately 8.4 m/s were used).

Table 4.5. ECR and Operational Parameters (Adamson et al. 2009)

Representative Condition	Approximate Total UDS Mass Fraction (Gibbsite, SiC)	Sediment Depth (in.)[(a)]	Nozzle Velocity (U_0) (m/s)	ECR (in)[(b)]	ECR/U_0D_0[(c)]
AZ-101	0.03 [0.90, 0.10]	0.76	0.8	2.75	0.15
			1.7	6	0.17
			2.5	10	0.18
			3.3	12.5	0.17
			4.2	14	0.15
			5.0	15.75	0.14
Intermediate UDS Loading	0.06[(d)] [0.84, 0.16]	NA[(e)]	0.8	0	0
			1.7	4	0.11
			2.5	6.5	0.12
			3.3	8.5	0.12
			4.2	14	0.15
			5.0	16.5	0.15
AY-102	0.09 [0.90, 0.10]	2.49	0.8	0	0
			1.7	3.5	0.10
			2.5	6.25	0.12
			3.3	7.75	0.11
			4.2	12.5	0.14
			5.0	14.75	0.14

(a) UDS mass fraction of the sediment for the AZ-101 and AY-102 conditions can be estimated at 0.49.
(b) Average ECR with and without obstructions in the test vessel.
(c) Nozzle diameter D_0 = 0.27 in..
(d) Computed with the assumption that the liquid mass was the average of that estimated for the AZ-101 and AY-102 tests.
(e) No sediment depth reported.

ECR as a function of nozzle velocity from Table 4.5 is shown in Figure 4.27. As noted above for Figure 4.25 regarding the difference between the ECRs of AZ-101 and SY-101, increased sediment depth (total UDS concentration) apparently reduces the ECR for equivalent pump conditions (although no rheology data are available, the equivalent UDS composition and concentration in the sediment for the Adamson et al. [2009] AZ-101 and AY-102 tests indicates that the materials has equivalent rheology). Similarly, the scaled ECR/U_0D_0 values (Table 4.5) are shown to be impacted by the UDS concentration (Figure 4.28). No comparison can be made to the prior scaled experiential data nor the full-scale tests (i.e., as in Figure 4.26) given the lack of sediment shear strength data.

The effect of increased UDS loading causing a decrease in the ECR in the scaled testing of Adamson et al. (2009) supports the expectations described in Wells and Ressler (2009) and referenced in Sections 3.1, 3.3, and 4.1. Changes in the quantity of sediment that is mobilized will change the suspended UDS concentration, which then affects the cohesiveness of the slurry.

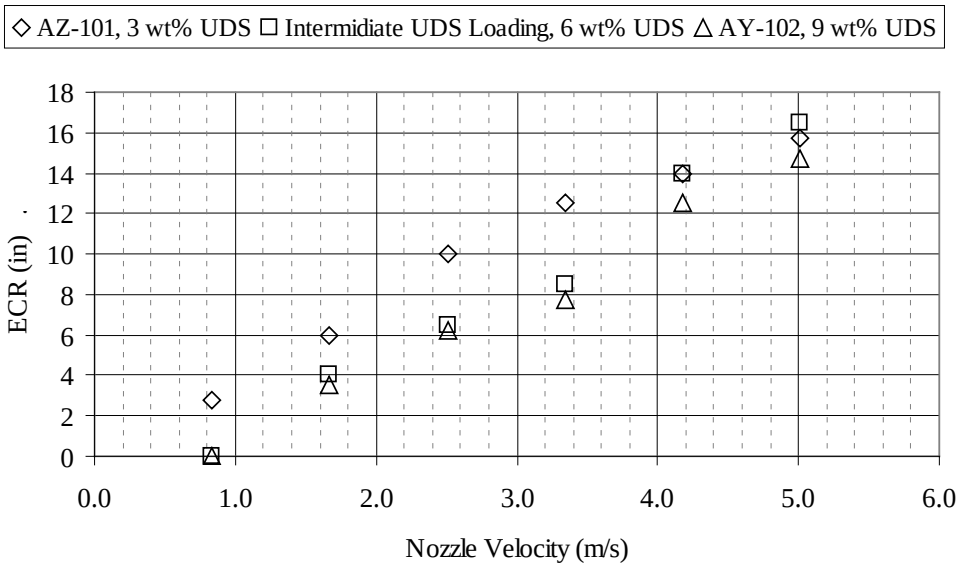

Figure 4.27. ECR as a Function of Nozzle Velocity for a Range of UDS Representing AZ-101, an Intermediate Loading, and AY-102 (Adamson et al. 2009)

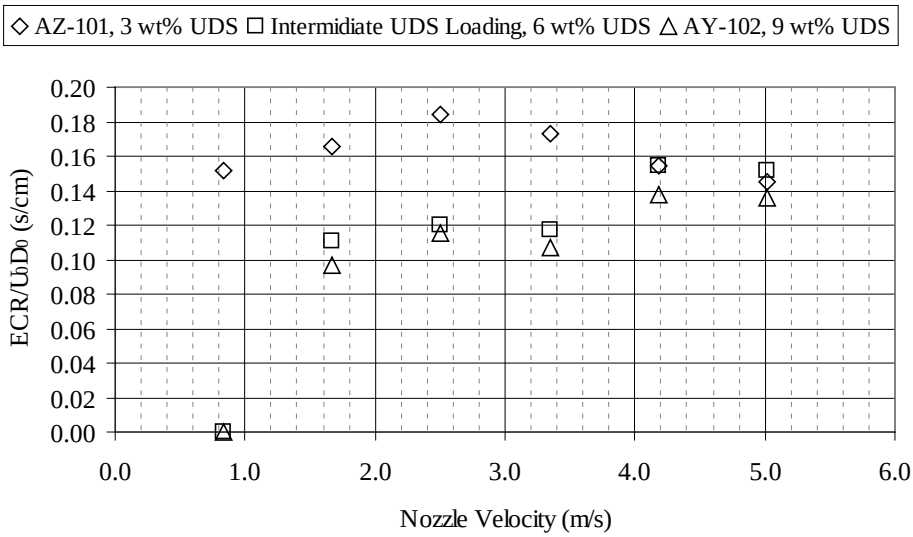

Figure 4.28. ECR/U_0D_0 as a Function of Nozzle Velocity (Adamson et al. 2009)

4.5 Region 5: Erosion of Weak Newly Settled Bed

There is very little information on the erosion of the material that is deposited at a distance from the jet after being mobilized from the region near the jet. In general, a newly formed bed will be much weaker and easier to mobilize than the original bed. However, it is still reasonable that a weak newly formed bed at sufficient distance from the jet will not be readily mobilized.

4.6 Region 6: Shear Strength of Original Bed

Particle cohesion is one of the main factors that affect the shear strength of the original bed, and the magnitude of the cohesive inter-particle forces also affects how a settled bed erodes. For example, for the same shear strength, material with different degrees of cohesive inter-particle forces will erode differently. Powell et al. (1995b) discussed how kaolin erodes differently than other clays. His erosion studies showed a weak shear strength (τ_s) dependence for kaolin, which was described as slightly cohesive, and a marked shear strength dependence for bentonite/kaolin mixtures, which were described as more cohesive than kaolin. Accordingly, the magnitude of the cohesive effects will affect erosion through both changes in the strength of a sediment layer and the mechanisms of erosion.

5.0 Discussion

In Section 4, previous studies were reviewed and analyzed to estimate the role of cohesive particle interactions on physical phenomena and specific regions that are important for the jet mixing and mobilization of settling particles. In addition to evaluating the direct and indirect roles of cohesive particles, brief discussions of scale-up behavior and how a small-scale test will behave was also presented. While each region was evaluated separately, the overall behavior of a jet mixed tank is a result of all the regions and their interactions. In the discussion below, the overall impact of cohesive particle interactions on solids uniformity in the mixed region of a tank is presented together with an overall assessment of the scale-up behavior that can be expected.

5.1 Overall Impact of Cohesive Properties

The evaluations in Section 4 show that cohesive particle interaction will have multiple effects through a number of different mechanisms. Some of the effects improve solids uniformity while others will likely degrade uniformity. To estimate the overall role of cohesive interaction, an overall assessment is needed for the combined behavior. Table 5.1 gives a summary of the estimated effects as described in Section 4.

Table 5.1. Summary of Role of Cohesive Particle Interactions on Solids Uniformity in Each Region

	Region	Impact of Cohesive Particle Interactions	Section
1	Pump Head	Negligible	4.2
2	Jet Velocity Decay	Uniformity worse – jet velocity decays faster when cohesive slurries are sufficiently concentrated to be non-Newtonian yield stress fluids, or any strongly shear thinning fluid, and evidence shows that a lower stratified region will be sufficiently concentrated to be non-Newtonian and affected by cohesive particle interactions	4.3 & 4
3, 4	Surface and Mass Erosion of Original Solids Bed	Uniformity Worse – erosion by turbulent jets is less effective when the jet is a non-Newtonian yield stress fluid, which is likely to occur due to stratification	4.4
5	Erosion of Weak Newly Settled Bed	Uniformity slightly worse – the newly settled bed should be sufficiently weak to fully erode; if not, the behavior will follow Region 3 & 4	4.5
6	Shear Strength of Original Bed	No direct effect	4.6
7	Mixing (Lifting and Settling) of Suspended Particles	Better – if cohesive interactions increase effective viscosity and slow particle settling Worse – if particle flocculation causes faster settling Worse – if upward jet velocity is reduced (see also Region 2)	4.1
	Overall	Potentially Worse	

Tank farm and scaled-test data suggest that a substantial fraction of the waste solids are not lifted above the bottom region of the tank but remain toward the bottom as a stratified layer. The evaluation

suggests that it is likely that the solids concentration in this layer is sufficiently high that the slurry will be non-Newtonian with a small but still significant yield stress. The yield stress is thought to be caused primarily by cohesive particle interactions. Studies have shown that even a small yield stress reduces the jet momentum away from the jet and reduces the ability of the jet to mobilize solids. It is expected that any significant shear thinning behavior in a non-Newtonian fluid will have the same effect as a fluid having a yield stress, which is a specific type of shear thinning fluid. Accordingly, the impact on jet velocity decay, shown in Table 5.1, is a greater reduction in jet velocity with cohesive particles, and this will ultimately reduce particle lifting and make uniformity worse. Surface and mass erosion will also occur less readily if the slurry has a small but still significant yield stress, and the impact shown in Table 5.1 for this region is that erosion will be less effective and this will ultimately make achieving uniformity worse. Regions 5 and 6 have a relatively small effect on the overall uniformity. The particle lifting and settling that occurs in Region 7 have a number of opposing effects, and it is difficult to estimate for this region the direct impact of cohesive particle interactions. Region 7, which can be considered the upper mixed region of the tank, is indirectly affected by changes in Regions 2, 3, and 4. Considering the overall interaction of all the regions, this evaluation suggests that the achieving uniformity in the mixed region will be potentially worse due to cohesive particle interactions, but the magnitude of the change is difficult to estimate.

The data and analysis given in Section 4.1 for the mixed region also shows that for the particles that are lifted into the upper region of the tank, the total particle concentration and the relative amounts of different size particles are extremely uniform in the upper region. However, in comparison to the overall concentration in the tank and the initial relative amounts of particles of different size, the material in the upper region is clearly different.

Finally, this study conducted an extensive review of the literature on the uniformity of suspended solids in jet mixed tanks. There are no existing studies or data that specifically quantify the role of cohesive interactions on uniformity. Simply based on the absence of any data, the conclusion is that testing with only non-cohesive particles will not be sufficient to meet the objectives of the Tank Mixing and Sampling Demonstration Program.

Because there is so little data to estimate the role of cohesive particle interactions on the suspension of settling particles, scoping experiments that would provide some results on the general behavior would be useful. Ultimately, careful quantitative tests will be needed to obtain performance data and scale-up behavior.

5.2 Overall Impact of Scale Up

There are two significantly different scale-up behaviors, discussed in Section 4, and there are additional interactions described in Section 4 that are known to be important but where there is too little information to judge their overall impact on scale up. The discussion in Section 4.1.3 highlighted some mixing studies that are relevant to jet mixing in DSTs, where the scale-up relationships for the just-suspended condition with non-cohesive particles followed constant power-per-unit volume. If actual scale-up behavior is similar to constant power-per-unit-volume, then the appropriate jet velocity in small-scale tests will be reduced in comparison to full-scale jet velocities. The discussion in Section 4.4.3 shows that for the erosion of a settled cohesive layer, the appropriate jet velocity to use in a small-scale test is the full-scale jet velocity. This assumes tests are conducted until steady state erosion conditions are

achieved. For any test that does not reach steady state conditions, the erosion rate needs to be considered, but there is little information on how to account for the erosion rate in scaled tests when tests do not reach steady state. Finally, with any non-Newtonian fluid the shear rate will be higher in smaller tests if the smaller tests are conducted at the full-scale velocity, so the viscosity will be affected by the scale of the test through the shear thinning behavior of a non-Newtonian fluid. Finally, the scale-up behavior of settling particles with cohesive particle interactions has not been determined in any test, and it is difficult to estimate based on the existing studies. Because there are at least two significant and different scaling behaviors (reduced velocity for one behavior and full velocity of another behavior), it will be challenging to determine the true scale-up behavior from small-scale mixing tests. However, quantitative test results will be significantly more definitive than estimates based on analysis of data from existing studies.

6.0 Conclusions and Recommendations

The evaluation shows that cohesive particle interaction will have multiple effects through a number of different mechanisms. The conclusion of this overall assessment is that stratification with an elevated particle concentration in the lower region of the tank will likely occur, and cohesive particle interactions in this lower region will reduce the fraction of particles lifted into the upper region of the tank although the magnitude of the impact could not be estimated. The cohesive particle interactions do not, on their own, cause the stratified layer and reduced particle lifting to occur, but the cohesive interactions will accentuate this behavior to some degree when stratification is present. Hence, testing with only non-cohesive particles will create technical uncertainty in meeting the objectives of the Tank Mixing and Sampling Demonstration Program.

The evaluation also shows that for the particles that are lifted into the upper region of the tank, the total particle concentration and the relative amounts of different size particles are extremely uniform in the upper region (the volume above the settled layer). However, in comparison to the overall concentration in the tank and the initial relative amounts of particles of different size, the material in the upper region is clearly different. It is possible that cohesive particle interactions cause flocculation in the upper region and potentially faster settling of particle agglomerates, but this is difficult to confirm.

Finally, this study conducted a fairly extensive review of the literature on the uniformity of suspended solids in jet mixed tanks. There are no existing studies or data that specifically quantify the role of cohesive interactions on concentration uniformity. The absence of definitive data further suggests that at least some testing with cohesive particles as part of the Tank Mixing and Sampling Demonstration Program will be needed to determine the impact of the cohesive particle interactions.

Based on the evaluation presented in this report and the absence of definitive studies, the recommendation is to conduct scoping tests to determine the magnitude of the impact caused by cohesive particle interactions on mixing. If the impact is determined to be significant, the recommendation is to conduct quantitative mixing tests at multiple scales with cohesive particles to augment the initial testing with non-cohesive particles. If initial testing can demonstrate that the impact of cohesive interactions is small over the range of important test conditions, then extensive scaled testing should not be necessary.

7.0 References

Adamson DJ, MR Poirier, and TJ Steeper. 2009a. *Demonstration of Internal Structures Impacts on Double Shell Tank Mixing Effectiveness.* SRNL-STI-2009-00326, Savannah River National Laboratory, Aiken, South Carolina.

Adamson DJ, MR Poirier, and TJ Steeper. 2009b. *Demonstration of Simulated Waste Transfers from Tank AY-102 to the Hanford Waste Treatment Facility.* SRNL-STI-2009-00717, Savannah River National Laboratory, Aiken, South Carolina.

Allemann RT, JD Hudson, ZI Antoniak, JJ Irwin, WD Chvala, NW Kirch, LE Efferding, TE Michener, JG Fadeff, FE Panisko, JR Friley, CW Stewart, WB Gregory, and BM Wise. 1994. *Mitigation of Tank 241-SY-101 by Pump Mixing: Results of Testing Phases A and B.* PNL-9423, Pacific Northwest Laboratory, Richland, Washington.

Allemann RT, ZI Antoniak, LL Eyler, and LM Liljegren. 1992. *Conceptual Models for Waste Tank Mechanistic Analysis Status Report - January 1991.* PNL-8011, Pacific Northwest Laboratory, Richland, Washington.

Allemann RT. 1989. *Analytical Evaluation of Jet Mixer Forces on Equipment in Waste Tanks.* ESD-88-113, Pacific Northwest Laboratory, Richland, Washington

Ancey C and H Jorrot. 2001. "Yield Stress for Particle Suspensions Within a Clay Dispersion." *Journal of Rheology* 45(2):297–319.

Antoniak ZI and KP Recknaggle. 1997. *Initial Parametric Study of the Flammability of Plume Releases in Hanford Waste Tanks.* PNNL-11639. Pacific Northwest National Laboratory, Richland, Washington.

Antoniak ZI and KP Recknagle. 1995. *Thermal Modeling of Tanks 241-AW-101 and 241-AN-104 with the TEMPEST Code.* PNL-10683, Pacific Northwest Laboratory, Richland, Washington.

Antoniak ZI. 1993. *Historical Trends in Tank 241-SY-101 Waste Temperatures and Levels.* PNL-8880, Pacific Northwest Laboratory, Richland, Washington.

Atkinson CM and HK Kytomaa. 1992. "Acoustic Wave Speed and Attenuation in Suspensions." *Int J Multiphase Flow* 18(4):577–592.

Atkinson CM and HK Kytomaa. 1991. "Acoustic Properties of Solid-Liquid Mixtures and the Limits of Ultrasound Diagnostics: Experiments." FED-Vol 118 *Liquid Solid Flows*, ASME, New York, New York, 145–158.

Bamberger JA, PA Meyer, JR Bontha, JA Fort, F Nigl, JM Bates, CW Enderlin, ST Yokuda, DE Kurath, AP Poloski, HD Smith, GL Smith, and MA Gerber. 2008. "Evaluating Pulse Jet Mixing with Non-Newtonian Slurries." *Proceedings of IMECE2007 2007 ASME International Mechanical Engineering Congress and Exposition*, 8 (IMECE2007-42223):1909–1930. American Society of Mechanical Engineers, New York.

Bamberger JA, LM Liljegren, CW Enderlin, PA Meyer, MS Greenwood, PA Titzler, and G Terrones. 2007. *One-Twelfth-Scale Mixing Experiments to Characterize Double-Shell Tank Slurry Uniformity*. PNNL-16859, Pacific Northwest National Laboratory, Richland, Washington.

Bamberger JA and PA Meyer. 2007. "Characterizing Pulsating Mixing of Slurries." *Proceedings of FEDSM2007 5th Joint ASME/JSME Fluids Engineering Conference* 2 (FEDSM2007-37666):201–205. American Society of Mechanical Engineers, New York.

Bontha JR, CW Stewart, DE Kurath, PA Meyer, ST Arm, CE Guzman-Leong, MS Fountain, M Friedrich, SA Hartley, LK Jagoda, CD Johnson, KS Koschik, DL Lessor, F Nigl, RL Russell, GL Smith, W Yantasee, and ST Yokuda. 2005. *Technical Basis for Predicting Mixing and Flammable Gas Behavior in the Ultrafiltration Feed Process and High-Level Waste Lag Storage Vessels with Non-Newtonian Slurries*. PNWD-3676 (WTP-RPT-132 Rev. 0), Battelle–Pacific Northwest Division, Richland, Washington.

Bamberger JA and MS Greenwood. 2004a. "Using Ultrasonic Attenuation to Monitor Slurry Mixing in Real Time." *Ultrasonics*, Vol. 42, pp. 145-148. PNNL-SA-40033, Pacific Northwest National Laboratory, Richland, Washington.

Bamberger JA and MS Greenwood. 2004b. "Measuring Fluid and Slurry Density and Solids Concentration Noninvasively." *Ultrasonics*, Vol. 42, pp. 563–567. PNNL-SA-40035, Pacific Northwest National Laboratory, Richland, Washington.

Bamberger JA and MS Greenwood. 2004c. *Real-Time Ultrasonic Characterization of Fluids and Slurries: Process Techniques Applicable in the Offshore Environment*. PNNL-SA-41080. Proceedings of OMAE04 23rd International Conference on Offshore Mechanics and Arctic Engineering, June 20–25, 2004, Vancouver, British Columbia, Canada.

Bamberger JA and MS Greenwood. 2003. *Evolution of a Non-Invasive Sensor for Fluid Density and Solids Concentration Measurement using Ultrasound. FEDSM2003-45590*, Proceedings of FEDSM'03, 4th ASME-JSME Joint Fluids Engineering Conference, Honolulu, Hawaii, July 611, 2003. PNNL-SA-38375.

Bamberger JA, and MS Greenwood. 2002. *Using Ultrasonic Signal Reflection to Characterize the Density and Viscosity of Fluids and Slurries*. ASME International Mechanical Engineering Congress, Symposium: Rheology and Fluid Mechanics of Non-Linear Materials, New Orleans, Louisiana, November 17–22, 2002. PNNL-SA-36868, Pacific Northwest National Laboratory, Richland, Washington.

Bamberger JA, BL Burks, KD Quigley, SW Butterworth, and DD Falter. 2001. *Technical Review of Retrieval and Closure Plans for the INEEL INTEC Tank Farm Facility*. PNNL-13651, Pacific Northwest National Laboratory, Richland, Washington.

Bamberger JA, and MS Greenwood. 2001a. *Development of a Density Sensor for In-Line Real-Time Process Control and Monitoring of Slurries during Radioactive Waste Retrieval and Transport Operations at DOE Sites.* PNNL-13719, Pacific Northwest National Laboratory, Richland, Washington

Bamberger JA and PA Meyer. 2001. *Using Oscillating Jets to Maintain Solids in Suspension – An Integrated Experimental and Computational Investigation*. PNNL-SA-34149, Pacific Northwest National Laboratory, Richland, Washington.

Bamberger JA. 2000. *An Assessment of Technologies to Provide Extended Sludge Retrieval from Underground Storage Tanks at the Hanford Site.* PNNL-13048, Pacific Northwest National Laboratory, Richland, Washington.

Bamberger, JA and MS Greenwood. 2000. *Measuring Slurry Density and Viscosity In-Situ in Real Time During Pipeline Transport Using an Ultrasonic Sensor.* FEDSM00-11121, Proceedings of the ASME 2000 Fluids Engineering Division Summer Meeting, June 11–15, 2000, Boston, Massachusetts. American Society of Mechanical Engineers, New York.

Bamberger JA and GF Boris. 1999. *Oak Ridge National Laboratory Old Hydrofracture Facility Waste Remediation Using the Borehole-Miner Extendible-Nozzle Sluicer*. PNNL-12225, Pacific Northwest National Laboratory, Richland, Washington.

Bamberger JA, GF Boris, and DG Alberts. 1999a. *Using the Borehole Miner Extendible-Nozzle Sluicing System to Dislodge and Mix Settled Sludge and Supernate in the Old Hydrofracture Tanks During Remediation*. PNNL-SA-30852, Pacific Northwest National Laboratory, Richland, Washington.

Bamberger JA, LJ Bond, and MS Greenwood. 1999b. *Ultrasonic Measurements for On-Line Real-Time Food Process Monitoring.* PNNL-SA-32024, AIChE Annual Meeting, Dallas, Texas.

Bamberger JA, CW Enderlin, and G Terrones. 1999c. *Effects of Lateral Suction Flow on Attaching Jet Velocity Profiles and the Dynamic Response of a Flexible Hose Impacted By the Attaching Jet.* FEDSM99-7067 (PNNL-SA-31009), ASME, San Francisco, California.

Bamberger JA, DG Alberts, CW Enderlin, and M White. 1998a. *Borehole Miner-Extendible Nozzle Development for Radioactive Waste Dislodging and Retrieval from Underground Storage Tanks*. PNNL-11730, Pacific Northwest National Laboratory, Richland, Washington.

Bamberger JA, MS Greenwood, and HK Kytomaa. 1998b. "Ultrasonic Characterization of Slurry Density and Particle Size." FEDSM98-5075 (PNNL-29822), 1998 ASME Fluids Engineering Division Summer Meeting, ASME, New York, New York.

Bamberger JA, HK Kytomaa, and MS Greenwood. 1998c. "Slurry Ultrasonic Particle Size and Concentration Characterization." In *Science and Technology for Disposal of Radioactive Tank Wastes*, (Eds) WW Schulz and NJ Lombardo. PNNL-SA-29277. Plenum Press, New York, New York, 485–495.

Bamberger JA and LM Liljegren. 1994. *Test Plan for 1/12-Scale Scoping Studies for the Double-Shell Tank Uniformity Task.* PNL-8900, Pacific Northwest National Laboratory, Richland, Washington.

Bamberger JA, MA McKinnon, DA Alberts, DE Steele, and CT Crowe. 1994. *Development of a Multi-Function Scarifier Dislodger with an Integral Pneumatic Conveyance Retrieval System for Single-Shell Tank Remediation.* PNL-8901, Pacific Northwest Laboratory, Richland, Washington.

Bamberger JA, JM Bates, JK Keska, MR Elmore, and NJ Lombardo. 1993a. *Strategy to Develop and Test a Multi-Function Scarifier End Effector with an Integral Conveyance System for Waste Tank Remediation.* PNL-8477, Pacific Northwest Laboratory, Richland, Washington.

Bamberger JA, LL Eyler, and RE Dodge. 1993b. *Mathematical Modeling of Mixer Pump Performance for Agitation of Radioactive Slurries in One-Million-Gallon Underground Storage Tanks at Hanford*. PNL-8295, Pacific Northwest Laboratory, Richland, Washington.

Bamberger JA and LM Liljegren. 1993. *Strategy Plan A Methodology to Define the Flow Rate and Pressure Requirements for Transfer of Double-Shell Tank Waste Slurries.* PNL-7664, Pacific Northwest Laboratory, Richland, Washington.

Bamberger JA and DE Steele. 1993. *Developing a Scarifier to Retrieve Radioactive Waste from Hanford Single-Shell Tanks*. PNL-SA-22721, Pacific Northwest Laboratory, Richland, Washington.

Bamberger JA. 1992. *Test Plan Characterization of Jet Forces upon Waste Tank Components.* PNL-7820, Pacific Northwest Laboratory, Richland, Washington.

Bamberger JA, JM Bates, and ED Waters. 1992. "Experimental Characterization of Jet Forces on Waste Tanks Components." Vol 1, *Proc 3rd Int Conf High Level Radioactive Waste Management*, American Nuclear Society, La Grange Park, Illinois, 628–635 (PNL-SA-19999).

Bamberger JA, JM Bates, and ED Waters. 1990a. *Experimental Characterization of Jet Static Forces Impacting Waste Tank Components: Final Report*. PNL-7394, Pacific Northwest Laboratory, Richland, Washington.

Bamberger JA, LM Liljegren, and PS Lowery. 1990b. *Strategy Plan – A Methodology to Predict the Uniformity of Double-Shell Tank Waste Slurries Based on Mixing Pump Operation.* PNNL-7665, Pacific Northwest National Laboratory, Richland Washington.

Barker SA and AR Lechelt. 2000. *Determination of Waste Groupings for Safety Analyses*. RPP-6171 Rev. 0, CH2M HILL Hanford Group, Inc., Richland Washington.

Barker SA, WB Barton, DR Bratzel, M Epstein, PA Gauglitz, GD Johnson, SN Maruvada, CE Olson, ML Auer, SE Slezak, CW Stewart, and J Young. 1999. *Flammable Gas Safety Analysis Review*. SNL-000198, Sandia National Laboratories, Albuquerque, New Mexico.

Bates JM, JW Brothers, JM Alzheimer, DE Wallace, and PA Meyer. 2003. *Test Results for Pulse Jet Mixers in Prototypic Ultrafiltration Feed Process and High-Level Waste Lag Storage Vessels.* PNWD-3496 (WTP-RPT-110 Rev. 0), Battelle–Pacific Northwest Division, Richland, Washington.

Bell KE. 2001. *Tank 241-AZ-101 Grab Samples From Mixer Pump Test Events 5, 7, 8, and 9 Analytical Results for the Final Results for the Report*. HNF-6062, Rev 0, Fluor Hanford, Richland, Washington.

Bontha JR, DE Kurath, AP Poloski, WC Buchmiller, WH Combs, ED Johnson, HC Webber, and KL Herman. 2007. *Pulse Jet Mixer Controller and Instrumentation Testing*. PNWD-3828 (WTP-RPT-146 Rev. 0), Battelle–Pacific Northwest Division, Richland, Washington.

Bontha JR, CW Stewart, DE Kurath, PA Meyer, ST Arm, CE Guzman-Leong, MS Fountain, M Friedrich, SA Hartley, LK Jagoda, CD Johnson, KS Koschik, DL Lessor, F Nigl, RL Russell, GL Smith, W Yantasee, and ST Yokuda. 2005. *Technical Basis for Predicting Mixing and Flammable Gas Behavior in the Ultrafiltration Feed Process and High-Level Waste Lag Storage Vessels with Non-Newtonian Slurries*. PNWD-3676 (WTP-RPT-132 Rev. 0), Battelle–Pacific Northwest Division, Richland, Washington.

Bontha JR, TE Michener, DS Trent, JM Bates, and MD Johnson. 2003a. *Development and Assessment of the TEMPEST CFD Model of the Pulsed Jet Mixing Systems*. PNWD-3261 (WTP-RPT-061 Rev. 0), Battelle–Pacific Northwest Division, Richland, Washington.

Bontha JR, JM Bates, CW Enderlin, and MG Dodson. 2003b. *Large Tank Experimental Data for Validation of the FLUENT CFD Model of Pulsed Jet Mixers*. PNWD-3303 (WTP-RPT-081 Rev. 0), Battelle–Pacific Northwest Division, Richland, Washington.

Bontha JR, GR Golcar, and N Hannigan. 2000. *Demonstration and Optimization of BNFL's Pulsed Jet Mixing and RFD Sampling Systems Performance Using NCAW Simulant*. PNWD-3054 (BNFL-RPT-048 Rev. 0), Battelle–Pacific Northwest Division, Richland, Washington.

Bradley RF, FA Parsons, CB Goodlett, and RM Mobley. 1977. *A Low-pressure Hydraulic Technique for Slurrying Radioactive Sludges in Waste Tanks.* DP-1468, Savannah River Laboratory, Aiken, South Carolina.

Buscall R, IJ McGowan, PDA Mills, RF Stewart, D Sutton, LR White, and GE Yates. 1987. "The Rheology of Strongly Flocculated Suspensions." *Journal of Non-Newtonian Fluid Mechanics* 24:183–202.

Callaway WS. 2000. *Results of Retrieval Testing of Sludge from Tank 241-AZ-101*. HNF-7078, Rev. 0, Fluor Hanford, Richland, Washington.

Camenen B. 2008. "Simple and General Formula for the Settling Velocity of Particles." *Journal of Hydraulic Engineering - ASCE* 133(2):229–233.

Carlson AB, PJ Certa, TM Hohl, JR Bellomy III, TW Crawford, DC Hedengren, AM Templeton, HS Fisher, SJ Greenwood, DG Douglas, and WJ Ulbright Jr. 2001. *Test Report, 241-AZ-101 Mixer Pump Test*. RPP-6548, Rev. 1, Numatec Hanford Corporation, Richland, Washington.

Carlstrom RF. 1994. *Packaging Design Criteria, Transfer and Disposal of 102-AP Mixer Pump*. WHC-SD-TP-PDC-026, Westinghouse Hanford Company, Richland, Washington.

Carstens MR. 1982. *Flow Characteristics of Simulated Slurries, Report by Georgia Ironworks Hydraulic Test Laboratory.* DPST-82-955, du Pont Savannah River Laboratory Report by Georgia Ironworks Hydraulic Test Laboratory.

Ceo RN, MB Sears, and JT Shor. 1990. *Physical Characterization of Radioactive Sludges in Selected Melton Valley and Evaporator Facility Storage Tanks*. ORNL/TM-11653, Oak Ridge National Laboratory, Oak Ridge, Tennessee.

Certa PJ, and MN Wells. 2009. *River Protection Project System Plan*. ORP-11242, Rev. 4, U.S. Department of Energy, Office of River Projection, Richland, Washington.

Chang SC and TR Beaver. 1993. *Subscale Mixing Test for Tank 101-SY*. WHC-SD-WM-ER-178, Westinghouse Hanford Company, Richland, Washington.

Channell GM and CF Zukoski. 1997. "Shear and Compressive Rheology of Aggregated Alumina Suspensions." *AIChE Journal* 43(7):1700–1708.

Churnetski BV. 1982. "Prediction of Centrifugal Pump Cleaning Ability in Waste Sludge." *Nuclear and Chemical Waste Management* Vol 3, pp 199–203.

Churnetski BV. 1981. *Effective Cleaning Radius Studies.* DPST-81-282, Savannah River Laboratory, Aiken, South Carolina. (Memorandum to JF Ortaldo).

Coleman CJ, MS Hay, and KB Martin. 2003. *Compositing and Characterization of Samples from 241-AY-102/C-106*. WSRC-TR-2003-00205, Rev. 0, Westinghouse Savannah River Company, Aiken, South Carolina.

Comly IV, C. 1979. *Tank 16 Demonstration Multipump Test Results.* DPST-79-17-17, Savannah River Laboratory, Aiken, South Carolina. (Memorandum to OM Morris).

Cuta JM, KG Carothers, DW Damschen, WL Kuhn, JA Lechelt, K Sathyanarayana, and LA Stauffer. 2000. *Review of Waste Retrieval Sluicing System Operations and Data for Tanks 241-C-016 and 241-AY-102*. PNNL-13319, Pacific Northwest National Laboratory, Richland, Washington.

Dahl TL, AC Lay, SA Taylor, and JW Moore. 1999. *C-Tank Transfers: Transuranic Sludge Removal From the C-1, C-2, and W-23 Waste Storage Tanks at Oak Ridge National Laboratory*. BJC/OR-279, Bechtel Jacobs Company LLC, Oak Ridge, Tennessee.

Day RW. 2006. *Foundation Engineering Handbook: Design and Construction with the 2006 International Building Code*. McGraw-Hill, New York.

De Lorenzo DS, AT DiCenso, LC Amato, MI Weyns-Rollosson, DJ Smith, BC Simpson, and TL Welsh. 1994. *Tank Characterization Report for Double-Shell Tank 241-AP-102*. WHC-SD-WM-ER-358, Rev. 0, Los Alamos Technical Associates, Kennewick, Washington.

Dimenna RA, SY Lee, DA Tamburello, and DR Rector. 2008. *Advanced Mixing Models.* SRNL-STI-2008-00417, Savannah River National Laboratory, Aiken, South Carolina.

Doron P and D Barnea. 1996. "Flow Pattern Maps for Solid-Liquid Flow in Pipes." *Int J Multiphase Flow* 22(2):273–283.

Doron P and D Barnea. 1995. "Pressure Drop and Limit Deposit Velocity for Solid-Liquid Flow in Pipes." *Chemical Engineering Science* 50(10):1595–1604.

Doron P and D Barnea. 1993. "A Three-Layer Model for Solid-Liquid Flow in Horizontal Pipes. *Int J Multiphase Flow* 19(6):1029–1043.

Douglas DG. 2000. *AZ-101 Mixer Pump Demonstration and Tests: Data Management (Analysis) Plan*. HNF-3840 Rev 0, Vista Engineering Technologies LLC, Richland, Washington.

Ehrlich RD and HO Weeren. 1979. *Safety Assessment Document Gunite Tank Sludge Removal*. ORNL/M-1919, Oak Ridge National Laboratory, Oak Ridge, Tennessee.

Enderlin CW, G Terrones, CJ Bates, BK Hatchell, and B Adkins. 2003. *Recommendations for Advanced Design Mixer Pump Operation in Savannah River Site Tank 18F*. PNNL-14443, Pacific Northwest National Laboratory, Richland, Washington.

Enderlin CW, OD Mullen, and G Terrones. 1997. *Performance Evaluation of the Quarter-Scale Russian Retrieval Equipment for the Removal of Hazardous Waste*. PNNL-11740, Pacific Northwest National Laboratory, Richland, Washington.

Eschbach EJ and CW Enderlin. 1993. *1/12-Scale Mixing Interface Visualization and Buoyant Particle Release Tests in Support of Tank 241-SY-101 Hydrogen Mitigation.* PNL-8892, Pacific Northwest Laboratory, Richland, Washington.

Estey SD. 1998. *Flow Velocity Analysis for Avoidance of Solids Deposition During Transport of Hanford Tank Waste Slurries.* HNF-2728, Lockheed Martin Hanford Corp, Richland, Washington.

Eyler LL and LA Mahoney. 1995. *Computer Simulation of Mobilization and Mixing of Kaolin with Submerged Liquid Jets in 25,000-Gallon Horizontal Cylindrical Tanks*. PNL-10503, Pacific Northwest Laboratory, Richland, Washington.

Eyler LL, G Terrones, and JA Fort. 1993. *Modeling of Submerged Liquid Jet Mixing in Waste Storage Tanks with Non-Newtonian Settled Sludge*. PNL-SA-22782, Pacific Northwest National Laboratory, Richland, Washington. (Submitted to ASME Fluids Engineering Meeting Lake Tahoe, Nevada, June 19–23, 1994).

Eyler LL, DS Trent, and MJ Budden. 1993. *TEMPEST: A Computer Program for Three-Dimensional Time-Dependent Computational Fluid Dynamics, Vol. II: Assessment and Verification Results*. PNL-4348 Vol. II Rev. 0, Pacific Northwest Laboratory, Richland, Washington.

Eyler LL and TE Michener. 1992. *Computer Modeling of Forced Mixing in Waste Storage Tanks*. PNL-SA-20258, Pacific Northwest National Laboratory, Richland, Washington. (In High Level Radioactive Waste Management, Proceedings of the Third International Conference, Las Vegas, Nevada, April 12–16, 1992, Vol 1 pp. 636–642).

Eyler LL, NJ Lombardo, and JS Barnhart. 1982. *FY 1980 and 1981 Progress Report - Hydrotransport Plugging Study*. PNL-3621, Pacific Northwest Laboratory, Richland, Washington.

Eyler LL and NJ Lombardo. 1980. *FY-1979 Progress Report Hydrotransport Plugging Study.* PNL-3203, Pacific Northwest Laboratory, Richland, Washington.

Fazio JM and MA Ebra. 1987. *Results of Sludge Slurry Pipeline Pluggage Tests.* DPST-87-271, Savannah River Laboratory to Ebra, Aiken, South Carolina.

Fellinger AP, MW Rinker, EJ Berglin, RL Minichan, MR Poirier, PA Gauglitz, BA Martin, BK Hatchell, E Saldivar, OD Mullen; NF Chapman, BE Wells, and PW Gibbons. 2009. *EM-21 Retrieval Knowledge Center: Waste Retrieval Challenges.* PNNL-18356 (SRNL-STI-2009-00231), Pacific Northwest National Laboratory, Richland, Washington.

Fort JA, PA Meyer, JA Bamberger, CW Enderlin, PA Scott, MJ Minette, and PA Gauglitz. 2010. *Scaled Testing to Evaluate Pulse Jet Mixer Performance in Waste Treatment Plant Mixing Vessels*. WM2010-10487, Waste Management 2010 Conference, March 7–10, 2010, Phoenix, Arizona. PNNL-SA-69746, Pacific Northwest National Laboratory, Richland, Washington.

Fort JA, JA Bamberger, PA Meyer, and CW Stewart. 2007. *Initial Investigation of Waste Feed Delivery Tank Mixing and Sampling Issues*. PNNL-17043, Pacific Northwest National Laboratory, Richland, Washington.

Fort JA, JA Bamberger, JM Bates, CW Enderlin, and MR Elmore. 1993. *1/12-Scale Physical Modeling Experiments in Support of 241-SY-101 Hydrogen Mitigation.* PNL-8476, Pacific Northwest Laboratory, Richland, Washington.

Fow CL, DE Kurath, and BA Pulsipher. 1989. *Evaluation of the Mixing System for the West Valley Melter Feed Hold Tank*. PNL-6724, Pacific Northwest Laboratory, Richland, Washington.

Francis CW and SE Herbes. 1997. *Summary Review of the Chemical Characterization of Liquid and Sludge Contained in the Old Hydrofracture Tanks*. ORNL/ER-395, Oak Ridge National Laboratory, Oak Ridge, Tennessee.

Gauglitz PA, BE Wells, JA Fort, and PA Meyer. 2009. *An Approach to Understanding Cohesive Slurry Settling, Mobilization, and Hydrogen Gas Retention in Pulsed Jet Mixed Vessels*. PNNL-17707 (WTP-RPT-177, Rev. 0), Pacific Northwest National Laboratory, Richland, Washington.

Gauglitz PA and JT Aikin. 1997. *Waste Behavior During Horizontal Extrusion: Effect of Waste Strength for Bentonite and Kaolin/Ludox Simulants and Strength Estimates for Wastes from Hanford Waste Tanks 241-SY-103, AW-101, AN-103, and S-102*. PNNL-11706, Pacific Northwest National Laboratory, Richland, Washington.

Geeting JGH, RT Hallen, LK Jagoda, AP Poloski, RD Scheele, and DR Weier. 2002. *Filtration, Washing, and Caustic Leaching of Hanford Tank AZ-101 Sludge*. PNWD-3206 (WTP-RPT-043), Battelle—Pacific Northwest Division, Richland, Washington.

Giaquinto JM, JM Keller, and TP Mills. 1997. *Miscellaneous Data for the 1996-1997 Sampling and Analysis Campaigns of the MVST, BVEST, and OHF Tank Complexes.* ORNL/TM-13455, Oak Ridge National Laboratory, Oak Ridge, Tennessee.

Golcar GR, NG Colton, JG Darab, and HD Smith. 2000. *Hanford Tank Waste Simulant Specification and Their Applicability for the Retrieval, Pretreatment, and Vitrification Processes.* PNWD-2455, Battelle Pacific Northwest Division, Richland, Washington.

Goslen AQ. 1984. *Tank 19 Salt Removal*. DPSP-84-17-7, Savannah River Plant, Aiken, South Carolina.

Gray WJ, ME Peterson, RD Scheele, and JM Tingey. 1993. *Characterization of the Second Core Sample of Neutralized Current Acid Waste From Double-Shell Tank 101-AZ.* PNNL-13027, Pacific Northwest National Laboratory, Richland, Washington.

Greenwell RD. 2009. *Integrated Waste Feed Delivery Plan*. RPP-40149, Rev. 0, Washington River Protection Solutions, Richland, Washington.

Greenwood MS and JA Bamberger. 2002. *Self-Calibrating Sensor for Measuring Density through Stainless Steel Pipeline Wall.* 2002 ASME International Mechanical Engineering Congress, Symposium: Advances in Materials Processing Science, New Orleans, Louisiana, November 17–22, 2002, PNNL-SA-36689, Pacific Northwest National Laboratory, Richland, Washington.

Greenwood MS, JL Mai, and MS Good. 1993. "Attenuation Measurements of Ultrasound in a Kaolin-Water Slurry: A Linear Dependence upon Frequency." *J Acoust Soc Am*. 94(2):908–916.

Guerrero HA and M Restivo. 2004. *Final Report UFP Restart and Sparger Testing*. WSRC-TR-2004-00488, Rev. 0, SRNL-RPP-2004-00066 Rev. 0, Westinghouse Savannah River Company, Aiken, South Carolina.

Hall MN. 2008. *ICD 19 - Interface Control Document for Waste Feed*. 24590-WTP-ICD-MG-01-019, Rev. 4, River Protection Project, Waste Treatment Plant, Richland Washington.

Hamm BA, WL West, and GB Tatterson. 1989. *Sludge Suspension in Waste Storage Tanks.* DP-MS-89-61, Savannah River Laboratory, Aiken South Carolina. (A paper proposed for Mixing XII Potosi, Missouri, August 6–11, 1989).

Hanks RW. 1987. "Low Reynolds Number Turbulent Pipeline Flow of Pseudohomogeneous Slurries." *Hydrotransport 5 Fifth International Conference on the Hydraulic Transport of Solids in Pipes*, BHRA Fluid Engineering, Cranfield, England.

Hansen EK and V Williams. 2005. P*hysical Properties of Kaolin/Sand Slurry used during Submersible Mixer Tests at TNX*. WSRC-TR-2004-00401, Rev. 1, Savannah River Technology Center, Aiken, South Carolina.

Hatchell BK, MW Rinker, and OD Mullen. 1995. *Hazardous Waste Retrieval Strategies Using a High Pressure Water Jet Scarifier.* PNL-SA 25132, Pacific Northwest Laboratory, 8th American Water Jet Conference, Houston, Texas, August 27–30, Richland, Washington.

Hay MS and ED Lee. 1994. *Hydrogen Evolution and Sludge Suspension during the Preparation of the First Batch of Sludge at the Savannah River Site.* WSRC-MS-94-0541, Westinghouse Savannah River Company, Aiken, South, Carolina.

Hill AJ Jr, and FA Parsons. 1977. T*echnical Data Summary. Removal of Sludge and Chemical Cleaning of Tank 16-H.* DPSTD-241-TK-16H, Savannah River Laboratory, Aiken, South Carolina.

Hill AJ. 1967. *Removal of Sludge from High Activity Waste Tanks.* DP-1093, E.I. du Pont de Nemours & Company, Savannah River Laboratory, Aiken, South Carolina.

Horowitz JB. 1980. *One-Twelfth Scale Mock-up of Tank 16 Cleaning Demonstration.* DPST-80-496, Savannah River Laboratory, Aiken, South Carolina. Memorandum to JK Okeson.

Hunter VL. 1988. Operability Test Report for the In-Tank Mixer Pump. SD-WM-OTR-081, Richland, Washington.

Hunter VL. 1987. *Operability Test Report for the In-Tank Mixer Pump*. SD-WM-OTR-081, Westinghouse Hanford Company, Richland, Washington.

Hydraulic Institute. 2000. *American National Standards for Centrifugal Pumps.* Hydraulic Institute Parsippany, New Jersey.

Hylton TD, RL Cummins, EL Youngblood, and JJ Perona. 1995. *Sludge Mobilization with Submerged Nozzles in Horizontal Cylindrical Tank*. ORNL/TM- 13036, Oak Ridge National Laboratory, Oak Ridge, Tennessee.

Hylton TD, EL Youngblood, and RL Cummins, 1994. *Fluid Dynamic Studies for a Simulated Melton Valley Storage Tank Slurry*. ORNL/TM-12781, Oak Ridge National Laboratory, Oak Ridge, Tennessee.

ICD 19. 2008. *ICD 19 - Interface Control Document for Waste Feed,* 24590-WTP-ICD-MG-01-019, Rev 4, River Protection Project, Richland, Washington.

Ilievski D and ET White. 1994. "Agglomeration During Precipitation: Agglomeration Mechanism Identification for $Al(OH)_3$ Crystals in Stirred Caustic Aluminate Solutions." *Chemical Engineering Science,* 49(19):3227–3239.

Johnson GD, NW Kirch, RE Bauer, JM Conner, CW Stewart, BE Wells, and JM Grigsby. 2000. *Evaluation of Hanford High-Level Waste Tank 241-SY-101*. RPP-6517, Rev. 0, CH2M HILL Hanford Group, Inc., Richland, Washington.

Johnson MD, MA Gerber, JR Bontha, AP Poloski, RT Hallen, SK Sundaram, and DE Wallace. 2005. *Hybrid Mixing System Test Results for Prototype Ultrafiltration Feed Process and High-Level Waste Lag Storage Vessels.* PNWD-3586 (WTP-RPT-128) Rev. 0, Battelle–Pacific Northwest Division, Richland, Washington.

Johnson MD, JR Bontha, and JM Bates. 2003. *Demonstration of Ability to Mix in a Small-Scale Pulsed-Jet Mixer Test Facility.* PNWD-3273 (WTP-RPT-077 Rev. 0), Battelle – Pacific Northwest Division, Richland, Washington.

Keller JM, JM Giaquinto, and AM Meeks. 1997a. *Characterization of the BVEST Waste Tanks Located at ORNL*. ORNL/TM-13358, Oak Ridge National Laboratory, Oak Ridge, Tennessee.

Keller JM, JM Giaquinto, and AM Meeks. 1997b. *Characterization of the Old Hydrofracture Facility (OHF) Waste Tanks Located at ORNL*. ORNL/TM-13394, Oak Ridge National Laboratory, Oak Ridge, Tennessee.

Keller JM, JM Giaquinto, and WH Griest. 1996. *Characterization of Selected Waste Tanks from the Active LLLW System*. ORNL/TM-13248, Oak Ridge National Laboratory, Oak Ridge, Tennessee.

Kent TE, SA Taylor, JW Moore, JL Stellern, and KM Billingsley. 1998. *Demonstration of Fluidic Pulse Jet Mixing for a Horizontal Waste Storage Tank*. ORNL/TM-13578, Oak Ridge National Laboratory, Oak Ridge, Tennessee.

Krieg SA. 1992. *A Description of the Hanford Single-Shell Tanks and Their Contents* (Includes photos of interiors and C-106). WHC-SD-TD-TI-001, Westinghouse Hanford Company, Richland, Washington.

Kurath DE, PW Eslinger, SM Barnes, RL Aaberg, BD Hanson, JL Huckaby, EC Golovich, PM Aker, MJ Minette, JM Billing, SD Rassat, CE Guzman-Leong, DL Baldwin, PS Sundar, CF Brown, ML Kimura, BM Rapko, GJ Josephson, JGH Geeting, SK Sundaram, LA Mahoney, JJ Toth, GJ Sevigny, RP Pires, PP Schonewill, ST Yokuda, AJ Casella, BE Wells, RC Daniel, EBK Baer, JR Bontha, and OP Bredt. 2009. *Pretreatment Engineering Platform Phase 1 Final Test Report*. PNNL-18894 (WTP-RPT-197 Rev. 0), Pacific Northwest National Laboratory, Richland, Washington.

Kurath DE, PA Meyer, JR Bontha, AP Poloski, JA Fort, WH Combs, WC Buchmiller, ID Welch, and MD Bleich. 2007. *Assessment of Pulse Tube Mixing for Vessels Containing Non-Newtonian Slurries.* PNWD-3827 (WTP-RPT-155) Rev. 0, Pacific Northwest National Laboratory, Richland, Washington.

Kytomaa HK and SW Corrington. 1994. "Ultrasonic Imaging Velocimetry of Transient Liquefaction of Cohesionless Particulate Media." *Int J Multiphase Flow* 20(5):915–926.

Kytomaa HK. 1993. "Theory of Sound Propagation in Suspensions: A Guide to Particle Size and Concentration Characterization." *Powder Technology* 115–121.

Lee SY and RA Dimenna. 2008. *Slurry Pump Mixing Effectiveness in Tank 50H.* WSRC-STI-2008-00151, Savannah River National Laboratory, Aiken, South Carolina.

Lee SY, RA Dimenna, R Leishear, and D Stefanko. 2007. *Analysis of Turbulent Mixing Jets in Large Scale Tank.* WSRC-STI-2007-00160, Savannah River National Laboratory, Aiken, South Carolina. (Submitted to Journal of Fluids Engineering).

Lee SY and RA Dimenna. 2005. *FLUENT Test and Verification Document.* WSRC-TR-2005-00563, Westinghouse Savannah River Company, Aiken, South Carolina.

Lee SY. 2004. *Tank 5 Model For Sludge Removal Analysis.* WSRC-TR-2004-00418, Westinghouse Savannah River Company, Aiken, South Carolina.

Lee SY and RA Dimenna. 2004. *CST Suspension Analysis for Slurry Pumps of Tank 40.* WSRC-TR-2004-00207, Westinghouse Savannah River Company, Aiken, South Carolina.

Lee SY. 2003a. *Evaluation of Sludge Removal Capabilities for ADMP Mixer in Tank 8.* WSRC-TR-2003-00166, Savannah River Technology Center, Aiken, South Carolina.

Lee SY. 2003b. *Sludge Heel Removal Analysis for Slurry Pumps of Tank 11.* WSRC-TR-2003-00308, Savannah River Technology Center, Aiken, South Carolina.

Lee SY. 2002. *Agitator Mixing Analysis In A HB-Line Flat Tank.* WSRC-TR-2002-00219, Savannah River Technology Center, Aiken, South Carolina.

Lee SY and RA Dimenna. 2002. *Heel Removal Analysis for Mixing Pumps of Tank 8.* WSRC-TR-2002-00460, Savannah River Technology Center, Aiken, South Carolina.

Lee SY and RA Dimenna. 2001a. *Design Analysis For A Scaled Erosion Test.* WSRC-TR-2001-00591, Savannah River Technology Center, Aiken, South Carolina.

Lee SY and RA Dimenna. 2001b. *Performance Analysis for Mixing Pumps in Tank 18.* WSRC-TR-2001-00391, Savannah River Technology Center, Aiken, South Carolina.

Lee SY and RA Dimenna. 2000. *Three-Dimensional CFD FLYGT Mixer Model and Results.* WSRC-TR-2000-00205, Savannah River Technology Center, Aiken, South Carolina.

Lee SY and RA Dimenna. 1995. *Validation Analysis for the Calculation of a Turbulent Free Jet in Water using CFDS-FLOW3D and FLUENT.* WSRC-TR-95-0170, Savannah River Technology Center, Aiken, South Carolina.

Leishear RA, MJ Augeri, M Hubbard, JL Thomas, SY Lee, RA Dimenna, and DB Stefanko. 2004. *ADMP Mixing of Tank 18F: History, Modeling, Testing, and Results.* WSRC-TR-2004-00036, Savannah River National Laboratory, Aiken, South Carolina (ASME Fluids/Heat Transfer Conference, Charlotte, North Carolina).

Liljegren LM and JA Bamberger. August 1992. "A Methodology to Predict the Uniformity of Double-Shell Waste Slurries Based on Mixer Pump Operation." *American Society of Chemical Engineers National Summer Meeting*, Minneapolis. PNL-SA-20281, Pacific Northwest National Laboratory, Richland, Washington.

Litzenberger CG. 2003. *Rheological Study of Kaolin Clay Slurries.* Masters Thesis, University of Saskatchewan, Saskatoon, Saskatchewan.

MacLean GT. 2000. *AZ-101 Mixer Pump Test Mt Fury Suspended Solids Profiler Application & Testing*. RPP-5644 Rev 0, Fluor Federal Services, Richland, Washington.

Mahoney LA and DS Trent. 1995. *Correlation Models for Waste Tank Sludge and Slurries.* PNL-10695, Pacific Northwest Laboratory, Richland, Washington.

Mahoney LA, G Terrones, and LL Eyler. 1994. *Modeling and Analysis of ORNL Horizontal Storage Tank Mobilization and Mixing*. PNL-9961, Pacific Northwest Laboratory, Richland, Washington.

McKay RL, FF Erian, CJ Call, and EA Daymo. 1994. *Slurry Transport of Hanford Tank Wastes: Open Technical Issues and Recommended Actions.* DSTRPT-CY94-012, Pacific Northwest Laboratory, Richland, Washington.

McMahon CL. 1990. *Design Characteristics of the Sludge Mobilization System.* DOEME/44139-63. NTIS Report No. DE93014680, West Valley Nuclear Services Company, Inc. West Valley, New York.

Meyer PA and JA Fort. 1993. *TEMPEST: A Computer Program for Three-Dimensional Time-Dependent Computational Fluid Dynamics, Vol. 3: Validation and Verification*. PNL-8857 Vol. 3 Rev. 0, Pacific Northwest Laboratory, Richland, Washington.

Meyer PA, JA Bamberger, CW Enderlin, JA Fort, BE Wells, SK Sundaram, PA Scott, MJ Minette, GL Smith, CA Burns, MS Greenwood, GP Morgen, EBK Baer, SF Snyder, M White, GF Piepel, BG Amidan, A Heredia-Langner, SA Bailey, JC Bower, KM Denslow, DE Eakin, MR Elmore, PA Gauglitz, AD Guzman, BK Hatchell, DF Hopkins, DE Hurley, MD Johnson, LJ Kirihara, BD Lawler, JS Loveland, OD Mullen, MS Pekour, TJ Peters, PJ Robinson, MS Russcher, S Sande, C Santoso, SV Shoemaker, SM Silva, DE Smith, YF Su, JJ Toth, JD Wiberg, XY Yu, and N Zuljevic. 2009. *Pulse Jet Mixing Tests With Noncohesive Solids*. PNNL-18098 (WTP-RPT-182, Rev. 0), Pacific Northwest National Laboratory, Richland, Washington.

Meyer PA and AW Etchells. 2007. "Mixing with Intermittent Jets with Application in Handling Radioactive Waste Sludges." *Chemical Engineering Research and Design* 85(5):691–696.

Meyer PA, DE Kurath, JA Bamberger, AW Etchells and SM Barnes. 2006. "Scaling Laws for Reduced-Scale Tests of Pulse Jet Mixing Systems in Non-Newtonian Slurries: Mixing Cavern Behavior." 2006 Waste Management Symposium, Tucson, Arizona, WM Symposia, Inc. Available online at http://www.wmsym.org/abstracts/2006/index.html.

Meyer PA, DE Kurath, and CW Stewart. 2005. *Overview of the Non-Newtonian Pulse Jet Mixer Test Program*. PNWD-3677 (WTP-RPT-127) Rev. 0, Pacific Northwest National Laboratory, Richland, Washington.

Meyer PA and BE Wells. 2000. *Understanding Gas Release Events in Hanford Double Shell Tanks*. PNNL-SA-32640, Pacific Northwest National Laboratory, Richland, Washington.

Meyer PA, LR Pederson, ME Brewster, CW Stewart, SA Bryan, G Terrones, and G Chen. 1997. *Gas Retention and Release Behavior in Hanford Double-Shell Waste Tanks*. PNNL-11536, Rev. 1, Pacific Northwest Laboratory, Richland, Washington.

Meyer PA. 1994. *Computer Modeling of Jet Mixing in INEL Waste Tanks*. PNL-9063, Pacific Northwest Laboratory, Richland, Washington.

Motyka T. 1981a. *Slurry Pump Efficiency on Very Thick Slurries.* DPST-81-633, Savannah River Laboratory, Aiken, South Carolina. (Memorandum to JF Ortaldo).

Motyka T. 1981b. *Slurry Transport Through Inter-Area Transport Line.* DPST-81-324TL, Savannah River Laboratory See Motka, Aiken, South Carolina.

Motyka T. 1983. *Slurry Pipeline Tests in Support of the In-Tank Sludge Processing Program*. DPST-83-266, EI du Pont de Nemours & Co Savannah River Laboratory, Aiken, South Carolina.

Olsen J. 2008a. *Determination of Mixing Requirements for Pulse-Jet-Mixed Vessels in the Waste Treatment Plant.* 24590-WTP-ES-PT-08-002, Rev. 0, Bechtel National Incorporated, Richland, Washington.

Olsen J. 2008b. *Determination of Mixing Requirements for Pulse-Jet-Mixed Vessels in the Waste Treatment Plant.* 24590-WTP-ES-PT-08-002, Rev. 1. Bechtel National Incorporated, Richland, Washington.

Onishi Y and BE Wells. 2004. *Feasibility Study on Using Two Mixer Pumps for Tank 241-AY-102 Waste Mixing*. PNNL-14763, Pacific Northwest National Laboratory, Richland, Washington.

Onishi Y, JM Tingey, BE Wells, J Lui, G Terrones, KP Recknagle, ST Yokuda, and M Quinn. 2003a. *Retrieval and Pipeline Transfer Assessment of Hanford Tank 241-AN-105 Waste*. PNNL-14144. Pacific Northwest National Laboratory, Richland, Washington.

Onishi Y, BE Wells, ST Yokuda, and G Terrones. 2003b. *Feasibility Study on Using a Single Mixer Pump for Tank 241-AN-101 Waste Retrieval*. PNNL-14105, Pacific Northwest National Laboratory, Richland, Washington.

Onishi Y, DS Trent, BE Wells, and LA Mahoney. 2003c. *Assessment of Tank 241-S-112 Liquid Waste Mixing in Tank 241-SY-101*. PNNL-14399, Pacific Northwest National Laboratory, Richland, Washington.

Onishi Y and BE Wells. 2001. "Chemically Active Non-Newtonian Waste Mixing." *Proceedings of the International Conference on Multiphase Flow-2001*. New Orleans, Louisiana.

Onishi Y, DA Yuen, JR Rustad, BE Wells, TE Michener, AR Felmy, DS Trent, AA Ten, and CA Hier. 2001a. *Numerical Modeling of Mixing of Chemically Reacting, Non-Newtonian Slurry for Tank Waste Retrieval*. Final Report for DOE EMSP Project No. 65371.

Onishi Y, BE Wells, AA Ten, CA Hier, and DA Yuen. 2001b. "Reactive Transport Modeling of Radioactive Waste Mixing." American Chemical Society 222nd National Meeting, Chicago, Illinois.

Onishi Y, KP Recknagle, and BE Wells. 2000. *Pump Jet Mixing and Pipeline Transfer Assessment for High-Activity Radioactive Wastes in Hanford Tank 241-AZ-102*. PNNL-13275, Pacific Northwest National Laboratory, Richland, Washington.

Onishi Y and Recknagle KP. 1999. *Simulation of Hanford Tank 241-C-106 Waste Release into Tank 241-AY-102*. PNNL-12179. Pacific Northwest National Laboratory, Richland, Washington.

Onishi Y and DS Trent. 1999. "Mobilization Modeling of Erosion-Resisting Radioactive Tank Waste." *Proceedings of the Rheology in the Mineral Industry II*, Kahuku, Hawaii. United Engineering Foundation, New York, pp. 45–56.

Onishi Y and KP Recknagle. 1998. *Tank 241-AZ-101 Criticality Assessment Resulting from Pump Jet Mixing Sludge Mixing Simulations*. PNNL-11486. Pacific Northwest National Laboratory, Richland, Washington.

Onishi Y and KP Recknagle. 1997a. *Performance Evaluation of Rotating Pump Jet Mixing of Radioactive Wastes in Hanford Tanks 241-AP-102 and -104*. PNNL-11486. Pacific Northwest National Laboratory, Richland, Washington.

Onishi Y and KP Recknagle. 1997b. *Tank AZ-101 Criticality Assessment Resulting from Pump Jet Mixing: Sludge Mixing Simulations*. PNNL-11486, Pacific Northwest National Laboratory, Richland, Washington.

Onishi Y and JD Hudson. 1996. *Waste Mixing and Diluent Selection for the Planned Retrieval of Hanford Tank 241 -SY-102: A Preliminary Assessment*. PNNL-10927, Pacific Northwest National Laboratory, Richland, Washington.

Onishi Y, R Shekarriz, KP Recknagle, PA Smith, J Liu, YL Chen, DR Rector, and JD Hudson. 1996. *Tank SY-102 Waste Rheological Measurements and Pump Jet Mixing Simulations*. PNNL-11352, Pacific Northwest National Laboratory, Richland, Washington.

Pacquet EA and GA Leshikar. 2000. *Evaluation of Flygt Propeller Mixers for Double-Shell Tank High-Level Waste Auxiliary Solids Mobilization*. RPP-6421 Rev 0, CH2M HILL Hanford Group, Inc., Richland, Washington.

Parker SP. 1984. *McGraw-Hill Dictionary of Scientific and Technical Terms*, 3rd Edition, McGraw-Hill, New York.

Perona JJ, TD Hylton, EL, Youngblood, and RL Cummins. 1994. *Jet Mixing Long Horizontal Storage Tanks*. ORNL/TM-12876, Oak Ridge National Laboratory, Oak Ridge, Tennessee.

Peterson ME, RD Scheele, and JM Tingey. 1989. *Characterization of the First Core Sample of Neutralized Current Acid Waste from Double-Shell Tank 101-AZ*. PNL-7758, Pacific Northwest Laboratory, Richland, Washington.

Poirier MR, D Herman, FF Fondeur, E Hansen, and SD Fink. 2003. *MST/Sludge Agitation Studies for Actinide Removal Process and DWPF*. WSRC-TR-2003-00471, Rev. 0, Savannah River National Laboratory, Aiken, South Carolina.

Poirier MR and PO Rodwell. 1999. *Phase C Flygt Mixer Test Results*. WSRC-TR-99-OO097, Westinghouse Savannah River Company, Aiken, South Carolina.

Poirier MR, H Gladki, MR Powell, and PO Rodwell. 1999. *Mobilization of Cohesive Sludge in Storage Tanks Using Jet Mixers*. WSRC-MS-99-00870, Westinghouse Savannah River Company, Aiken, South Carolina. (At 10th European Conference on Mixing, Delft (NL).

Poirier MR and PR Monson. 1998. *Gas - Liquid Mass Transfer In Agitated Tanks Containing Non-Newtonian Fluids*. WSRC-MS-98-00784, Savannah River Technology Center, Aiken, South Carolina.

Poirier MR, MR Powell, H Gladki, and PO Rodwell. 1998a. *Suspending Zeolite Particles in Tanks*. WSRC-MS-98-00893, Savannah River Technology Center, Aiken, South Carolina.

Poirier MR, MR Powell, H. Gladki, and PO Rodwell. 1998b. "Suspending Zeolite Particles in Tanks." FEDSM99-7787. *3rd ASME/JSME Joint Fluids Engineering Conference*, July 18–23, 1999, San Francisco, California.

Poirier MR, MR Powell, and H Gladki. 1998c. *Suspending Insoluble Solids in Waste Tanks with Shrouded Axial Impeller Mixers*. WSRC-MS-98-00785, Savannah River Technology Center, Aiken, South Carolina.

Poirier MR. 1995. *Slurry Pump Operation in Tank 48*. WSRC-RP-94-01223, Rev. 1, Savannah River Laboratory, Aiken, South Carolina.

Poloski AP, HE Adkins, Jr, MJ Minette, J Abrefah, AM Casella, RE Hohimer, F Nigl, JJ Toth, JM Tingey, and ST Yokuda. 2009a. *Deposition Velocities of Newtonian and Non-Newtonian Slurries in Pipelines.* PNNL-17639 (WTP-RPT-175 Rev. 0), Pacific Northwest National Laboratory, Richland, Washington.

Poloski, AP, HE Adkins, ML Bonebrake, J Chun, AM Casella, KM Denslow, MD Johnson, ML Luna, PJ MacFarlan, JM Tingey, and JJ Toth. 2009b. *Deposition Velocities of Non-Newtonian Slurries in Pipelines: Complex Simulant Testing.* PNNL-18316 (WTP-RPT-189 Rev. 0), Pacific Northwest National Laboratory, Richland, Washington.

Poloski AP, BE Wells, JM Tingey, LA Mahoney, MN Hall, SL Thomson, GL Smith, ME Johnson, JE Meacham, MA Knight, MG Thien, JJ Davis, and Y Onishi. 2007. *Estimate of Hanford Waste Rheology and Settling Behavior*. PNNL-16857 (WTP-RPT-154 Rev. 0), Pacific Northwest National Laboratory, Richland, Washington.

Poloski AP, ST Arm, JA Bamberger, DB Barnett, RS Brown, BJ Cook, CW Enderlin, MS Fountain, M Friedrich, BG Fritz, RP Mueller, F Nigl, Y Onishi, LA Schienbein, LA Snow, S Tzemos, M White, and JA Vucelick. 2005. *Technical Basis for Scaling of Air Sparging Systems for Mixing in Non Newtonian Slurries*. PNWD-3541, Battelle Pacific Northwest Division, Richland, Washington.

Powell MR, BK Hatchell, JR Farmer, MR Poirier, H Gladki, and PO Rodwell. 1999a. *Evaluation of Flygt Mixers for Application in Savannah River Site Tank 19 Test Results from Phase A: Small-Scale Testing at ITT Flygt.* PNNL-12094, Pacific Northwest National Laboratory, Richland, Washington.

Powell MR BK Hatchell, WH Combs, MA Johnson, JR Farmer, MR Poirier, H Gladki, and PO Rodwell. 1999b. *Evaluation of Flygt Mixers for Application in Savannah River Site Tank 19 Test Results from Phase B: Mid-Scale Testing at PNNL*. PNNL- 12093, Pacific Northwest National Laboratory, Richland, Washington.

Powell MR, JR Farmer, H Gladki, BK Hatchell, MA Johnson, MR Poirier, and PO Rodwell. 1999c. *Evaluation of Flygt Mixers for Application in Savannah River Tank Summary of Test Results from Phase A, B, and C Testing.* PNNL-12168, Pacific Northwest National Laboratory, Richland, Washington.

Powell MR, Y Onishi, and R Shekarriz. 1997. *Research on Jet Mixing of Settled Sludges in Nuclear Waste Tanks at Hanford and Other DOE Sites: A Historical Perspective*. PNNL-11686, Pacific Northwest National Laboratory, Richland, Washington.

Powell MR. 1996. "Prediction of Mixer Pump Effectiveness for Sludge Mixing." Proc. of the *International Topical Meeting on Nuclear and Hazardous Waste Management: Spectrum* '96. American Nuclear Society, Inc. La Grange Park, Illinois, pp. 2355–2362.

Powell MR, CM Gates, CR Hymas, MA Sprecher, and NJ Morter. 1995a. *Fiscal Year 1994 1/25th-Scale Sludge Mobilization Testing*. PNL-10582, Pacific Northwest National Laboratory, Richland, Washington.

Powell MR, GR Golcar, CR Hymas, and RL McKay. 1995b. *Fiscal Year 1993 1/25th-Scale Sludge Mobilization Testing.* PNL-10464, Pacific Northwest National Laboratory, Richland, Washington.

Rajaratnam, N. 1982. "Erosion by Submerged Circular Jets." *J Hydraulics Division* Vol 108 HY2:262–267.

Rajaratnam N. 1981. "Erosion by Plane Turbulent Jets." *J Hydraulic Research* 19(4):339–358.

Rajaratnam N. 1980. "Erosion by Circular wall Jets in Cross Flow." *J Hydraulics Division* Vol 106 HY11:1867–1883

Rajaratnam N and S Beltaos. 1977. "Erosion by Impinging Circular Turbulent Jets." *J Hydraulics Division* Vol 103 HY10:1191–1205.

Rajaratnam N and B Berry. 1977. "Erosion by Circular Turbulent Wall Jets." *J Hydraulic Research* 15(3):277-289.

Rajaratnam N. 1976. *Turbulent Jets.* Elsevier Science Publishers, New York.

Rassat SD, CW Stewart, BE Wells, WL Kuhn, ZI Antoniak, JM Cuta, KP Recknagle, G Terrones, VV Viswanathan, JH Sukamto, and DP Mendoza. 2000. *Dynamics of Crust Dissolution and Gas Release in Tank 241-SY-101*. PNNL-13112, Pacific Northwest National Laboratory, Richland, Washington.

Rast RS. 2009. *Operating Specifications for the Double-Shell Storage* Tanks. OSD-T-151-00007 Rev. 2. Washington River Protection Solutions, Richland, Washington.

Recknagle KP and A Shekarriz. 1998. "Laminar Impeller Mixing of Newtonian and Non-Newtonian Fluids: Experimental and Computational Results." Proceedings of *FEDSM'98 1998 ASME Fluids Engineering Division Summer Meeting*, June 21–25, 1998 Washington, D.C.

Rule VA, BL Burks, and SD Van Hoesen. 1998. *North Tank Farm Data Report for the Gunite and Associated Tanks at Oak Ridge National Laboratory, Oak Ridge, Tennessee*. ORNL/TM-13630, Oak Ridge National Laboratory, Oak Ridge, Tennessee.

Russel WB, DA Saville, and WR Schowalter. 1989. *Colloidal Dispersions.* Cambridge University Press, Cambridge.

Schatzmann M, P Ficher, and GR Bezzola. 2003. "Rheological Behavior of Fine and Large Particle Suspensions." *Journal of Hydraulic Engineering, ASCE* 129(10):796–803.

Schiffhauer MA and RE Inzana. 1987. *Scale Model Equipment Testing, Final Report for the Period of FY 1985 to 1987*. DOE/NE/44139-36, West Valley Nuclear Services, Co., Inc., West Valley, New York.

Schiffhauer MA, JT Groth, and DW Scott. 1985. "The Status of the Waste Removal System for the West Valley Demonstration Project." Proc. Symposium on Waste Management '85. Volume 2, RG Post, ed., pp. 611–619.

Sears MB, JM Giaquinto, WH Griest, RT Pack, T Ross, and RL Schenley. 1995. *Sampling and Analysis of Inactive Radioactive Waste Tanks W-17, W-18, WC-5, WC-6, WC-8 and WC-11 through WC-14 at ORNL (BVEST Area)*. ORNL/TM-13017, Oak Ridge National Laboratory, Oak Ridge, Tennessee.

Shekarriz A, BB Brenden, and HK Kytomaa. 1998. "Planar Ultrasonic Technique for Real-Time Visualization and Concentration Measurement in Dense Solid-Liquid Slurries." FEDSM98-5226, 1998 ASME Fluids Engineering Division Summer Meeting, ASME, New York, New York.

Shekarriz A and DM Sheen. 1998. "Slurry Pipe Flow Measurements Using Tomographic Ultrasonic Velocimetry and Densitometry." FEDSM 98-5076, 1998 ASME Fluids Engineering Division Summer Meeting, ASME, New York, New York.

Shekarriz A, KJ Hammad, and MR Powell. 1997a. *Evaluation of Scaling Correlations for Mobilization of Double-Shell Tank Waste.* PNNL-11737, Pacific Northwest National Laboratory, Richland, Washington.

Shekarriz A, Y Onishi, PA Smith, M Sterner, DR Rector, and J Virden. 1997b. *Cross-Site Transfer System at Hanford: Long-term Strategy for Waste Acceptance*. PNNL-11497, Pacific Northwest National Laboratory, Richland, Washington.

Shekarriz R. 1996. *Real-Time Slurry Rheology Measuremen*t. DE-AC06-76RL01830, Pacific Northwest Laboratory, Richland, Washington.

Shekarriz A, G Doulliard, and CD Richards. 1996. "Velocity Measurements in a Turbulent Non-Newtonian Jet." *Journal of Fluids Engineering*, 118:872–874.

Shekarriz A, JR Phillips, and TD Weir. 1995. "Quantitative Visualization of a Submerged Pseudoplastic Jet Using Particle Image Velocimetry." *Journal of Fluids Engineering*, 117, pp 369-373.

Shepard CL, CW Stewart, JM Alzheimer, G Terrones, G Chen, and NE Wilkins. 1995. *In Situ Determination of Rheological Properties and Void Fraction: Hanford Waste Tank 241-SY-103*. PNL-10865, Pacific Northwest National Laboratory, Richland, Washington.

Shepard CL, JB Colson, KO Pasamehmetoglu, C Unal, JN Edwards, and J Abbott. 1994a. T*heory of Operation for the Ball Rheometer.* PNL-10240, Pacific Northwest Laboratory, Richland, Washington.

Shepard CL, MA Chieda, LJ Kirihara, JR Phillips, A Shekarriz, G Terrones, J Abbott, C Unal, KO Pasamehmetoglu, A Graham, and TI Stokes. 1994b. *Acquisition and Reduction of Data Obtained from Tank 101-SY In-Situ Ball Rheometer*. PNL-10170, Pacific Northwest Laboratory, Richland, Washington.

Shor JT and RL Cummins. 1991. *MVST Scale-Model Sludge Mobilization Development*. ORNL/TM-11709, Oak Ridge National Laboratory, Oak Ridge, Tennessee.

Staehr TW. 1999. *Mixer Pump Test Plan for Double Shell Tank AZ-101*. HNF-SD-WM-PTP-027 Rev 4, Cogema Engineering Corporation, Richland, Washington.

Stanisich SN, RS Rice, and RG Schwaller. 1991. *Sampling and Analysis Plan for TAN-616, Liquid Waste Tanks V-1, V-2, V-3, and the TAN-640-Liquid Waste Tank at WRRTF (TK-735).* EGG-WM-8620, Rev. 1, Idaho National Engineering Laboratory, Idaho Falls, Idaho.

Stewart CW, SA Hartley, PA Meyer, and BE Wells. 2005. *Predicting Peak Hydrogen Concentrations from Spontaneous Gas Releases in Hanford Waste Tanks*. PNNL-15238, Pacific Northwest National Laboratory, Richland, Washington.

Stewart CW, JM Alzheimer, G Chen, and PA Meyer. 1998. *In Situ Void Fraction and Gas Volume in Hanford Tank 241-SY-101 as Measured with the Void Fraction Instrument.* PNNL-12033. Pacific Northwest National Laboratory, Richland, Washington.

Stewart CW, JM Alzheimer, ME Brewster, G Chen, RE Mendoza, HC Reid, CL Shepard, and G Terrones. 1996. *In Situ Rheology and Gas Volume in Hanford Double-Shell Waste Tanks*. PNNL-11296, Pacific Northwest National Laboratory, Richland, Washington.

Stewart CW, CL Shepard, JM Alzheimer, TI Stokes, and G Terrones. 1995. *In Situ Determination of Rheological Properties and Void Fraction in Hanford Waste Tank 241-SY-101*. PNL-10682, Pacific Northwest Laboratory, Richland, Washington.

Stewart CW, JD Hudson, JR Friley, FE Panisko, ZI Antoniak, TE Michener, JG Fadeff, LF Efferding, JJ Irwin, NW Kirch, and DA Reynolds. 1994. *Mitigation of Tank 241-SY-101 by Pump Mixing: Results of Full-Scale Testing*. PNL-9959, Pacific Northwest Laboratory, Richland, Washington.

Stewart CW. 1994. *Jet Mixer Pump Testing in Hanford Tank 241-SY-101*. PNL-SA-24429, Pacific Northwest Laboratory, Richland, Washington.

Tamburello DA, RA Dimenna, and SY Lee. 2009. *Tank 26 Evaporator Feed Pump Transfer Analysis*. SRNS-TR-2008-00026 Rev. 1, Savannah River National Laboratory, Aiken, South Carolina.

Tamburello DA, RA Dimenna, and SY Lee. 2008a. *Tank 32 Evaporator Feed Pump Transfer Analysis.* SRNL-TR-2008-00324, Savannah River National Laboratory, Aiken, South Carolina.

Tamburello DA, RA Dimenna, and SY Lee. 2008b. *F-Area Pump Tank 1 Mixing Analysis*. SRNL-TR-2008-00280, Rev. 0, Savannah River National Laboratory, Aiken, South Carolina.

Templeton AM. 2000. *Tank 241-AZ-101 Mixer Pump Test Grab Sampling and Analysis Plan*. RPP-5533 Rev 1, CH2M HILL Hanford Group, Inc., Richland, Washington.

Terrones G and LL Eyler. 1993. *Computer Modeling of OWL Storage Tank: Sludge Mobilization and Mixing*. PNL-8855, Pacific Northwest Laboratory, Richland, Washington.

Thorne CR. 1981. "Field Measurements of Rates of Bank Erosion and Bank Material Strength." *Erosion and Sediment Transport Measurement* (Proceedings of the Florence Symposium, June 1981). IAHS Publ. No. 133, 503–512.

Townson PS. 2009. *Tank Farm Mixing Demonstration Plannin*g Workshop. RPT-1741-0001, Rev. 0, Energy Solutions, Richland, Washington.

Trent DS and LL Eyler. 1991. *TEMPEST: A Computer Program for Three-Dimensional Time-Dependent Computational Fluid Dynamics, Vol. 1: User's Manual*. PNWD-1536 Rev. 1, Battelle, Pacific Northwest Laboratory, Richland, Washington.

Trent DS and TE Michener. 1993. *Numerical Simulation of Jet Mixing Concepts in Tank 241-SY101*. PNL-8559, Pacific Northwest Laboratory, Richland, Washington.

Turian RM, JF Attal, DJ Sung, and LE Wedgewood. 2002. "Properties and Rheology of Coal-Water Mixtures Using Different Coals." *Fuel* 81:2019–2033.

Urie MW, GM Mong, PR Bredt, AP Poloski, JA Campbell, RD Scheele, OT Farmer, CZ Soderquist, SK Fiskum, RG Swoboda, LR Greenwood, MP Thomas, EW Hoppe, JJ Wagner, and LK Jagoda. 2002. *Chemical Analysis and Physical Property Testing of 241-AZ-101-Tank Waste—Supernatant and Centrifuged Solids*. PNWD-3215, Rev 1 (WTP-RPT-048, Rev 1), Pacific Northwest National Laboratory, Richland, Washington.

US Silica. 2010. *Minusil-40 Product Data*. Downloaded from http://www.u-s-silica.com/prodindex.htm on 2/21/2010.

Warrant RW. 2002. *Results of Retrieval Testing of Sludge from Tank 241-AZ-102*. RPP-9806 Rev. 0, Fluor Hanford Inc., Richland, Washington.

Warrant RW. 2001. *Results of Retrieval Testing of Sludge from Tank 241-AY-102*. RPP-8909 Rev. 0, Fluor Hanford Inc., Richland, Washington.

Waters ED and DT Heimberger. 1992. *Stress Cycles and Forces on In-Tank Components Resulting from Mixer Pump Operation in DST 101-AZ*. WHC-SD-W151-ER-001, Westinghouse Hanford Company, Richland, Washington.

Weast RC, Editor-in-Chief. 1985. *CRC Handbook of Chemistry and Physics*. ISBN-0-8493-0466-0. CRC Press, Inc., Boca Raton, Florida.

Weber RA. 2008. *Methodology and Calculations for the Assignment of Waste Groups for the Large Underground Waste Storage Tanks at the Hanford Site*. RPP-10006, Rev. 8, CH2M HILL Hanford Group, Inc., Richland, Washington.

Weeren HO. 1984. *Sluicing Operations at Gunite Waste Storage Tanks*. ORNL/NFW-84/42, Oak Ridge National Laboratory, Oak Ridge, Tennessee.

Wells BE, RL Russell, LA Mahoney, GN Brown, DE Rinehart, WC Buchmiller, EC Golovich, and JV Crum. 2010. *Hanford Sludge Simulant Selection for Soil Mechanics Property Measurement*. PNNL-19250, Pacific Northwest National Laboratory, Richland, Washington.

Wells BE and JJ Ressler. 2009. *Estimate of the Distribution of Solids within Mixed Hanford Double-Shell Tank AZ-101: Implications for AY-102*. PNNL-18327, Pacific Northwest National Laboratory, Richland, Washington.

Wells BE, CW Enderlin, PA Gauglitz, and RA Peterson. 2009. *Assessment of Jet Erosion for Potential Post-Retrieval K-Basin Settled Sludge*. PNNL-18831, Pacific Northwest National Laboratory, Richland, Washington.

Wells BE, MA Knight, EC Buck, SK Cooley, RC Daniel, LA Mahoney, PA Meyer, AP Poloski, JM Tingey, WS Callaway III, GA Cooke, ME Johnson, MG Thien, DJ Washenfelder, JJ Davis, MN Hall, GL Smith, SL Thomson, and Y Onishi. 2007. *Estimate of Hanford Waste Insoluble Solid Particle Size and Density Distribution*. PNWD-3824 (WTP-RPT-153, Rev. 0), Battelle—Pacific Northwest Division, Richland, Washington.

West WL. 1979. *Tank 16 Demonstration Single-Pump Test Results.* DPSP-79-17-12, Savannah River Laboratory, Aiken, South Carolina.

Winterwerp JC and WGM Van Kesteren. 2004. *Introduction to the Physics of Cohesive Sediment in the Marine Environment*. Developments in Sedimentology, 56. Elsevier Amsterdam, Netherlands.

Witwer KS, JA Bamberger, and MS Greenwood. 2001. *Results Of Performance Testing of the Ultrasonic Densitometer Used in the 241SY-101 Prefabricated Pump Pit*. RPP-7543, Rev. 0, Fluor Hanford, Inc., Richland, Washington.

Workman J Jr., DJ Veltkamp, S Doherty, BB Anderson, KE Creasy, M Koch, JF Tatera, AL Robinson, L Bond, LW Burgess, GN Bokerman, AH Ulhman., GP Darsey, F Mozayeni, JA Bamberger, and MS Greenwood. 1999. "Process Analytical Chemistry." *Analytical Chemistry* 71(12):121R–180R.

Youngblood EL, JB Berry, and JR De Vore. 1991. "Predicting Transport Behavior for Radioactive Sludges at Oak Ridge National Laboratory." Presented at the AIChE Summer Meeting, August 18–21, 1991, Pittsburgh, Pennsylvania. Martin Marrietta Energy Division, Oak Ridge National Laboratory, Oak Ridge, Tennessee.

Zhou Z, MJ Solomon, PJ Scales, and DV Boger. 1999. "The Yield Stress of Concentrated Flocculated Suspensions of Size Distributed Particles." *Journal of Rheology* 43(3):651–671.

Distribution

No. of Copies

2 **DOE Office of River Protection**

JS Shuen (2) H6-60

5 **Washington River Protection Solutions**

SJ Lepka B1-55
DJ Tedeschi B1-55
M Thien (3) B1-55

No. of Copies

29 **Pacific Northwest National Laboratory**

JA Bamberger K7-15
J Chun K6-24
KM Denslow K5-26
JA Fort K7-15
PA Gauglitz (20) K7-15
JJ Jenks K7-15
PA Meyer K7-15
TE Michener K7-15
DR Rector K7-15
BE Wells K7-15

Pacific Northwest
NATIONAL LABORATORY

U.S. DEPARTMENT OF
ENERGY

Proudly Operated by Battelle *Since 1965*

902 Battelle Boulevard
P.O. Box 999
Richland, WA 99352
1-888-375-PNNL (7665)
www.pnl.gov